POLITECNICO DI TORINO

KUNGLIGA TEKNISKA HOGSKOLAN

Master’s degree in Civil Engineering

The Master Thesis

HSI effects on pedestrian bridges

Tutors

Prof. Cecilia Surace

Prof. Raid Karoumi

Lc.PhD Daniel Colmenares

Lc.PhD Marco Civera

Candidate

Giancarlo Costa

Academic year 2020/2021

Acknowledgement

I would like to thank all the people who have supported me in this project and have helped me in writing my thesis with observations, suggestions, and critics.

Firstly, I would like to thank my family for all the support they give me throughout this master's degree.

I would like thank Lc.PhD Daniel Colmenares and prof. Raid Karoumi, who drove me throughout my project in KTH. I hope we will continue our collaboration in the next journal paper, and we will enjoy working together again.

I would like to thank prof. Cecilia Surace and Dr. Civera who helped throughout the thesis with suggestions and observations.

I thank all the 35 people who took part in the experiment and without collaboration I could not finish my thesis.

I thank Treesa and Giovanni for the help in checking my English.

Finally, last but not least, all my friends who add value to my personal life.

Abstract

The study on Human Structure Interaction (HSI) effects represent a new research field in the design of pedestrian bridges. The presence of pedestrians on the structure affects the dynamic properties of the bridge, and these changes may be quantified in order to design pedestrian bridges in a more efficient way. The Dynamic Amplification Factor (DAF) curve shifts downward and towards the left when increasing number of pedestrians. The thesis, which is strictly connected to a journal paper to be submitted in 2021, includes a new formulation of the dynamic response through the DAF curves and an experimental campaign to verify the shift. A HSI model, based on Caprani continuous formulation, was created on MATLAB.

To perform the experimental campaign, the Folke Bernadotte Bridge in Stockholm was chosen. The dynamic response due to a hammer test, was registered without pedestrians and with 35 pedestrians on the bridge. The dynamic properties of the bridge, such as natural frequencies, damping, mode-shapes, Frequency Response Function (FRF) are estimated in both cases. A Finite Element Model (FEM) is built on Abaqus, natural frequencies and mode-shapes are compared. Moreover, a running test is performed on the bridge and the single pedestrian loading is modelled as a moving harmonic. This test brings different values of stiffness and damping for the pedestrian to be compared to the values assumed in the HSI model for standing pedestrians.

A quantification of the variation of the bridge properties due to Human structure interaction may lead to a new way to design pedestrian bridges considering pedestrians not only as loading sources of the structural system but also as dynamic vibration adsorbers (DVA).

Table of contents

List of Figures

List of tables

Nomenclature

HSI – Human Structure Interaction

SDOF – Single Degree of Freedom

MDOF – Multiple Degree of Freedom

VDA – Viscous Dynamic Adsorbers

FEM – Finite Element Model

DAF – Dynamic Amplification Factor

MF – Moving Force

MM – Moving Mass

SMD – Spring Mass Damper

MSMD - Moving Spring Mass Damper

H2SI – Human to Structure Interaction

S2HI – Structure to Human Interaction

MAC – Modal Assurance Criterion

CoMAC – Coordinate Modal Assurance Criterion

DFT – Discrete Fourier Transformation

FFT - Fast Fourier Transformation

DLF – Dynamic Load Factor

SLE - Serviceability Limit State

1. Introduction

This chapter presents a general view on the thesis background, aim and scope, contribution, and context.

1.1. Background

In recent years there has been an increasing awareness of the importance of infrastructures for pedestrians. Cities need to be re-designed facing environmental, economic, and social challenges.

In this context, pedestrian bridges improve the liveability of cities connecting spaces, shortening travel distances and making a safer environment not only for pedestrians but also for cyclists seeking a more environmentally friendly method of transport.

Modern footbridges are built slender, lighter, and longer and have different dynamic properties from the ones which were built in the past. A new problem with discomfort regarding the vibration of the structure due to external loading has been noticed, studied, and analysed. The London Millennium Bridge and the Solferino footbridge in Paris are examples of how modern footbridges experience excessive vibration due to pedestrian loading. The two famous bridges needed to be closed soon after the opening day because of the lateral swaying of the structure induced by pedestrian loading.

Pedestrian loading is difficult to model due to the variety in inter and intra-pedestrian properties such as weight, walking speed, synchronization, damping, and stiffness. Dynamic analysis is not extensively covered in Eurocode and the standards leave the reasonable estimation of parameters for the designers.

The difference of dynamic behaviour on the new footbridges rather than the older ones, lies mainly in the slenderness and the lightness pursued, which are the cause of lower resonance frequencies in the new bridges. Human-induced loading is more likely to be near to the resonance frequencies of the pedestrian bridges which causes an amplification of the dynamic response.

Human structure interaction (HSI) effects represent a new research field in the design of pedestrian bridges. The presence of pedestrians on the structure affects the properties of the bridge. Several studies, as it will be shown in the next chapter, demonstrates how humans behave as dampers dissipating energy. It is important to quantify these changes to pursue a more efficient design.

1.2. Aims and Scope

The overall aim of this Master Thesis is to analyse HSI and provide a quantification on bridge properties changes due to the HSI, to be taken into account in the design phase of a pedestrian bridge.

The thesis analyses the different approaches to model HSI and later focuses on the continuous approach. The quantification of the variation of the bridge properties can lead to a new way to design bridges. Pedestrians can be considered not only as loading components of the structural system but as dynamic vibration adsorbers (DVA).

This thesis aims to propose an innovative and more efficient method for the design of footbridges including HSI.

1.3. Methodology

A summary of the current proposed guidelines is presented and an explanation of the modelling of human-induced vibrations is provided. Human Structure Interaction is introduced and analysed. A literature review is conducted, and the continuous method is assumed for the analysis.

A new way to model HSI effects in real cases is studied and coded on MATLAB. Afterwards, an experimental campaign is performed in order to test how HSI affects the properties of the new Folke Bernadotte Bridge in Stockholm. The results are compared with the ABAQUS FEM model based on the drawings provided by the bridge design company. The HSI model is verified by the second experiment when 35 pedestrians are requested to stand while performing a hammer test.

1.4. Limitations

The analyses in the thesis are limited to the study of simply supported structures in one span using two-dimensional analysis.

Literature accounts for two different methods to model HSI: the Modal Analysis Method and the Finite Element Method. In this thesis, only the former method is developed and implemented in the analysis.

The analysis focuses on the only vertical vibration of the system. Lateral, torsional, and mixed modes can be analysed in the same method but are not included in the thesis.

1.5. Literature Review

Cost-effectiveness and environmental impact are two of the main features of newly built civil engineering structures. Pedestrian bridges need to be light, slender, aesthetically pleasant and optimized for cost. Slenderness and lightness permit a lower use of material while making the structure more susceptible to excessive vibrations caused by human-induced loads, e.g. pedestrians crossing the bridge.

To ensure comfort for pedestrians, today's design guidelines for pedestrian bridges require the limitation of vibrations and the verification of comfort criteria. Human structure interaction (HSI) effects may have a significant impact on the dynamic properties of the bridge. In presence of a single pedestrian or of crowds, the natural frequencies of the bridge change as well as the damping, and the Dynamic Amplification factor (DAF). Predicted acceleration might be overestimated and the comfort criteria might be too conservative. On the other hand, running pedestrians might cause excessive vibrations which are not analysed in the current design guidelines.

In the thesis, the Caprani continuous formulation of Human Structure Interaction [10] is adopted and the continuous flow of pedestrians is assumed. Several studies have been conducted on the themes of the load on footbridges and on the Human Structure Interaction. A literature review is presented below.

The London Millennium bridge unexpected lateral movements are well analysed in the paper of Dallard et al., (2001) [1]. After the description of the bridge components, the author emphasizes that the reason for the excessive motion was given by the low frequency of resonance in the horizontal direction. If enough pedestrians apply a horizontal force on the deck of the bridge, in so-called lock-in phenomenon, a significant lateral motion is caused. Thirty-seven viscous dampers were installed just down the deck to limit the problem.

1.5.1 Load Modelling

Caprani (2013) [2] formulates a computationally efficient methodology to determine footbridge vibration response when subjected to pedestrian excitation suitable for use in a Monte Carlo framework. Pedestrian loading models usually idealize walking as a perfectly periodic force. However, it is demonstrated that "imperfect walking" occurs, and it is the key source of the differences between measured and estimated vibration responses. The Modal Precise Integration Method (MPIM) is formulated by Caprani on the base of Zhong and Williams' previous works in order to efficiently and accurately estimate the dynamic response of a bridge when subjected to pedestrian loading taking into consideration inter-pedestrian variability through a Monte Carlo analysis.

Živanović et al.,(2007) [3] criticize how in vibration serviceability a force induced by a single person is usually modelled as a harmonic force with the same frequency as the footbridge natural one, and how footbridges are usually modelled as SDOF. These assumptions can significantly overestimate the footbridge vibration response. Their paper aims to formulate a multi-harmonic force model for the calculation of the multimode response in footbridges. The intersubject variability is modelled via probability distributions of walking frequencies, force amplitudes and step lengths. The intra-subject variability is modelled in frequency domain. The multimode response of pedestrian bridges can be predicted with sufficient accuracy.

The existing walking models used for vibration serviceability assessment assume perfect periodicity of the loading, easily describable by the Fourier series. Brownjohn et al. (2004) [4] in their paper examine real continuous walking forces and the effect of their imperfection through time simulations of the structural response. These differences are most significant for higher harmonics where the simulated vibration response is simulated. The measurement of the walking force function in a continuous manner permitted researchers to study its randomness.

A computation of crowd loads using a nonlinear equation is conducted by Ebrahimpour et al. (1991) [5]. A floor is designed, built, and instrumented with strain gauges and displacement transducers. For four patterns of groups formed by 10, 20, 30 and 40 people, the results are measured experimentally. These results are later compared with the computer simulation model developed previously. The average deviation between the measured and the simulated values were less than 8%.

The dynamic loading and the footbridges response are studied further by Ranier et al. (1988) [6]. The maximum dynamic load was found to be nearly twice as large as those recommended in the 1983 Ontario Highway Bridge Design Code or the British Standard BS5400. In their studies, a procedure for evaluating the response of simply supported bridges to walking, running, and jumping excitations at the resonance frequencies, is described. Newer design codes permit the designer to consider other loading functions that may be applicable for footbridges like when the excitation arises for the second harmonic component of the pedestrian movement.

A literature review on the pedestrian induced lateral vibrations on footbridges is conducted by Ingólfsson et al. (2012) [7]. The scope of their research is to provide the link between the mathematical models and the empirical observation. Based on the measured responses Charles and Bui (2005) [8] defined the equivalent number of single resonant pedestrians walking at a frequency that matches the bridge natural frequencies. Dallard et al. (2000) [1] explained that the excessive oscillations were caused by synchronous horizontal loading as a consequence of the phenomenon of lock-in between the pedestrians.

Ingólfsson and Georgakis (2011) [9] use the experimentally obtained forces to define a total induced lateral force F(t), as an equivalent static force and additional equivalent damping and inertia forces.

1.5.2 Modelling Human Structure Interaction

Considering Human Structure interaction leads to many issues which are analysed by several authors. The modelling of the pedestrian, the mutual effects, the pedestrian properties, the inter and intra-subject variability are studied and discussed.

Caprani and Ahmadi (2016) [10] model the walking pedestrian vertical forces in three different ways. A pedestrian is in turn modelled as a moving force (MF), a moving mass (MM) and a moving spring-mass-damper (SMD). In each case, the single pedestrian is firstly studied and then extended to consider a crowd of pedestrians. Depending on the crowd-to-bridge mass ratio, the dynamic properties of the human structure system change. High ratios lead to large changes in the natural frequencies and damping of the system. The response prediction depends on the choice of the force model. It is demonstrated as the SMD spring mass damper force model is the most accurate in the prediction of the dynamic response.

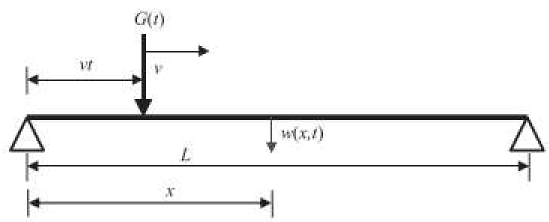

Fig. 1. The MF model of a pedestrian (showing simply-supported beam as an example structure).

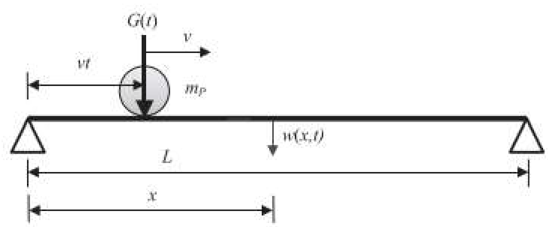

Fig. 2. The MM model of a pedestrian (showing simply-supported beam as an example structure).

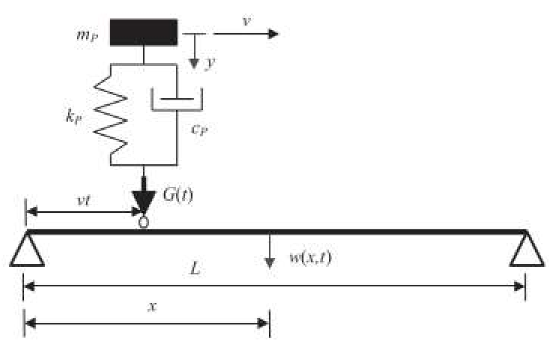

Fig. 3. The SMD model of a pedestrian (showing simply-supported beam as an example structure).

Figure 1: MF, MM and SMD modelling. Source [10]

In another study, Ahmadi et al. (2018) [11] analyse how the structure and human interact with each other in a mutual sense. Two kinds of interaction are considered the Human-To-Structure and the Structure-to-Human. The H2SI and the S2HI effects are usually considered mutually exclusive. Ahmadi's work experimentally investigates the existence of H2SI and the S2HI effects by isolating their influence on the vibration response. Five tests were conducted on a rigid and on a flexible bridge model. Modal analysis is implemented, and Newmark-beta integration used. The mode shape can be approximately described by a half-sine function which means that the bridge is considered as simply supported. H2SI is found to be a far stronger influence than S2HI for the bridge study. The intensity of both S2HI and H2SI is found to increase as the mass ratio between the human and structure increases. At resonance, where vibration amplitude reaches its peak, the HSI effects are the most pronounced.

Van Nimmen et al. (2017) [12] study a detailed crowd model and evaluate the impact of various simplifying assumptions and inter and intra-person variabilities. Their results show that for the low-frequency dynamic behaviour of bridges, HSI leads to an effective damping ratio which is significantly higher than the inherent damping ratio of the empty structure. Moreover, they demonstrate how the detailed moving crowd model can be well approximated by a time-invariant crowd-structure model. Their studies suggest an increase in the effective damping ratio up to 10 % for the high pedestrians-bridge mass ratio. The posture is even analysed, and it was shown how standing, walking or a posture with slightly bent legs give different effect on damping.

Caprani et al. (2015) [13] conduct a comprehensive experimental programme to quantify the magnitude of human structure interaction. A range of test subjects were considered, walking at a range of pacing frequencies on both rigid and flexible surfaces. Loading was conducted with the aid of Tekscan in-shoe foot pressure sensors in order to efficiently describe the dynamic pressure, force and timing for foot function and gait analysis. Their studies suggest an increase in damping up to 2-3 times during resonance and a slight shift in the bridge resonance frequency.

Ahmadi and Caprani (2015) [14] model each pedestrian as a spring-mass-damper (SMD). The bridge was modelled as a simply supported bridge and the eigenvalue analysis was carried out to obtain the frequency and the damping matrices of the HSI system at each time. It was concluded that the bridge frequency and damping significantly change due to the interaction between the bridge and a crowd of pedestrians.

Ahmadi et al. (2017) [15], in their work, point out how the deterministic moving force (MF) model may not be the most suitable to describe slender, lightweight, low-damping, and low-frequency pedestrians bridges. On the other hand, the SMD is able to incorporate human mass, stiffness, and damping into the vibration response prediction. The moving spring mass damper (MSMD) schematization for the pedestrian includes an external pulsating force and permits the evaluation of the actual motion of the pedestrian. However, it introduces relevant unknown parameters which requires a high level of knowledge from both the programmer and the designer. The solution, they adopt, is to consider SMDs in fixed positions assuming a stationary location of the pedestrian who "walks on the spot". Their work aims to define an equivalent damping that considers HSI to use directly in the design process.

Younis et al. (2017) [8] focuses on the analysis of dynamic loading and emphasises the differences in the different human activities such as walking, jogging, and running. The two main parameters used to quantify the vibration response are amplitude and frequency. While in movement, the human body passes through the double, the single or zero support stage (while running for example). There are two types of randomness in human walking, the inter-subject given by the variety of pedestrians and the intra-subject variability given by the possible interaction between pedestrians. For example, the lock-in or sailor's walk is the phenomenon of synchronization of the pacing rate of walking pedestrians.

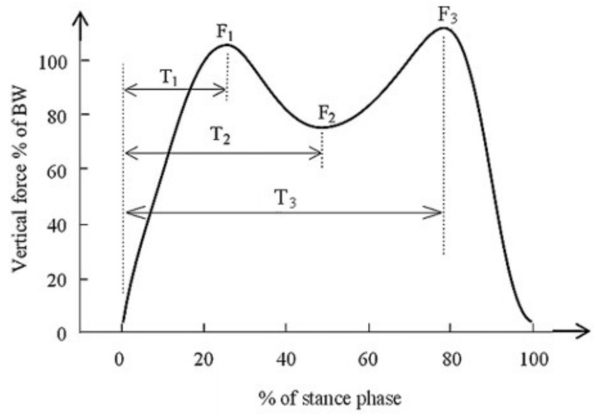

Figure 2: Vertical force caused by a walking pedestrian. Source [8]

Several authors describe the moving load problem in the finite element method adopting different techniques to solve the time-dependent and the unsymmetric element matrices properties of the system. Olsson [17] significantly reduces the number of equations to solve by adopting modal coordinates, which are eventually analysed by Newmark. Lin and Trethewey [18] solve the system with the Runge-Kutta integration scheme and Hino et al. [19] adopt the Wilson technique to obtain the dynamic response of the support beam and of the moving system. A critical comparison of the three techniques was conducted and it was concluded that modal coordinate formulation permits a faster and simpler solution of the vibration response.

Moreover, Lin and Trethewey [18] adopt more accurate modelling of the pedestrian. A two feet spring dynamic system represented an effective schematization of the human body even though a more difficult formulation was needed.

Pu and Liu [20] in the description of a vehicle or a train moving on a multi-span continuous bridge with a non-uniform cross-section with the Finite Element Method, as well considers the effect of the inertial, the Coriolis and the centrifugal force by means of the additive matrices. Time dependency and friction are considered in the description of the system, and the numerical integration scheme of Romberg is adopted to solve the system.

Živanović et al. (2009) [21] compare the results of modal testing of a footbridge in three different setups: empty structure, bridge occupied by a passive standing crowd and eventually an active walking crowd. Their study emphasises the intrinsic damping of the human-structure system: modal testing showed higher damping for systems occupied either by a passive or an active crowd than for the empty structure. With the change in damping a shift in the frequency of resonance was noticed.

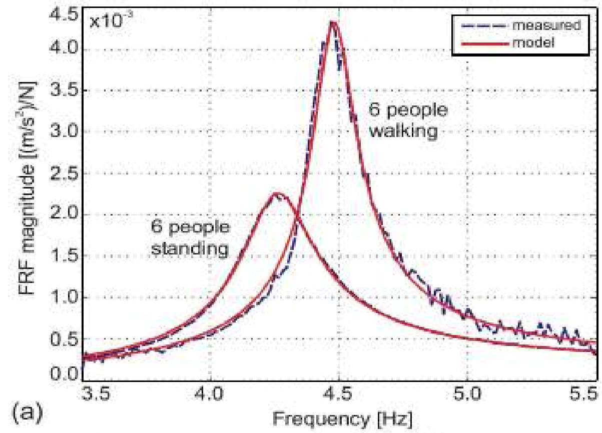

Figure 3: FRF magnitude of 6 standing and 6 walking pedestrians. Source [21]

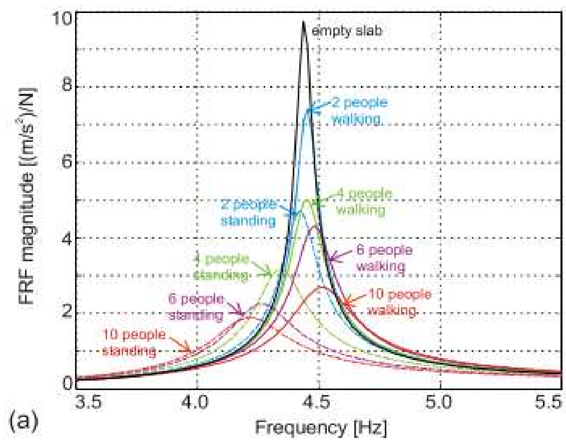

Figure 4: FRF Magnitude of walking and standing pedestrians. Source [21]

In their study, Živanović et al. (2010) [22] focus on the possible factors that cause discrepancies between measured and estimated vibration responses. Multi-person traffic is usually considered as a multiple of the response to a single person excitation and a factor which is a function of the number of people crossing the bridge at the same time. This approach originated from Matsumoto et al. (1978) [23] and it is commonly used because of its simplicity. The authors emphasise as most guidelines involve time-domain analyses while frequency domain analyses such as Brownjohn et al. (2004) [24], Butz (2008) [25] and Georgakis (2008) [26] are more suitable to describe inter and intra-variability in the description of pedestrian loading.

Piccardo e Tubino (2009) [27] analyse the vibration serviceability of footbridges subjected to realistic pedestrian traffic conditions, based on a probabilistic characterization of the pedestrian induced forces. The aim of the paper is to provide an evaluation of the vibration serviceability avoiding the numerical analyses. The study characterizes the essential non-dimensional parameters governing the dynamic response and defines the Equivalent Amplification Factor and the Equivalent Synchronization Factor. The identification of a simplified procedure to evaluate realistic levels of peak accelerations permitted to assess the vibration serviceability in a closed form. It is shown how the guidelines sometimes suggest a too conservative and sometimes slightly unconservative loading condition.

Yao et al. (2002) [28] study the behaviour of human subjects bouncing or jumping on a flexible structure. A unique test rig, which is a single degree of freedom platform supported by a cantilever and a moveable support, was used. The configuration of the system permitted them to adapt its own natural frequencies to match critical frequencies for bouncing and jumping. A human bouncing or jumping changes the dynamic properties of the system. The experimental results show that there are significant differences between the bouncing and jumping forces and the corresponding responses produced on stiff and flexible structures.

Fanning et al. (2005) [29] describe the modelling strategies used to simulate the interaction between a flexible ultra-lightweight pedestrian bridge and a crossing pedestrian. A finite element model of the footbridge was created, and it was analysed under transient load condition. Later comparison of the measured and predicted responses displayed agreement apart from when the pacing frequency of the test subject, modelled as an SMD, was near the resonant case. In this case, it was noted how the simulations overestimated the actual response.

In 2011 Archbold et al. [30] conduct a parametric analysis to compare the moving force model and the spring-mass-damper (SMD) model as a description of the pedestrians on the footbridge. The parameters which were investigated included the pacing frequency, leg stiffness, pedestrian mass, and step length. In the analysis, the pacing frequency was found to have by far the greatest influence on the bridge vibration response. Within its typical frequency range (1.8-2.2 Hz), the force model resulted conservative and the SMD model more appropriate. In their studies, Archbold et al. explained as there are two principal approaches in the design guidelines for dealing with the pedestrian-induced-vibration on a footbridge system. The first one is to ensure that the lower natural frequencies of the bridge are outside the pedestrian expected frequency's ranges, whereas the second is to limit the induced structural acceleration below certain prescribed acceptable limits. Therefore, the calculation of the natural frequencies, by the stiffness and the mass of the structure, needs to be conducted early in the design phase. The adjustment of these two main features can significantly vary the natural frequencies making them further from the pedestrian expected frequency. By increasing the mass, the frequency decreases, increasing the stiffness the frequency increases. However, in the case of slender and light bridges, it can be difficult to change mass and stiffness because of the design. Viscous dampers can be adopted to decrease the Dynamic Amplification Factor if needed. Due to the cumbersome dimensions and the relatively high cost, dampers should be considered in the design process and not only for later solutions as for the London Millennium Bridge.

In 2009 Venuti and Bruno [31] provided a critical analysis of the literature regarding the crowd-structure interaction phenomena on pedestrian bridges. The problem of Synchronous Lateral Excitation where the dependence of the force exerted by the pedestrians on the structural response, the triggering of the lock-in and the force self-limitation are analysed. The paper emphasises the need of more studies as the mechanisms which drive these phenomena are still not completely known. Modelling the parts of the complex crowd structure is widely applied in practice. However, crowd models are difficult to define and require the continuity assumption, which does not hold for very low densities.

In this thesis, the same continuity assumption is made. A certain number of pedestrians are modelled and positioned on the bridge assuming that the number of people on the bridge is constantly on time.

1.6. General Layout

Chapter 2 presents the theoretical background of this work of the thesis. The chapter includes the bases of Structural Dynamics, the concepts of modal analysis, signal analysis, damping evaluation, and time-stepping methods. Human Structure Interaction formulations from Caprani and Colmenares are presented. Finally, a brief synthesis of the current guidelines is presented.

Chapter 3 presents the methodology which has been followed through the tasks of the thesis. The HSI formulation is analysed, while the value of the parametric analysis and error surface is recognized. A case study is introduced, and the experiments described. Finally, a methodology for the extraction of the natural frequencies, mode-shapes and damping is defined.

Chapter 4 summarizes the result obtained in this work of the thesis. The HSI validity is checked through the parametric analysis and error surface. The case study dynamic properties are presented and the CoMAC applied. The second experiment permitted the verification of the HSI model.

Chapter 5 comprehends the discussion of the results. The dynamic properties, the HSI parametric analysis, the error surface as well as the running test results are the main focuses of this section.

Chapter 6 includes the conclusions of the study. The purpose of this section is to summarize the most relevant results of the thesis and to suggest further studies which can be conducted in the future.

2. Theoretical Background

A solid theoretical background is fundamental to understand the dynamic evaluation of a structure and the function that HSI can have in the design process.

2.1. Single Degree of freedom systems

A single degree of freedom system (SDOF) is a system where properties can be described by only one parameter. Therefore, the simplest structure can be described as an SDOF and its equation of motion accounts for just one parameter. An SDOF system can comprehend elastic, dissipating, and inertial components. These correspond to a spring, a viscous damper and eventually the mass. (Figure 5)

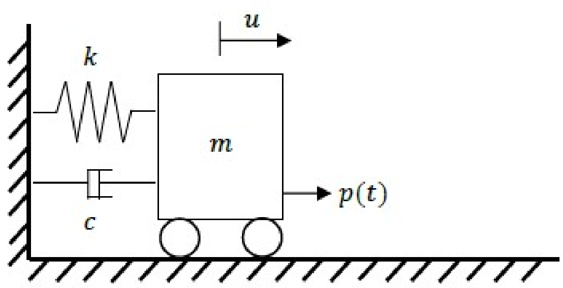

Figure 5: Single degree of freedom system

In the system the mass m is a point mass, k is the stiffness of the spring, c the damping coefficient of the viscous damper, p(t) represents an applied force to the system which varies in time. The describing parameter u indicates the direction of motion. Its derivates are velocity and acceleration.

A structure is usually composed of different parts behaving dynamically in various ways. Its complexity can be simplified in multiple independent SDOF systems.

The equation of motion of an SDOF can be obtained through Newton's Second Law:

$$\sum F = m\, a \tag{2.1}$$

where on the left side there is the sum of all the applied forces to the system and on the right mass and acceleration.

By the free body diagram of the system, it can be noted as three forces which are applied to the system: the external force $p(t)$, the spring generated force on the system F_s, and the damper generated force on the system F_d.

The force F_s is an expression of the Hooke's Law:

$$F_s = ku \tag{2.2}$$

where k corresponds to the stiffness of the spring and u to the displacement associated to the motion.

The force F_d is defined as:

$$F_d = c\,\dot{u} \tag{2.3}$$

Where c is the damping coefficient and $\dot{u}$ as the velocity.

Hence, the equation of motion for a Single degree of freedom system can be written as:

$$m\ddot{u} + c\dot{u} + ku = p(t) \tag{2.4}$$

The equation of motion represents the base of structural dynamics, and it can be solved both analytically and numerically. Mathematically, equation 2.4 corresponds to a second-order differential equation for which the solution consists of a particular solution $u_p(t)$ strictly dependant on the force $p(t)$ applied to the system and a characteristic (or homogeneous) solution $u_c(t)$ related to the natural motion of the system. The sum of $u_c(t)$ and $u_p(t)$ describes the total response of the structure.

$$u(t) = u_c(t) + u_p(t) \tag{2.5}$$

The equation of motion for a single degree of freedom system can be rewritten as:

$$\ddot{u} + 2\xi\omega_n\dot{u} + {\omega_n}^2 u = {\omega_n}^2\frac{p(t)}{k} \tag{2.6}$$

Defining:

- the undamped natural frequency of the system $\omega_n = \sqrt{\frac{k}{m}}$,
- the critical damping factor $c_{cr} = 2\,\omega_n m = 2\sqrt{km}$

- the viscous damping factor $\xi = \frac{c}{c_{cr}}$

Depending on the value of ξ a system can be defined as underdamped ($\xi < 1$), critically damped ($\xi = 1$), or over damped ($\xi > 1$). The propagation of the vibration strictly depends on the properties of the system and on the damping. An underdamped system experiences several cycles before the dynamic response cancels out. On the other hand, for critically damped and overdamped structures the motion decays rapidly. Civil structures are lightly damped systems with damping ratio below 0.05.

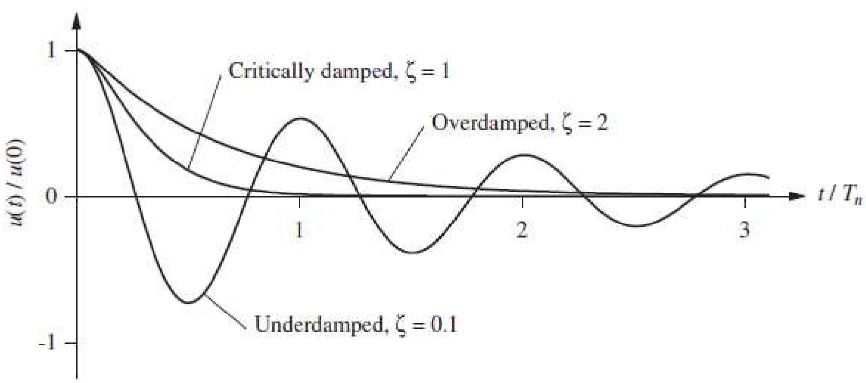

Figure 6: Damping ratios. Source [35]

The equation of motion for a non-damped structure is:

$$m\ddot{u} + ku = p_0 cos(\Omega t) \tag{2.7}$$

Assuming a solution in the form $u(t) = A\ cos(\omega_n t) + B\ sin(\omega_n t)$, the constants can be determined applying the boundary conditions to the system.

$$u(0) = A \quad and \quad \dot{u}(0) = v_0 = B\omega_n \tag{2.8}$$

The expression for the characteristic solution is:

$$u_c(t) = u_0 cos(\omega_n t) + \frac{v_0}{\omega_n} sin(\omega_n t) \tag{2.9}$$

The particular solution depends strictly on the applied force on the system, as mentioned. As the system is undamped, the force causes a motion that does not decay in time.

$$u_p(t) = Ucos(\Omega t) \tag{2.10}$$

Hence, the total response of the system is:

$$u(t) = u_c(t) + u_p(t) = u_0 cos(\omega_n t) + \frac{v_0}{\omega_n} sin(\omega_n t) + Ucos(\Omega t) \tag{2.11}$$

When the free vibration of a SDOF is considered, the applied force on the system is set equal to zero, $p(t) = 0$. The equation of motion can be written as:

$$\ddot{u} + 2\xi\omega_n\dot{u} + {\omega_n}^2 u = 0 \tag{2.12}$$

2.2. Multi Degree of freedom systems

The dynamic analysis of continuous systems requires the solution of a partial differential equation which may be difficult to obtain or may not exist. Therefore, the approximation of continuous systems as multi-degree of freedom (n-DOF) is usually conducted for simplicity of analysis. A multi-degree of freedom system requires one coordinate and one equation of motion for each degree of freedom. The equations of motion can be obtained by Newton's second law of motion, through the influence coefficients, or by using the Lagrange equation. There are n natural frequencies, to which correspond n mode shapes for an n degrees of freedom system. The mode shapes are orthogonal to each other which often enables simplifications.

Normal mode vibrations are the free vibrations that depend only on mass and on stiffness of the system. These are important to define to resonance spectrum of the system and to analyse the behaviour of the system under a certain loading. Damping limits the amplitude of vibration of the system.

Hence continuous structures can be schematized as spring-mass-damper systems and will be described by the Mass (M), Stiffness (K) and Damping (C) matrixes.

A 2-DOF is a multi-degree of freedom system which require 2 coordinates to describe the motion of the system.

The derivation of the equation of motion can be conducted through Newton's second law. Suitable coordinates to describe the positions of masses and rigid bodies directions are defined. Hence, the static equilibrium configuration is determined and the free-body diagram of each mass, or rigid body, is drawn. Forces by the springs, dampers or externally applied loads are represented. Finally, Newton's second law can be applied.

$$m_1\ddot{x}_1 + (c_1 + c_2)\dot{x}_1 - c_2\dot{x}_2 + (k_1 + k_2)\, x_1 - k_2x_2 = F_1 \qquad (2.13)$$

$$m_2\ddot{x}_2 - c_2\dot{x}_1 + (c_2 + c_3)\dot{x}_2 - k_2x_1 + (k_2 + k_3)x_2 = F_2 \qquad (2.14)$$

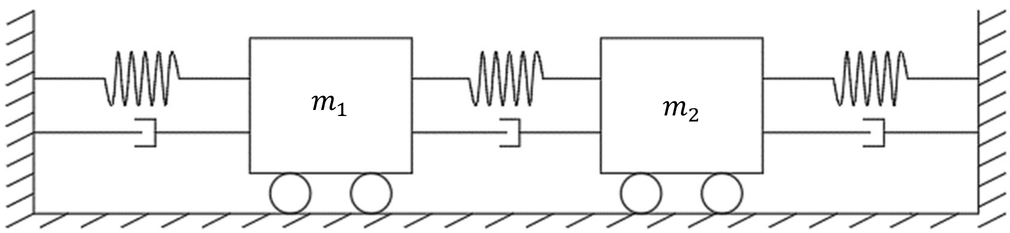

Figure 7: Two degree of freedom system

The equation of motion can be written in a matrixial form.

$$[\mathbf{M}]\ddot{x} + [\mathbf{C}]\dot{x} + [\mathbf{K}]x = F \qquad (2.15)$$

Where $[\mathbf{M}]$, $[\mathbf{C}]$ and $[\mathbf{K}]$ are mass, damping and stiffness matrixes, and $\ddot{x}$, $\dot{x}$ and x are vectors containing the accelerations, the velocities, and the displacements of the n points of the systems.

In the case of the 2 DOF:

$$[\mathbf{M}] = \begin{bmatrix} m_1 & 0 \\ 0 & m_2 \end{bmatrix} \qquad [\mathbf{C}] = \begin{bmatrix} c_1 & c_{12} \\ c_{21} & c_2 \end{bmatrix} \qquad [\mathbf{K}] = \begin{bmatrix} k_1 & k_{12} \\ k_{21} & k_2 \end{bmatrix}$$

$$\ddot{x} = \begin{pmatrix} \ddot{x}_1 \\ \ddot{x}_2 \end{pmatrix} \qquad \dot{x} = \begin{pmatrix} \dot{x}_1 \\ \dot{x}_2 \end{pmatrix} \qquad x = \begin{pmatrix} x_1 \\ x_2 \end{pmatrix}$$

The differential equations of the spring-mass system are coupled which means that each equation involves more than one coordinate. The equations cannot be solved individually but need to be solved at the same time.

Another method to define the K and M matrixes is through the influence coefficients. The equation of motion of a multi-degree system can be written in terms of influence coefficients. In the case of a simple linear spring, the force necessary to cause a unit elongation is called stiffness. When analysing more complex systems the relation between the displacements of the points and the force applied can be described by the influence coefficients. Given a system of two points, the displacement of the first point is set equal to 1 and the second is set fixed. The stiffness coefficients correspond to the force necessary to maintain the configuration of equilibrium.

Lagrange equations can be used as well, to describe the motion. Lagrange's equation can be stated as:

$$\frac{d}{dt}\left(\frac{\delta T}{\delta \dot{q}_j}\right) - \frac{\delta T}{\delta q_j} + \frac{\delta V}{\delta q_j} = Q_j^{(n)} \tag{2.16}$$

The equation of motion can be derived from equation 2.16 provided that the energy expressions are available.

The equations of motion need to be solved to calculate the mode-shape and the frequency of the system. Typically, the undamped system free vibration system can be solved through the calculations of the eigen values and eigen vectors.

Assuming a solution in the form $x_1(t) = C_1 cos(wt - \varphi)$ and $x_2(t) = C_2 cos(wt - \varphi)$

The equation: $[M]\,\ddot{x} + [K]\,x = 0$ can be written as:

$$([\mathbf{K}] - w^2[\mathbf{M}])x = 0 \tag{2.17}$$

Substituting $\lambda = w^2$, and posing the determinant equal to zero, the natural frequencies can be calculated.

Eigenvalues correspond to the natural frequencies while eigenvectors correspond to the mode-shapes. The mode-shape describes the deformation that the component shows when vibrating at the natural frequency.

2.3. Modal Analysis

The dynamic response of a multi degree of freedom system can be expanded in terms of modal contributions.

$$u(t) = \sum_{r=1}^{N} \phi_r q_r(t) = \phi q(t) \tag{2.18}$$

where $u(t)$ is the geometric coordinate vector, ϕ_r is the mode vector r, $q_r(t)$ is the modal generalized coordinate vector.

Using equation 2.18, the coupled equation $m\ddot{u} + ku = p(t)$, valid for a linear MDOF without damping, can be transformed to a set of uncoupled equations with modal coordinates $q(t)$ as unknowns.

The modal equations for a damped structure can be written as:

$$m\ddot{u} + c\dot{u} + ku = p(t) \tag{2.19}$$

Unlike the case of a non-damped system the substitution by equation 2.18, may not lead to the uncoupling of the equations. However, uncoupling can be obtained by adopting certain formulations of damping. Substituting equation 2.18,

$$\sum_{r=1}^{N} m\phi_r \ddot{q_r}(t) + \sum_{r=1}^{N} c\phi_r \dot{q_r}(t) + \sum_{r=1}^{N} k\phi_r q_r(t) = p(t) \tag{2.20}$$

Pre-multiplying each term by ${\phi_n}^T$, the following equation is obtained:

$$\sum_{r=1}^{N} {\phi_n}^T m\phi_r \ddot{q_r}(t) + \sum_{r=1}^{N} {\phi_n}^T c\phi_r \dot{q_r}(t) + \sum_{r=1}^{N} {\phi_n}^T k\phi_r q_r(t) = {\phi_n}^T p(t) \tag{2.21}$$

Natural modes corresponding to different natural frequencies are shown to be orthogonal and linearly independent. Therefore, most terms in the summation are equal to zero. Terms for which $r = n$ and damping matrix values are not equal to zero.

The previous equation is reduced to:

$$(\phi_n{}^T m\phi_n)\ddot{q}_n(t) + \sum_{r=1}^{N}\left(\phi_n{}^T c\phi_r\right)\dot{q}_r(t) + (\phi_n{}^T k\phi_n)q_n(t) = \phi_n{}^T p(t) \tag{2.22}$$

The Modal Mass Matrix $\mathbf{M}_n$, the Modal Stiffness Matrix $\mathbf{K}_{nr}$, the Damping Matrix $\mathbf{C}_{nr}$, and the Force Vector $P_n(t)$ are defined as:

$$\mathbf{M}_n = \phi_n{}^T m\phi_n \qquad \mathbf{C}_{nr} = \phi_n{}^T c\phi_r \qquad \mathbf{K}_n = \phi_n{}^T k\phi_n \qquad P_n(t) = \phi_n{}^T p(t)$$

Equation 2.22 can be expressed as:

$$\mathbf{M}_n\ddot{q}_n(t) + \sum_{r=1}^{N}\mathbf{C}_{nr}\dot{q}_r(t) + \mathbf{K}_n q_n(t) = P_n(t) \tag{2.23}$$

The previous equation exists for each $n = 1$ to N . The set of N equations can be written in the matrix form as:

$$\mathbf{M}\ddot{q} + \mathbf{C}\dot{q} + \mathbf{K}q = P(t) \tag{2.24}$$

Where M and K are diagonal matrixes as defined above, $P(t)$ is the force vector varying in time, and C is a non-diagonal matrix of coefficients C_{nr}. The N equations in modal coordinates $q_n(t)$ are coupled through the damping matrix.

In the case of non-damped structure c is always equal to zero. In case of classical damping for damped systems, $C_{nr} = 0$ if $n \neq r$. Hence, the N equations are uncoupled and the modal coordinate $q_n(t)$ and the displacement $u_n(t)$ can be calculated independently from the other modes.

2.4. The Dynamic Amplification Factor (DAF)

The study of the Dynamic Amplification Factor (DAF) curve is of great importance in the determination of the dynamic properties of a structure. The DAF is usually plotted in an XY plane with the loading frequency on the x-axis and it represents the multiplication factor of the static displacement to obtain the dynamic one.

From the dynamic equilibrium of a single degree of freedom system. Equation 2.25 can be written.

$$m\ddot{u} + c\dot{u} + ku = p(t) \tag{2.25}$$

Given a harmonic loading, $p(t) = p_0\ sin(\omega t)$, the solution comprehending the complementary and particular solution, corresponding to the transient and the steady state response, is:

$$u(t) = u_c(t) + u_p(t) = u_0(t)sin(\omega_D t - \alpha) + \frac{p_0}{k}\frac{sin(\omega t - \varphi)}{\sqrt{\left(1 - \frac{\omega^2}{{\omega_n}^2}\right)^2 + 4\left(\xi\,\frac{\omega}{\omega_n}\right)^2}} \tag{2.26}$$

Where the first term represents the transient part and the second one the steady response. In equation 2.26 $u_0(t)$ is a transient displacement related term, ω_D is the damped natural frequency of the system, α is the phase lag associated to the transient state, $\frac{p_0}{k}$ is the static deformation due to the load p_0, k is the stiffness of the system, ω is the loading frequency, ω_n is the natural frequency of the system, φ is the phase lag associated to the steady-state and ξ is the damping ratio.

The dynamic amplification factor can be defined as the ratio of the dynamic displacement over the static one. By the steady state response term in equation 2.26, the dynamic amplification factor (DAF) can be written as:

$$R_d = \frac{1}{\sqrt{\left(1 - \frac{\omega^2}{{\omega_n}^2}\right)^2 + 4\left(\xi\,\frac{\omega}{\omega_n}\right)^2}} \tag{2.27}$$

The dynamic displacement can be written as the multiplication of the static response and the Dynamic amplification factor:

$$u_{dyn} = R_d\, u_{st} \tag{2.28}$$

The DAF curve can be plotted as function of the ratio $\frac{\omega}{\omega_n}$, the loading frequency over the natural frequency of the system. When the loading frequency tends to the natural frequency of the structure R_d assumes its maximum value and this condition is defined as Resonance. When the damping is equal to 0 and $\frac{\omega}{\omega_n} = 1$, R_d tends to infinity, the dynamic displacement tends to infinity.

In the next graph the R_d is plotted for several damping ratio. Higher the damping ratio is, lower is the R_d curve.

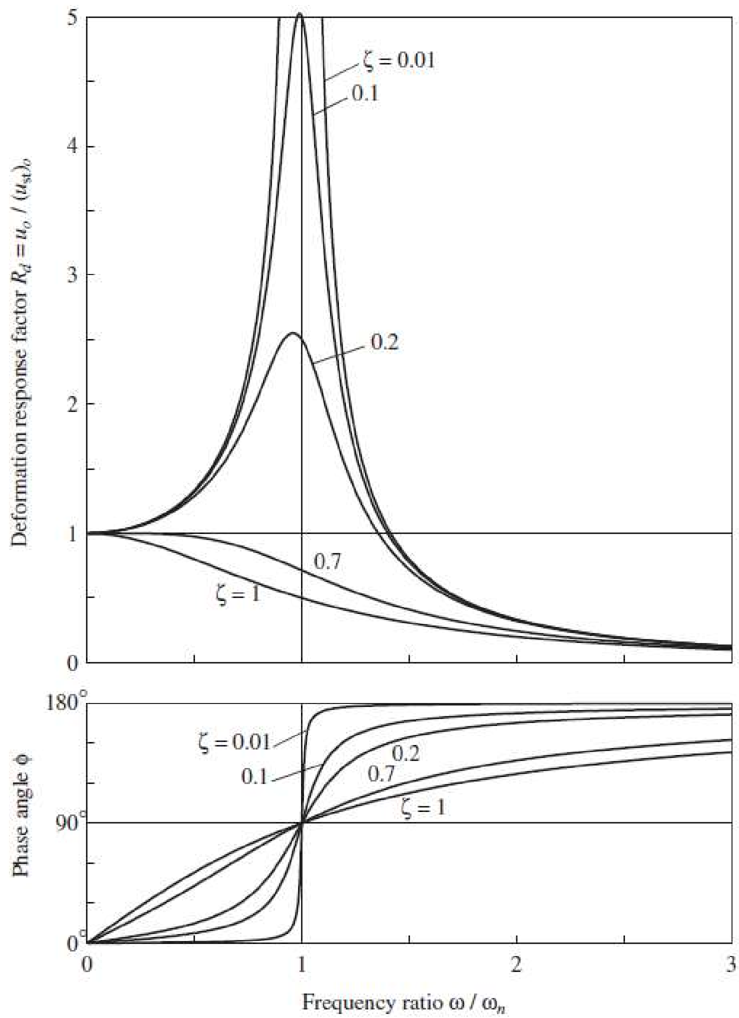

Figure 8. DAF curve and phase lag. Source [35]

The phase angle ϕ defines the delay of the dynamic response of the system when a force is applied to the system. For lightly damped systems when the frequency ratio $\frac{\omega}{\omega_n} \ll 1$ the phase angle ϕ is close to 0˚. Therefore, the displacement is essentially in phase with the applied force. On the other hand, when ratio $\frac{\omega}{\omega_n} \gg 1$, the phase angle ϕ is close to 180˚ and the displacement is essentially of opposite phase relative to the applied force. When $\frac{\omega}{\omega_n} = 1$, ϕ is equal to 90˚ for any damping value, and the displacement attains its peaks when the force assumes the value 0.

2.5. Signal Analysis

Studying Structural Dynamics implies the understanding of how displacement, velocity and acceleration vary in time. The signal analysis permits the investigation of these variations, and it can be performed by two different approaches: time domain analysis and frequency domain analysis.

Data acquisition systems allow direct or indirect recording of displacements. Direct recording implies the registration of the vibration directly on paper which is moving at constant velocity. On the other hand, in the indirect recording, the vibration is transduced in an electric signal which is amplified, recorded, and later plotted. The signal is registered by taking N equally spaced samples and then reconstructed as a continuous curve.

To analyse all signals, three different signal types are defined, and a different theoretical and practical approach is considered for each one. Signals are differentiated into periodic signals, transient signals, and random signals. Periodic signals can be originated by working machines, transient signals by impacts whereas random signals can be originated by the wind. A periodic signal is defined as the repetition in time of a portion defined over a time T and several forces can be defined as nearly periodic. The wave loading on an offshore platform, wind forces induced by vortex shedding on structures or vehicle travelling on a bridge are nearly periodic signals while earthquake ground motion and wind-induced vibration in general are not periodic.

By the definition of Jean Baptiste Fourier, all periodic signals can be described as a sum of pure sine and cosine waves with different amplitude and phase. Therefore, any periodic signal can be written as:

$$x(t) = \frac{a_0}{2} + \sum_{m=1}^{\infty} a_m cos(m\omega t) + b_m sin(m\omega t) \tag{2.29}$$

where a_0, a_m and b_m are defined as integrals in time and ω corresponds to $\frac{2\pi t}{T}$.

Moreover, it is important to define the transient and steady-state response. The former appears when the load is applied to the structure. It depends on the force, damping, stiffness, and initial conditions. On the other hand, the latter corresponds to the remaining vibration when the transient vibration disappears. The steady-state response gives an indication of the natural frequency of vibration of the structure.

2.5.1 Time Domain Analysis

As mentioned in the previous paragraphs, signals can be studied in the time domain. The amplitude of the signal is plotted in an XY plane where time is on the x-axis and displacement, velocity or acceleration is on the y axis. In studying a signal, the transient state and the steady-state response can be detected easily. The estimation of the natural frequencies needs to be performed in the steady-state and it can be difficult in the case of multi-frequency signals.

In the case of a Single Degree of Freedom system (SDOF), there is only one natural frequency of the structure. In the time domain, this frequency can be estimated by the period T of the signal. However, Multi Degree of Freedom systems (MDOF) have as many as the number of coordinates, the system is described by (e.g. the number of degree of freedom). A study in the frequency domain is preferable.

2.5.2 Frequency Domain Analysis

Frequency Domain Analysis is recommended for the study of MDOF structures and permits a better understanding of their dynamic response. As mentioned, any periodic signal can be written as a sum of sine and cosines. The frequency-domain analysis permits understanding the natural frequencies and the amplitude of the single elements in the sum which is the total signal. The spectrum corresponds to the XY graph where frequencies are on the x-axis while the amplitude is on the y-axis.

The spectrum permits the estimation of the several natural frequencies and the level of damping of a system. Exact periodic signals have a discrete frequency spectrum while non-periodic signals have continuous spectra.

An example of the representation of a signal in the time domain and the frequency-domain is shown in figure 9.

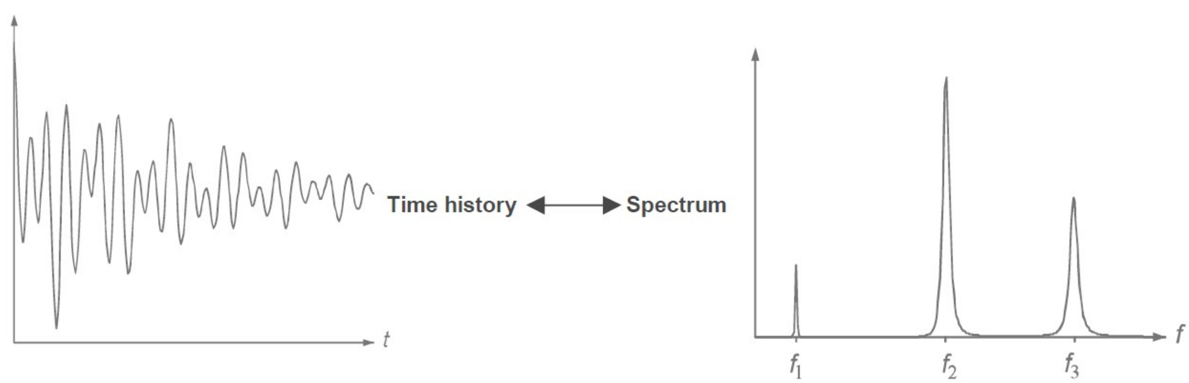

Figure 9: Time-domain and Frequency Domain. Source [35]

To determine the spectrum for a signal sampled with a certain frequency, the Discrete Fourier Transform (DFT) is used. However, a faster and smarter algorithm to calculate DFT is known as the Fast Fourier Transform (FFT) is usually implemented.

As the real signal is sampled in some points and then reconstructed, there is no exact representation in either domain. Therefore, the sampling frequency is a decisive factor in the signal analysis and needs to be chosen accordingly to the Nyquist theorem. Nyquist theorem specifies that the highest reproducible frequency in a digital system is equal to or less than one half of the sampling frequency. Consequently, a sampling frequency of 1200 Hz permits the detection of frequencies up to 600 Hz. In the analysis of civil structures, the main natural frequencies are usually below 10 Hz. Nevertheless, higher sampling frequencies lead to a better reconstruction of the signal, which is composed of several higher frequencies.

When the sampling theorem has not been respected the phenomenon of Aliasing occurs. The signal distortion, given by the low sampling frequency, can be solved using the application of filters. Bessel, Butterworth, Chebishev or the Elliptic filters are usually applied. However, assuming the correct sampling frequency is the best way to avoid aliasing.

Another issue in FFT processing is Leakage. Leakage is caused by truncation of a time-domain waveform applied in the Fast Fourier Transform (FFT)and can be solved by applying Window Function like the Hann and the Hamming ones.

2.6. Damping evaluation

The dynamic response of a structure is characterized by mass, stiffness, and damping. While mass and stiffness can be analysed or taken from the geometry and material properties, damping needs to be estimated through experiments. There are two main kinds of damping: Viscous damping and Hysteretic damping. The former depends on the frequency, and it is easily describable. The latter assumes nonlinear relations between stress and deformation. Damping is usually modelled as Viscous Damping.

Damping is generally expressed in percentage of the critical damping or damping ratio.

$$\zeta = \frac{c}{2\sqrt{k\,m}} \tag{2.30}$$

Where ζ is the damping ratio, c is the damping value, k is the stiffness of the system and m is the mass. The downer term corresponds to the critical damping.

Eurocode specifies a lower limit in the percentage of the critical damping to be used in the design of railways and other structures. The lower limit for a steel bridge of a span bigger than 20 meters is 0.5 %.

Damping is defined as the influence which reduces or prevents the oscillation within or upon an oscillatory system through dissipation of energy.

All structures exhibit damping, even though civil structures are usually lightly damped. The damping in bridges can have multiple sources as the energy dissipation through deformation from bending and shear effects, friction at supports, opening and closing of cracks, sliding and closing at the crack interface, aerodynamic damping, vehicle and pedestrian damping. Pedestrians' influence on damping is later described in the definition of Human Structure Interaction. Moreover, the factors which influence the damping in a bridge are the frequency and the mode of vibration, the amplitude of vibration cracked or uncracked concrete, ballast condition and temperature.

To estimate the damping ratio of a structure several methods can be implemented. The logarithmic method and the Half Power Bandwidth method are two commonly used methods. Another example of a more detailed estimation tool is the complex explanation method.

2.6.1 Logarithmic Decrement Method

The logarithmic decrement technique permits the estimation of the damping of a structure from a free vibration test and analysing the data in the time domain. It is a simple method that requires low-density instrumentation on the structure.

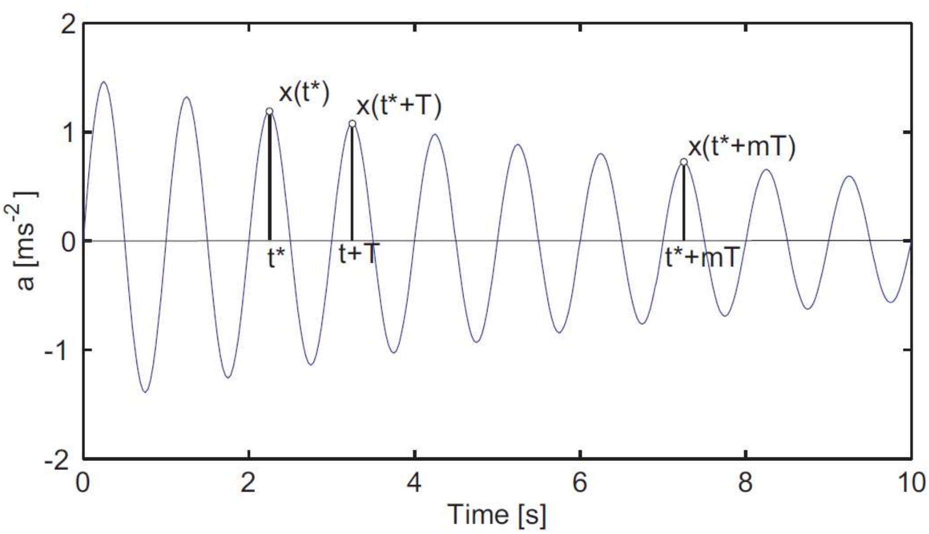

Figure 10: Logarithmic decrement Method. Source [35]

The free vibration part of a signal is analysed and usually a filter on the frequency of interest is applied. Two or more consecutive peaks of the signal are taken into consideration and the difference in the amplitude of the peaks give indication on the damping. The logarithmic decrement is defined as:

$$\delta = ln\left(\frac{x(t')}{x(t'+T)}\right) \tag{2.31}$$

Where $x(t')$ is the amplitude of the peak at time t', $x(t'+T)$ is the amplitude of the consecutive peak at time $t'+T$. A better result can be obtained considering the logarithmic decrement between two non-consecutive peaks, taking into consideration the number of peaks in the middle dividing the logarithmic parenthesis by it plus one.

The damping ratio can be found by explicating the following equation.

$$\delta = 2\pi\frac{\zeta}{\sqrt{1-\zeta^2}} \tag{2.32}$$

For small structural damping $\zeta = \frac{\delta}{2\pi}$

2.6.2 Half Power Bandwidth Method

The Half Power Bandwidth Method determines the amount of damping for each mode of a structure by the transfer function plot. Therefore, this technique is defined on the frequency response curve for the Dynamic Amplification Factor. As mentioned previously, in correspondence to the natural frequency the DAF assumes its largest value. When the forcing frequency matches the natural frequency of the structure the dynamic response is amplified by the peak value of the DAF curve.

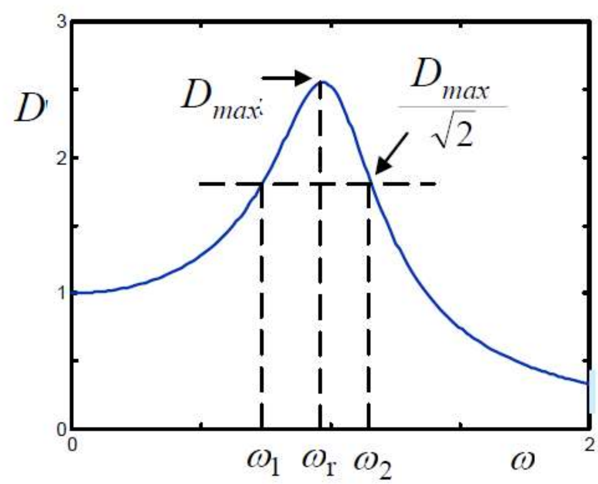

Figure 11: Half-Power Bandwidth Method. Source [35]

The Half Power Bandwidth method implies the detection of two forcing frequencies ω_a and ω_b, where correspondent dynamic amplification factors equal to $1/\sqrt{2}$ of the resonant amplitude.

For small damping ratios, e.g. $\zeta \leq 0.1$, the following equation is valid.

$$\frac{\omega_b - \omega_a}{\omega_n} = 2\zeta \tag{2.33}$$

Therefore, the damping ratio can be found as:

$$\zeta = \frac{\omega_b - \omega_a}{2\omega_n} \tag{2.34}$$

$$\zeta = \frac{f_b - f_a}{2f_n} \tag{2.35}$$

2.7. Time-stepping Methods

Analytical solution of the equation of motion for a single degree of freedom system is not possible in most cases. Indeed, if the applied force $p(t)$ varies arbitrarily or if the system is not linear, it is not possible to derive an equation for the displacement $u(t)$.

The numerical evaluation of the dynamic response can be performed through the time-stepping method for the integration of differential equations. The problem can be defined as:

$$m\ddot{u} + c\dot{u} + ku = p(t) \tag{2.36}$$

given the initial conditions $u_0 = u(0)$ and $\dot{u}_0 = \dot{u}(0)$

Time-stepping methods implement the discretization in time of the problem and the satisfaction of the equation of motion at a finite number of points. This procedure can be performed efficiently on a computer.

While the continuous formulation can be found in equation 2.36, the discrete formulation of the equation of motion can be written as:

$$m\ddot{u}_i + c\dot{u}_i + ku_i = p_i \tag{2.37}$$

Time is discretised in equally distributed points spaced so that:

$$t_{i+1} = t_i + \Delta t \tag{2.38}$$

Therefore, equilibrium is satisfied on the discretised points and not between them. In between assumptions and simplifications need to be made introducing error. Consequently, the dimension Δt between the points assumes importance and needs to be carefully chosen. The smaller it is, the numerical evaluation is more precise but more time consuming. For a Δt tending to zero, convergence should be obtained by each method.

There are two different types of methods: the explicit and the implicit ones. The explicit method imposes the equation of motion at the time $t = t_i$ and the initial conditions to find u_{i+1}. On the other hand, the implicit method imposes the equation of motion at the time $t = t_{i+1}$ and the initial conditions to find u_{i+1}, e.g. at the time the displacement is looked for. The Central Difference method is explicit whereas Newmark's methods are implicit.

Newmark's implicit Method imposes the equation of motion at the time $i + 1$ while looking for u_{i+1}. Between any given two points t_i and t_{i+1}, the acceleration is assumed as a value in between the acceleration at t_i and the one at t_{i+1}.

Newmark developed a set of time- stepping methods based on the equations:

$$\dot{u}_{i+1} = \dot{u}_i + [(1-\gamma)\Delta t]\ddot{u}_i + (\gamma\Delta t)\ddot{u}_{i+1} \tag{2.39}$$

$$u_{i+1} = u_i + \Delta t\dot{u}_i + [(0.5-\beta)(\Delta t)^2]\ddot{u}_i + [\beta(\Delta t)^2]\ddot{u}_{i+1} \tag{2.40}$$

$$m\ddot{u}_{i+1} + c\dot{u}_{i+1} + ku_{i+1} = p_{i+1} \tag{2.41}$$

The parameters β and γ define the variation of acceleration between the points over the time steps and they characterize the stability and accuracy of the system. The Average Acceleration method assumes $\gamma = \frac{1}{4}$ and $\beta = \frac{1}{4}$ while the Linear Acceleration method assumes $\gamma = \frac{1}{4}$ and $\beta = \frac{1}{6}$. Both Newmark's methods are stable and accurate. The two equations 2.39 and 2.40 and the equation of motion 2.41 applied at the end of each time step provide the basis to calculate $u_{i+1}, \dot{u}_{i+1}$ and $\ddot{u}_{i+1}$ at the time $i + 1$, from the displacement velocity and acceleration correspondent at time i.

Unlike the central difference method, a wrong definition on the time step results in incorrect but reasonable results. The choice on the time step needs to made taking into consideration this issue.

2.8. Human Structure Interaction (HSI)

As discussed in the literature review, section 1.5.2, several authors concentrated their work on studying Human Structure Interaction. However, Caprani’ s formulation of the problem and the assumption on the pedestrians as evenly distributed SMD, was the most suitable to carry out the study on the Human Structure Interaction in a more practical way. The new journal paper by Colmenares et al. [37] which will be published later in 2021, describes the formulation of HSI and verifies the formulation through the experiments of this work of thesis.

2.8.1 Caprani’s Formulation

As mentioned in the literature review, section 1.5.2, Caprani and Ahmadi (2016) [10] model the walking pedestrian vertical forces in three different ways: a moving force (MF), a moving mass (MM) and a moving spring-mass-damper (SMD). Each model is firstly developed for the single pedestrian and later for the crowd of pedestrians.

For the scope of the thesis, the spring-mass-damper model is adopted due to its major accuracy in the prediction of the dynamic response. In Caprani and Ahmadi’s paper, the arbitrary beam structure is modelled using either a formulation in modal coordinates or finite elements. The former is preferred, and the formulation of the problem is reported below.

The general equation of motion is written as:

$$\mathbf{M}\,\ddot{q} + \mathbf{C}\,\dot{q} + \mathbf{K}\,q = Q \tag{2.42}$$

In the case of a human spring mass, the equation can be expressed as:

$$m_p\ddot{y} + c_p(\dot{y} - \dot{w}) + k_p(y - w) = 0 \tag{2.43}$$

Where y, $\dot{y}$ and $\ddot{y}$ are the displacement, velocity, and acceleration of the human mass from the equilibrium position, w and $\dot{w}$ are the displacement and velocity of the bridge at the point the pedestrian is, m_p, k_p and c_p are the mass, stiffness and damping of the single pedestrian.

The interaction force between the beam and the mass is:

$$f(x,t) = \left[G(t) - m_p\ddot{y}\right]\delta(x - vt) \tag{2.44}$$

where $G(t)$ is the general force function and $\delta(x - vt)$ is the Dirac delta function which is required to locate the load on the beam.

The jth modal equation for the beam can be written as:

$$\ddot{q}_j + 2\xi_j\omega_j\dot{q}_j + \omega_j{}^2 q_j + m_p\ddot{y}\phi_j(vt) = G(t)\phi_j(vt) \qquad (2.45)$$

Where $\ddot{q}_j$, $\dot{q}_j$ and q_j are the modal coordinates, ξ_j is the damping ratio, ω_j is the natural frequency, $\phi_j(vt)$ is the mode-shape of the jth mode. $G(t)$ is the general force function and m_p is the mass of the single pedestrian.

For the human mass, using the modal expansion for the beam deflection, equation 2.43 becomes:

$$m_p\ddot{y} + c_p\dot{y} + k_p y - c_p\sum_{j=1}^{N}\dot{q}_j\phi_j(vt) - k_p\sum_{j=1}^{N}q_j\phi_j(vt) = 0 \qquad (2.46)$$

Caprani and Ahmadi, write equations 2.45 and 2.46 in $N + 1$ coupled equation in mass normalized matrix format as follows:

$$\mathbf{M} = \begin{bmatrix} I_{NxN} & M_{12} \\ 0_{1xN} & m_p \end{bmatrix} \qquad \mathbf{C} = \begin{bmatrix} C_{11} & 0_{1xN} \\ C_{21} & c_p \end{bmatrix} \qquad \mathbf{K} = \begin{bmatrix} K_{11} & 0_{1xN} \\ K_{21} & k_p \end{bmatrix} \qquad Q = \begin{Bmatrix} Q_b \\ 0 \end{Bmatrix}$$

Where the above sub-matrixes are:

$$\mathbf{M}_{12} = m_p\phi(vt) \qquad \mathbf{C}_{11} = diag[2\xi_j\omega_j] \qquad \mathbf{C}_{21} = -c_p\phi^T(vt)$$

$$\mathbf{K}_{11} = diag[\omega_j{}^2] \qquad \mathbf{K}_{21} = -k_p\phi^T(vt) \qquad Q_b = G(t)\phi_j(vt)$$

The formulation which has been reported is referred to a single pedestrian and needs to be rewritten in the pedestrian crowd formulation as shown in paper [10].

$$\mathbf{M} = \begin{bmatrix} I_{NxN} & \mathbf{M}_{12} \\ 0_{nxN} & m_p \end{bmatrix} \qquad \mathbf{C} = \begin{bmatrix} \mathbf{C}_{11} & 0_{Nxn} \\ \mathbf{C}_{21} & c_p \end{bmatrix}$$

$$\mathbf{K} = \begin{bmatrix} \mathbf{K}_{11} & 0_{Nxn} \\ \mathbf{K}_{21} & k_p \end{bmatrix} \qquad Q = \begin{Bmatrix} Q_b \\ 0_{nx1} \end{Bmatrix}$$

Some sub-matrixes change in order to include the multi pedestrians' system.

$$M_{12}[1, \ldots., N; i] = m_{p,i}\phi(v_i t) \qquad m_p = diag[m_{p,i}]$$

$$C_{12}[1, \ldots., N; i] = -c_{p,i}\phi^T(v_i t) \qquad K_{12}[1, \ldots., N; i] = -k_{p,i}\phi^T(v_i t)$$

As defined, the matrixes can be used in the equation of motion in order to include Human Structure Interaction in the evaluation of the dynamic response.

2.8.2 Multidimensional Dynamic Amplification Factors

In parallel to this work of thesis, a new journal paper on the bridge dynamics by Colmenares et al. is in progress and will be submitted in 2021. The formulation which been implemented in this thesis is taken from Colmenares's work. For this reason, the formulation on the HSI in the evaluation of the dynamic response of a structure is not entirely reported in this section.

In figure 12, a schematization of the system which has been modelled as described in Caprani formulation is presented. The work on the evaluation of the dynamic response considering Human structure Interaction is based on it.

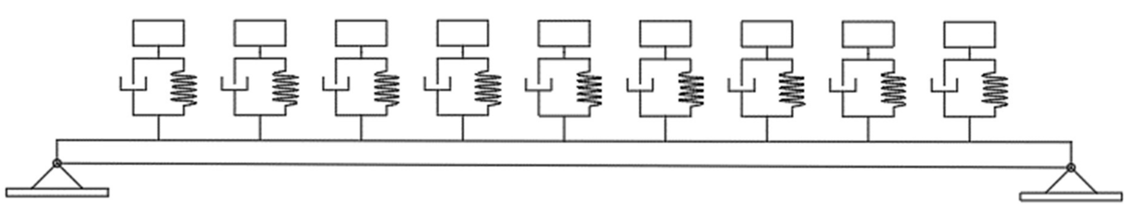

Figure 12: Caprani schematization of HSI

The proposal aims to formulate a more efficient and computer-friendly way to compute the dynamic response of a MDOF system without the time stepping methods.

From the equation of motion, through the Frequency response function, a new technique is developed and compared to Newmark's linear method. The formulation of the mass matrix M, stiffness matrix K, damping matrix C and load vector F are taken from Caprani continuous method with SMDs.

The impedance matrix can be written as:

$$Z = -\omega^2 * M + i\omega C + K \tag{2.47}$$

The Dynamic amplification factor which takes HSI into consideration and permits to calculate the maximum dynamic response of steady state from the static displacement is found as:

$$X_{dyn} = DAF_{HSI} X_{stat} \tag{2.48}$$

Where DAF_{HSI} is:

$$DAF_{HSI} = K * (Z(\omega))^{-1} \tag{2.49}$$

2.9. Current Guidelines

The following section focuses on the current guidelines for the estimation of the vibration response to multi-person traffic. The assumptions and the limitations for the application of each model are stated for each one.

Over the years, the vibration response due to multi-person traffic has been taken as a multiple of the response to a single person excitation. A factor that considers the number of pedestrians crossing the bridge at the same time is considered and used as a multiplication factor. This approach was based on the work of Matsumoto et al. (1978) [16] and it is still used because of its simplicity.

The Eurocode 5, the ISO 10137 Standard (ISO, 2007), the Sétra and the UK National Annex to Eurocode 1 analyse the issue from a time-domain perspective. The multi-person traffic vibration response is analysed from a frequency domain analysis by Brownjohn et al. (2004b), Butz.

2.9.1 Eurocode 5

Eurocode 5 is a guideline concerning the design of timber bridges. Nonetheless, the response model which is defined in the code is not timber specific and can be used to design and check bridges of any other material.

The calculation procedure involves the simplification of the bridge to analyse it into a simply supported bridge. The amplitude of the acceleration response under the load from N pedestrians is given as:

$$a_N = 0.23 a_1 N k \tag{2.50}$$

where a_1 is the amplitude of the steady-state response from a single pedestrian, N is the number of pedestrians and k is a reducing factor that considers the number of synchronised people if the natural frequencies of the bridge are far from the average pacing rate of the pedestrians. Each pedestrian is modelled as a stationary harmonic force matching the natural frequency of the bridge through the equation:

$$a_1 = \begin{cases} \dfrac{200}{M\zeta} \; for \; f_n \leq 2.5 \; Hz \\ \dfrac{100}{M\zeta} \; for \;\; 2.5 \; Hz \leq f_n \leq 5 \; Hz \end{cases} \tag{2.51}$$

Where M is the total mass of the bridge, ζ is the damping ratio of the mode shape solicited by walking, and f_n is the natural frequency of the bridge.

To model the first harmonic constant pedestrian force amplitude of 200 N is considered, to model the second, the constant force is taken as 100 N. The values of these forces are obtained assuming a single pedestrian, whose weight is 700 N, and considering the 40% of the total weight for the first harmonic and the 20% for the second harmonic.

A reduction factor of 0.7 is later applied as the steady-state cannot be achieved as the pedestrians spend a limited time on the bridge.

The above-mentioned method is only applicable to beam-like structures and does not take into account that the force amplitude is a function of the pacing rate of the pedestrians while walking. Moreover, the multiplication factor is linearly dependent on the number of pedestrians.

2.9.2 ISO 10137 standard (ISO, 2007)

The ISO 10137 standard (ISO, 2007) deals with the serviceability of walkways against vibrations. In this case, the vertical force induced by one single pedestrian is time-dependent and can be written as:

$$F_1(t) = W\left(1 + \sum_{n=1}^{k} \alpha_n sin\big(2\pi n f_p t + \phi_n\big)\right) \tag{2.52}$$

In the equation W is the weight of the pedestrian, α_n is the dynamic loading factor which indicates the proportion of the weight to be considered in the walking force harmonic definition, ϕ_n is the phase angle for the nth load harmonic and f_p is the pacing frequency.

The dynamic loading factor (DLF) is defined independently from the pacing rate f_p for the second harmonic onwards ($\alpha 2 = 0.1, \alpha 3 = \alpha 4 = \alpha 5 = 0.06$), while the first one is defined as $\alpha 1 = 0.37(fp - 1)$.

For a group of N not synchronized pedestrians the total effective pedestrian load is obtained by multiplication of the $F_1(t)$, found in equation 2.52 by $\sqrt{N}$. The guideline does not specify the pacing frequency f_p, although it was presumably meant to match the vibration mode of interest. Moreover, the ISO 10137 is not explicitly specified if the force model is stationary or moving across the bridge.

Differently from Eurocode 5, ISO 10137 defines the force model rather than the dynamic response. The assumption on the structural layout assumed like a beam structure, is no longer made and the modal properties can be used in the calculation for the estimation of the dynamic response.

However, the fact that the loading model for multi-person traffic is defined as $\sqrt{N}$ times the response of a single pedestrian, e.g. assuming that all pedestrians walk at the same frequency f_p with a random angle phase ϕ_n, often leads to an overestimation of the actual total response.

2.9.3 Sétra

The design guidelines known as Sétra were presented by the French road authorities in 2006. They are currently the most used guidelines for the verification of the comfort criteria.

In the guidelines, two different load models are presented: one for the sparse and dense crowds and another one for very dense crowds. The former crowd model is characterized by a pedestrian density of 0.5-0.8 pedestrians/m^2 and is more relevant for normal traffic conditions. A very dense crowd model is used in the case of urban pedestrian bridges subjected to very high traffic. A pedestrian density of 1 pedestrian/m^2 is taken into account in the crowd model.

The model assumes that the pacing rate of the walking pedestrians is distributed as a Gaussian curve. The dynamic load per unit area is defined as:

$$f_N(t) = 10.8\frac{F_0}{A}\sqrt{N\zeta}\psi cos(2\pi\, f_n\, t) \qquad (2.53)$$

Where F_0 is the load amplitude of a single pedestrian, equal to 280 N for the first and 70 N for the second harmonic, A is the area of the bridge deck, N is the number of pedestrians forming the crowd, ζ is the bridge damping ratio, ψ is a reducing factor for the loads having frequencies away from the average pacing rate, and f_n is the natural frequency.

For each vibration mode having a frequency below 5 Hz, a load case should be created according to equation 2.53 and be applied on the deck at the corresponding modal frequency. The direction of the load needs to be analysed to simulate the worst-case scenario. For the first vertical vibration mode, the load can be assumed to be acting all downwards but for the second vertical vibration mode, the same configuration of the loads would give a total acting force equal to zero. Therefore, the direction of the load needs to be studied in order to maximize the total acting force on the bridge.

The steady-state response to the load applied is considered as the estimation of the maximum amplitude of the vibration response under a crowd of people, with the 95% probability not to be exceeded.

The model definition considered 500 simulations for each configuration of interest and the peak response with 5% probability of exceedance was considered. The modal mass of the bridge is increased because of the presence of the pedestrians while the structural damping is assumed to remain constant.

The load model as described considers one harmonic at a time, neglecting the case in which more modes are excited at the same time. However, this procedure is common to many guidelines.

2.9.4 UK National Annex to Eurocode 1

UK National Annex to Eurocode 1 defines loading models given by people walking and jogging and for crowds. The crowd model which is considered is 0.4 pedestrians/m^2 or above in line with the values specified by Sétra. Moreover, the load is defined per unit area and the loading sign matches the vibration mode.

The load is defined as:

$$f_N(t) = 1.8\frac{F_0}{A}k\sqrt{\frac{\gamma N}{\lambda}}sin(2\pi f_n t) \qquad (2.54)$$

where F_0 is the reference load equal to 280 N, A is the area of the deck, factor k which takes into account the excitation potential of the force and the probability that the pedestrians are walking at the given resonant frequency, factor γ considers the limited correlation among the people in the crowd and in case of continuous stream assumption is equal to $\gamma = 7.40\zeta$, λ is the factor which considers the position of each pedestrian with regards to the vibration mode-shape, N is the number of pedestrians and f_n is the natural frequency of the mode shape it is considered.

In the case of sinusoidal mode $\lambda = 0.64$, and the equation 2.54 can be written as equation 2.53 from Sétra code, with the multiplying constant equal to 6.1 instead of 10.8. The magnitude of the load model in the two different guidelines differs of about 56% and the reason lies in the choice of the percentile value.

2.9.5 And the other in frequency domain

Most models are based on the study of the phenomena in the time domain perspective and study the crowd effects as a single pedestrian walking at a single natural frequency multiplied by several appropriate factors.

Differently, Brownjohn, Butz, Georgakis and Ingòlfsson analysed the multi-person traffic effects in the frequency domain. Brownjohn et al. method is based on the study of considering a Gaussian distribution of pacing rates for the pedestrians. Butz took into consideration even the pedestrian mass, the forcing amplitude and the pedestrian arrival times in a stream of pedestrians. The response spectrum method, by Georgakis and Ingòlfsson, was inspired by earthquake engineering and is a simpler way to deal with human-induced vibrations.

3. Methodology

The following section summarizes the methodology which has been followed to pursue the aim of the thesis. Initially, the HSI formulation is implemented on Matlab, a parametric analysis is run to verify the consistency of the code, then an error surface is drawn. Afterwards, a case study is taken, and two experiments are performed. The first one aims at the determination of the dynamic properties of the bridge while the second aims to verify the influence of the HSI on the dynamic properties. Moreover, a FEM model of the bridge is made to extract mode-shapes and frequencies to be compared to the experimental ones.

3.1. HSI formulation and coding

As mentioned in section 2.8.2, the MDOF system is modelled as an SDOF beam on which N spring-mass-dampers (SMD) are positioned in fixed positions. This way of modelling assumes the condition of a continuous flow of pedestrians which may not be correct when low conditions of traffic verify.

The definition of the single quantities is considered in detail as they significantly affect the final result. Initially, the HSI model is run for values found in literature or values considered as suitable for a raw analysis. The inputs are differentiated into two main categories: bridge and pedestrian properties.

The length, the linear mass, the damping ratio, one natural frequency and the associated mode-shape are the inputs for the bridge, which is defined as the primary system. The number of pedestrians, the mass of a single pedestrian, the damping ratio of a pedestrian and the pedestrian stiffness for the secondary system which is composed only by the evenly distributed pedestrians. Another categorization needs to be done as some data can be obtained by drawings or by literature reviews, and some other data is initially set to reasonable values but need to be changed according to the analysed case through an experimental campaign.

Known data is the length of the bridge set to 97 meters, the linear mass of the bridge set to 1031 kilograms per meter (calculated as the total mass divided by the total length), the mass of a pedestrian set to 70 kg by literature reviews [10], pedestrian damping set to 0.35 and pedestrian stiffness set to 23500 N/m [10]. On the other hand, initially, several assumptions need to be made. The mode-shape is assumed to be as: $\phi = \sin\left(\frac{\pi x}{L}\right)$, , the damping ratio of bridge equal to 0.03, the natural frequency of the bridge initially set as 1.9 Hz.

The number of evenly distributed pedestrians is modulated according to the case in analysis, and it is significant in the evaluation of the dynamic response. The variation of this number changes the mass ratio, and consequently, the Dynamic Amplification Factor curve and the frequency of resonance. The curve is lower and positioned more towards the left when a higher number of pedestrians is considered.

The mass ratio refers to the modal mass of the bridge over the modal mass of the pedestrians. The modal masses are obtained by the equations:

$$M_{bridge} = \int_0^L \phi(x)^2 \gamma \, dx \tag{3.1}$$

$$M_{pedestrians} = \sum_{j=1}^{N} \phi(x_j)^2 M_p \tag{3.2}$$

Where $\phi(x)$ is the mode-shape in the continuous form, $\phi(x_j)$ is the mode-shape in the discretized points where the pedestrians are positioned, γ is the linear mass of the bridge and M_p is the mass of the single pedestrian.

The mass matrix M, the stiffness matrix K and the damping matrix C are calculated following Caprani formulation. Their dimension depends strictly on the number of pedestrians which are considered, e.g. their dimension is $((N+1) \bullet (N+1))$ where N is the number of pedestrians.

The dynamic response can be obtained through Newmark's methods by the definition of a forcing vector and by the M, K and C matrixes. As explained in section 2.7.2, the choice on the time step can significantly affect the result and it is initially set to 0.0001 seconds. Afterwards, in order to make the process more efficient and less time consuming, it was set to 0.001 seconds. The force imposed by a single pedestrian is defined as:

$$p_d = g \; \alpha \; G_0 sin(\omega_{stp} t) \tag{3.3}$$

Where g is the standard acceleration due to gravity equal to $9.81 \; m/s^2$, α is the walking load factor which is equal to $\alpha = 0.4$, G_0 is the mass of a pedestrian in kg and is multiplied by 10 to have the corresponding weight in Newtons, ω_{stp} is the circular loading frequency even defined as the step frequency of the pedestrian set equal to $\omega_{stp} = 2\pi f_{stp} = 2 \; x \; 3.14 \; x \; 1.9 \; Hz = 11{,}93 \; rad/s$, and t is the time vector.

Therefore, the time vector is defined as a harmonic applied from each pedestrian in his own position on the bridge. The force vector F is defined as having in its first position the sum of the N forces modulated by the mode-shape, and then all zeros. Indeed, the force is applied on the bridge (first mode) by the pedestrians and not to the pedestrians (mode $[2\!:(N+1)]$).

Newmark's constant method is used to estimate the dynamic response of the bridge. The maximum displacement in the steady-state is stored and it will be later compared to the one obtained by the multiplication of the DAF and the static response.

The static displacement is obtained in two equivalent ways. The first method requires the definition of the inverse of matrix K and the static force as a vector. The first position of the force vector is set equal to the sum of the maximum dynamic force given by the N pedestrian modulated by the mode shape evaluated in the position of the pedestrians. The static displacement is obtained considering the first element in the vector obtained by the multiplication of the inverse of the K matrix and the force vector. On the other hand, the second method defines the static force as the sum of the static part of the dynamic response modulated in each position of the N pedestrians. The static displacement is obtained by the static force divided by the element (1,1) in the K matrix. The error between the two methods is equal to zero.

The dynamic amplification factor by the $\mathbf{M}, \mathbf{K}$ and $\mathbf{C}$ matrixes is calculated through the Frequency Response Function (FRF). The formulation that follows is extracted from Colmenares et al. (2021) [37] and implies the calculation of the impedance matrix:

$$\mathbf{Z} = -\omega^2 * \mathbf{M} + i\omega\mathbf{C} + \mathbf{K} \tag{3.4}$$

The Frequency response Function is calculated by the equation:

$$\boldsymbol{FRF_{HSI}} = \mathbf{Z}(\omega)^{-1} \tag{3.5}$$

And the Dynamic amplification Factor as:

$$\mathbf{DAF_{HSI}} = \|\mathbf{K} \bullet \mathbf{FRF_{HSI}}\| \tag{3.6}$$

Consequently, the maximum dynamic response is obtained by:

$$X_{dyn} = \boldsymbol{DAF_{HSI}}\left(f_{stp}\right) \bullet X_{stat} \tag{3.7}$$

The dynamic response is calculated by the multiplication of the DAF, evaluated at the loading frequency, and the statical displacement.

In conclusion, the error between the dynamic maximum displacement obtained by Newmark constant method and the one by the proposal, is calculated as:

$$error\,\% = \frac{X_{Dyn\,Newmark} - X_{Dyn\,DAF}}{X_{Dyn\,Newmark}} \bullet 100 \tag{3.8}$$

The evaluation of the natural frequencies, mode-shapes and damping is needed as inputs in the HSI model and are obtained by the experimental campaign and a Finite Element Model.

3.2. Parametric analysis and error surface

As described in the previous section, several parameters need to be chosen and can be adapted to the case in analysis. A parametric analysis is conducted to analyse the variation of the Dynamic Amplification factor and to better understand how the dynamic response varies.

The factors which are taken into consideration in the parametric analysis are detailed below.

$$\omega_{bridge} \qquad \omega_{loading} \qquad \omega_{pedestrian} \qquad \xi_{bridge} \qquad \xi_{pedestrian} \qquad N_{pedestrians}$$

Where ω_{bridge} is the natural cyclic frequency of the bridge, $\omega_{loading}$ is the loading frequency or step frequency, $\omega_{pedestrians}$ is the natural frequency of vibration of the pedestrians, ξ_{bridge} is the damping ratio of the bridge, $\xi_{pedestrian}$ is the damping ratio of the pedestrians, $N_{pedestrians}$ is the number of pedestrians on which depends the total mass of the pedestrians taken into consideration.

However, single dimensional parameters are more difficult to handle, and relevant conditions may be hard to detect. Therefore, to perform the parametric analysis, a set of 6 non-dimensional parameters are made to vary. The 6 non-dimensional parameters are detailed below.

$$\Pi_1 = \frac{\omega_{loading}}{\omega_{bridge}} \qquad \Pi_2 = \frac{m_{pedestrians}}{m_{bridge}} \qquad \Pi_3 = \frac{\omega_{pedestrians}}{\omega_{bridge}} \qquad \Pi_4 = \frac{\omega_{loading}}{\omega_{pedestrian}}$$

$$\Pi_5 = \xi_{pedestrian} \qquad \Pi_6 = \xi_{bridge}$$

Where Π_1 is a ratio which indicates the condition of resonance ($\Pi_1 = 1$), Π_2 is the modal mass ratio and indicates the entity of the problem, Π_3 represents the tuning of the secondary system with respect to the primary one and indicates if the energy, which causes vibration, is deviated to the pedestrians ($\Pi_3 = 1$), Π_4 is a ratio which indicates the condition of resonance for the pedestrians ($\Pi_4 = \frac{\Pi_1}{\Pi_3} = 1$), Π_5 and Π_6 are the damping ratios of the pedestrian and of the bridge which are already non-dimensional.

In the parametric analysis, which is conducted, the modal mass ratio Π_2 is made to vary between 0.02 and 0.10 in 0.02 steps, the frequency of the pedestrians is made to vary between 1 and 2.9 Hz with 0.1 Hz steps, the frequency of the loading is made to vary between 1 and 5 Hz with 0.01 Hz steps, the frequency of the bridge is assumed constant as well as the damping of the bridge and of the pedestrian. The analysis is conducted in only three dimensions to appreciate the results in a 3D graph. The frequency of the loading and the frequency of the pedestrians are shown as ratios on the frequency of the bridge, Π_1 and Π_3.

3.3. The case study, the Folke Bernadotte Bridge

Folke Bernadotte's Bridge is an important walking and cycling connection across the Djurgårdsbrunn Bay, in the town centre of Stockholm, Sweden. The pedestrian bridge, which was opened on September 19th, 2019, connects the southern and the northern part of Djurgården.

Figure 13: Folke Bernadotte Bridge

The structure was committed by the Kungliga Djurgården administration to Rundquist Arkitekter, one of the most famous architectural studios based in Stockholm, and the designer was Ramboll, a Danish technical consulting company which works worldwide.

The construction of the structure began in June 2018 starting from the foundations on both sides and the central part was installed in 2019. Supports and abutments are in concrete, and they are hidden under the ground. The total span of 97 meters is covered by a single arch bridge made of stainless steel that provides slenderness and lightness in its expression. The beam structure is designed as a truss, and all elements are welded together.

The structure system is composed of three main running pipes, 2 at the deck surface of cross-section CHS355.6X12.5, and one on the lower level of cross-section CHS298.5X25 within a CHS355.6X25. These three elements are connected by inclines members (cross-section CHS193.7X5.6) which form the truss system. The wooden deck is supported by a set of transversal rectangular elements and longitudinal trapezoid elements. The rectangular elements are welded to the lateral pipes while the longitudinal ones are connected to the transversal elements, only for shear. In order to provide major stiffness, additional diagonal elements crossing the transversal span are positioned.

Figure 14: Folke Bernadotte Bridge Detail

In accordance with the maritime traffic requirements, the bridge provides a 3 meters sail-free height. Nevertheless, its slender, modern, and effective profile suits the landscape and the historical context.

The choice of case study was made accordingly with other graduates working on a different thesis. The Folke Bernadotte bridge is considered suitable for the analysis as it experiences a significant dynamic response for loading with the frequency in the range of walking and jogging pedestrians.

3.4. Experimental Campaign

The verification of the Human Structure Interaction model on the prediction of the dynamic response of a structure needs to be implemented through an experimental campaign. The shift of the Dynamic Amplification factor curve and the decrease of its peak due to the presence of pedestrians is registered performing two hammer tests while on the bridge there are 2 or 35 people.

Two experiments were performed to verify the model on HSI. The first experiment was conducted in collaboration with other two graduates who are writing a thesis on a different topic but needed to experiment on the same bridge.

From the first experiment, the natural frequencies, damping and the mode-shapes of the bridge can be extracted. Moreover, the time history of the dynamic response of the bridge is reconstructed. In the second experiment the dynamic properties are re-estimated and compared with the ones obtained by the previous experiment, and the HSI model is verified. The shift and the lowering of the DAF curve due to the presence of pedestrians is registered and compared with the theoretical ones obtained by the HSI model.

3.4.1 First experiment

The first experiment of the experimental campaign permitted the estimation of the natural frequencies, the evaluation of the damping and the detection of the mode-shapes of vibrations.

The experiment was conducted on March 23rd 2021. The environmental conditions were favourable, with a temperature of 19 degrees and light wind coming from the west. The equipment included 3 laptops, 1 quantum module, 20 (1-20) accelerometers PCB 393B12, 10 (21-30) accelerometers PCB 393B31, 1(31) accelerometer PCB480B, 31 fibre optic cables, 15 large steel cylinders (6 of which can be supplied with a vertical and a horizontal accelerometer), 1 small steel cylinder, 1 hammer specially equipped to measure the intensity of the transmitted impulse to the bridge and three electricity cables.Two setups for the accelerometers were considered and are shown in figures 17 and 18.

Figure 15: Vertical and Horizontal accelerometers and fibre optic cables

Figure 16: Experiment 1. Hammer

The first setup provided 14 vertical accelerometers and 2 horizontal accelerometers. An additional vertical accelerometer was positioned in correspondence with accelerometer number 10 as a reference. Two excitations points (E1, E2) are considered for the hammer test. The second set-up involved the same number of accelerometers in different positions and two other excitation points.

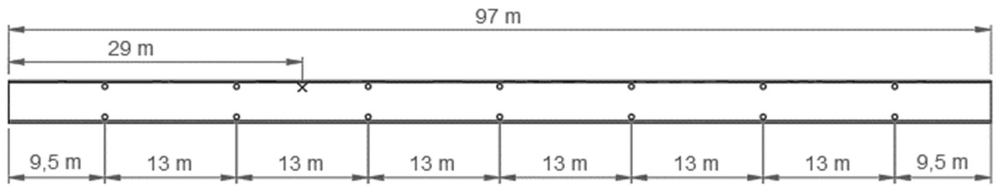

Figure 17: Experiment 1, set-up 1

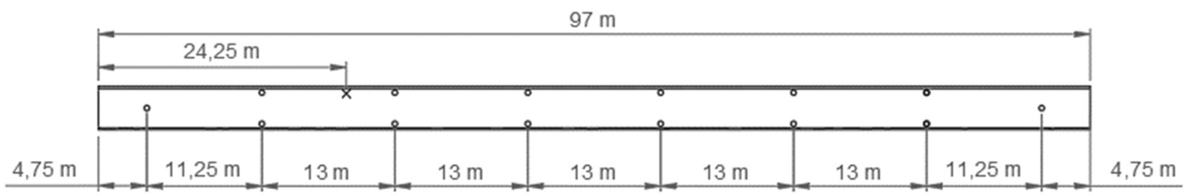

Figure 18: Experiment 1 set-up 2

The first test performed was the hammer test where a measured impulse force was transmitted through the hammer to the excitation point. 11 hits were made in each of the two hammer tests for each set-up. 30 seconds were measured between 2 consecutive hits to permit a frequency definition of 0.033 Hz. By the signal, it was possible to estimate the natural frequencies, the damping, and estimate the mode shape. 44 hits provided a sufficient amount of data to analyse.

Moreover, a jump test was performed in order to give an additional reference data system by four people at the quarter-span.

In addition, marching tests and running tests were performed. 5 frequencies (1.6 Hz, 1.8 Hz, 2 Hz, 2.2 Hz, 2.4 Hz) of loading were chosen. The given harmonic load to the structure by a moving person or group of people permitted the reconstruction of the time history. The marching tests were performed by 4 people, distributed in two rows marching on the western half of the bridge. The running tests were performed by a single pedestrian jogging at the abovementioned frequencies on the western side the bridge. Both of the tests needed to be performed on the same side as the measurement equipment was positioned at the midspan eastern side.

3.4.2 Second experiment

The second experiment took place on May 11th, 2021. The experiment aimed to estimate HSI effects on the Folke Bernadotte bridge and to verify the formulation described in section 3.1. Two hammer tests were conducted. The first test was to measure the dynamic response of the structure with only two pedestrians, necessary to conduct the test. The second hammer test was conducted in presence of 35 people on the bridge acting as Dynamic Vibration Adsorbers. The dynamic response of the bridge varied from one case to the other. The DAF curve shifted and decreased its peak.

To perform the experiment a different set-up from the first experiment, is chosen. Six accelerometers were distributed on the bridge according to figure 19:

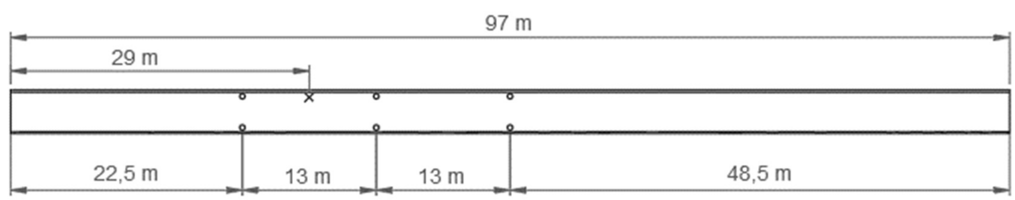

Figure 19: Experiment 2 set-up

However, to make a proper comparison, the same accelerometers were located in the same position. The number of accelerometers was reduced due to the interest in only the first and second vertical mode. Excitation point 2 was chosen as the hitting point.

Hammer test one included 11 hits with 100 seconds in between. The choice of the time in between the hits was calculated to permit a definition of 0.01 Hz. Due to the position of the excitation point, two people needed to stand on the bridge while performing the test. Weight and position are known and are considered in the theoretical simulation. The measurements were saved in 2 two files and signal analysis is conducted to construct the DAF curve.

Hammer test two included 12 hits with 100 seconds in between. 35 pedestrians were positioned on the bridge on the central 51 meters. The choice on the position and on the spacing was taken to maximize the effects on the first and second mode of vibrations. 1.5 meters distance was considered between two people. The weight and position of each person was noted. The average weight is calculated as 80 kg obtaining a model mass ratio of 5.16% for the second mode and 6.36% for the first mode.

The position of every pedestrian is shown in figure 20.

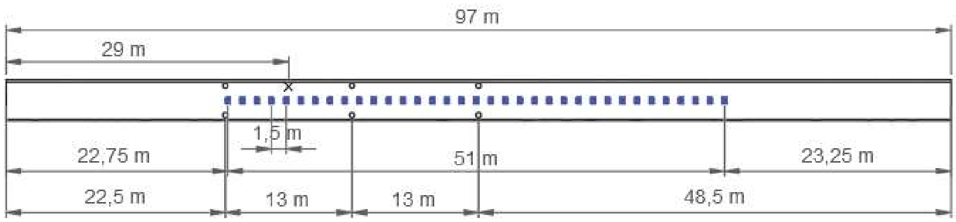

Figure 20: Pedestrians distribution on the bridge

Table 1 was compiled during the experiment. Each person was assigned a number indicating his/her position on the bridge. The second column shows the weight of each pedestrian. The second and third columns represent the contribution factor to mode 1 and 2.

Table 1: Pedestrians distribution, weights and modal contributions

Person Number	Weight (kg)	ϕ_1^2	ϕ_2^2	ϕ_3^2
1	76.1	0.092	0.482	0.980
2	93.8	0.126	0.594	1
3	63.2	0.168	0.701	0.951
4	69.5	0.216	0.796	0.842
5	102.4	0.271	0.871	0.686
6	94.5	0.332	0.921	0.507
7	74.5	0.398	0.940	0.327
8	56.3	0.468	0.928	0.170
9	68.5	0.540	0.883	0.057
10	78.8	0.612	0.809	0.003
11	69.9	0.683	0.710	0.014
12	69.4	0.751	0.593	0.089
13	89.9	0.814	0.467	0.216
14	69.0	0.870	0.340	0.377
15	87.5	0.917	0.223	0.546
16	57.1	0.955	0.123	0.698
17	73.8	0.981	0.049	0.808
18	110.0	0.995	0.008	0.857
19	103.1	0.996	0.002	0.840
20	62.0	0.985	0.032	0.757
21	69.0	0.962	0.098	0.622
22	104.5	0.927	0.194	0.458
23	80.9	0.881	0.313	0.290
24	77.9	0.827	0.448	0.145
25	96.1	0.765	0.586	0.043
26	85.2	0.697	0.718	0.001
27	62.2	0.626	0.834	0.023

28	84.0	0.553	0.923	0.107
29	98.0	0.480	0.980	0.242
30	73.4	0.409	1.000	0.409
31	70.3	0.342	0.981	0.586
32	88.5	0.279	0.927	0.749
33	62.0	0.222	0.842	0.876
34	101.0	0.172	0.733	0.949
35	72.4	0.129	0.610	0.956

Pedestrians were distributed in two middle quarter-spans to maximize the HSI effect. Studying the position of the pedestrians and weight was not permitted due to logistic difficulties.

A Normal standing posture was requested. The posture affects stiffness and damping, that are unknown in the problem.

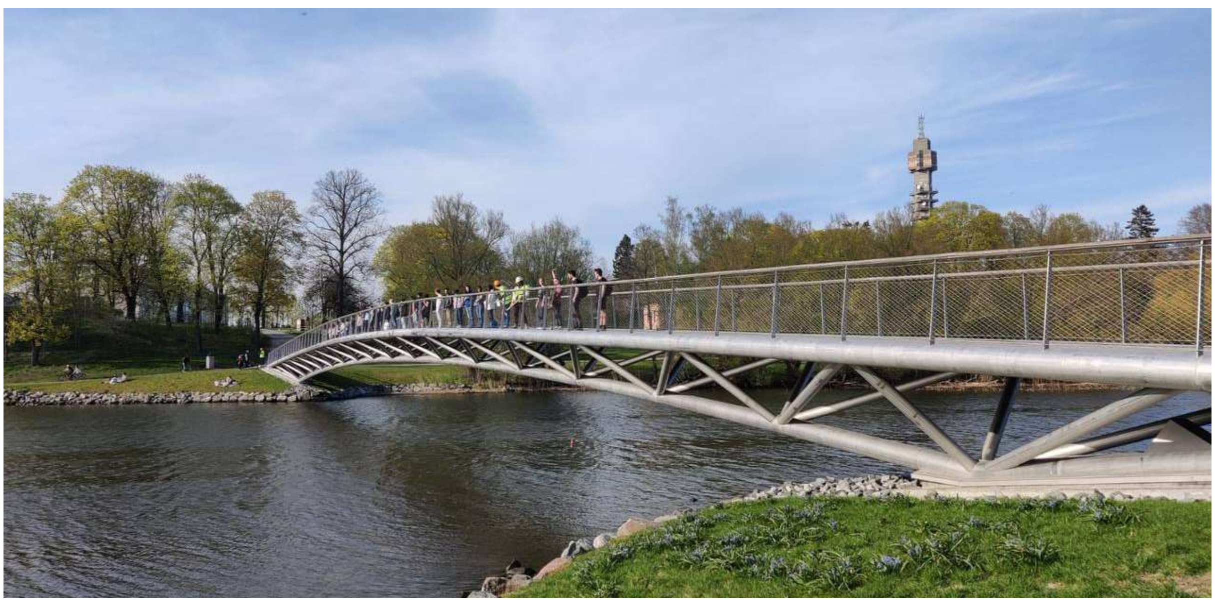

Figure 21: Experiment 2. Pedestrians on the bridge

Figure 22: Experiment 2. Pedestrians in position

3.5. The FEM Model

A Finite Element Model (FEM) of the Folke Bernadotte bridge is made to compare natural frequencies, mode-shapes, study the bearing conditions and ensure a better understanding of the bridge response itself.

The FEM model is implemented on the software ABAQUS. As mentioned in the previous paragraphs, the Folke Bernadotte Bridge is a steel arch bridge with a wooden deck. As the deck is positioned over the steel structure and only fixed at the extremes, it is considered as an applied load on the structure, and it is not designed in any part of the structure. The elements were not designed independently from each other but as merged in the four parts. Therefore, the interactions between the elements are assumed all clamped and transmitting normal forces, shear forces and moments. This assumption is correct for most connections, apart from the trapezoid elements under the deck which transmit only shear forces.

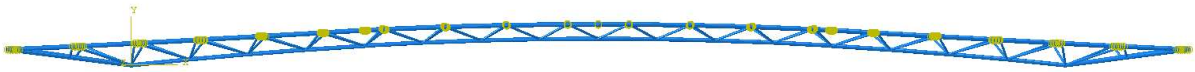

Figure 23: FEM model. Outline

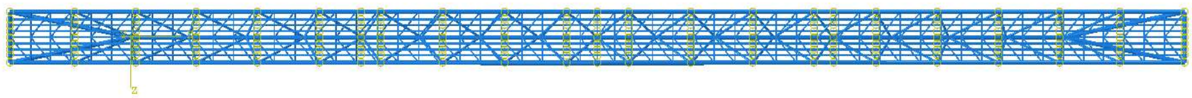

Figure 24: FEM model . Plan view

The bridge is modelled in four parts, sections of the bridge. The three main tubes, the truss elements, the transversal elements, the trapezoid elements supporting the deck and the diagonal elements stiffening the structure are designed in 3d space model as wires. Four parts are designed as the bridge is not symmetric. The diagonal elements just under the deck maintain the same V-shape along with the structure. Therefore, each part needs to be modelled and later assembled.

LDX2101 property material is created, and its properties defined. The density of the metal is initially set to $7850\ kg/m^3$ and later modified to $8860\ kg/m^3$ in order to include the deck and the railing which were not modelled. Therefore, the total mass of the bridge is set equal to $100300\ kg$ corresponding to the drawing's value. Seven cross-sections are defined and assigned to each element. The beam orientation is specified according to the position in space of the element. In the assembly module, the four parts are combined in space and the continuity of the structure is ensured by interactions. Tie constraints are defined by the longitudinal main girders, longitudinal trapezoids and diagonal elements of each part. A mesh of 0.2 is applied, after ensuring that more dense mesh does not increase the quality of the result.

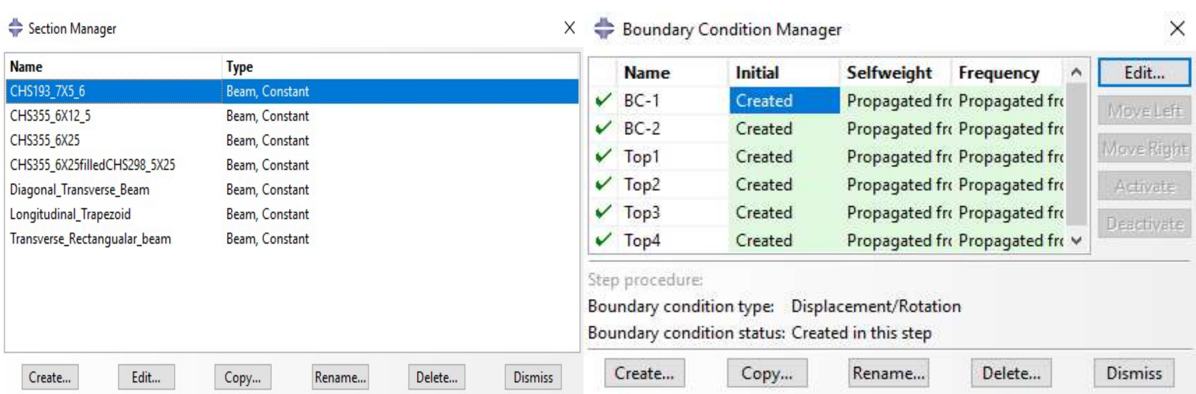

Figure 25: Abaqus Section and Boundary condition manager

The boundary conditions are defined in the load module. The bearings are initially set as specified in the drawings. The two lower bearings are defined to set all the translation equal to zero, the four upper ones not to allow the only vertical translation. A second configuration, in which one lower bearing allows longitudinal displacement is studied in order to create an upper and a lower bound for the natural frequencies as is explained in section 3.6.

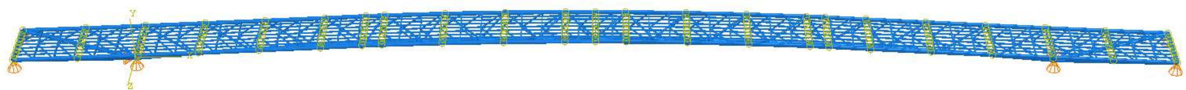

Figure 26: FEM model bearing configuration. Outline.

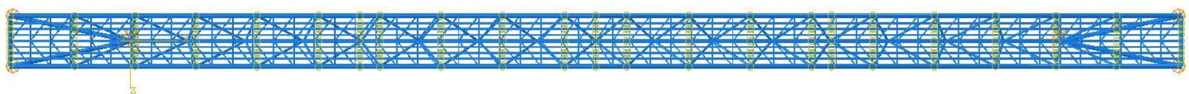

Figure 27: FEM model bearing configuration. Plan view

The only self-weight of the model is considered, and two steps are defined. The first step permits the calculation of displacements, stresses and sectional forces due to the self-weight. It is defined as a static procedure through linear perturbation. The second step permits the extraction of the natural frequencies of the model. 20 eigenvalues are requested and Lanczos procedure is requested. The first 20 natural frequencies and corresponding mode-shapes are obtained.

3.6. Extraction of the natural frequencies

By the FEM model, it was possible to extract the natural frequencies of the bridge and compare them with the estimations by experiment 1. On Abaqus 20 eigenvalues are requested, even though the main focus is on the first ten. To each frequency a correspondent mode is estimated. As mentioned, the study of the FEM model permits the understanding of the boundary conditions of the bridge. The natural frequencies from Abaqus were extracted for two bearing configurations. The first one was obtained by the drawing, the two bearing supports in the lower part are considered simply supported (translation in the three directions equal to 0), and the 4 bearing supports at the deck level were fixed only in the vertical direction. The second configuration allowed longitudinal displacement on one bearing at the base, while all the other bearing conditions remained the same.

From the experimental point of view, the four hammer tests were analysed. Each hammer test included eleven hits for each one of them and so it was possible to extract the natural frequencies of the bridge. The steady-state response after each hit was taken into account. The spectrum of the frequencies of the cut signal was shown and the peaks detected. The spectrum accounts for the Fourier Transformation, the signal and a later modulation.

The comparison of the natural frequencies obtained by the theoretical FEM model and the experiment can be performed and the bearing conditions studied.

3.7. Determination of the mode-shapes

The determination of the mode-shapes for the first two vertical bending modes is conducted. The theoretical results from the FEM model and the experimental results are obtained and compared. The Coordinate Modal Assurance Criteria (CoMAC) is applied to verify independence between the first and second mode and the correlation between the experimental and theoretical results.

The theoretical mode-shape is extracted for both the bearing configurations. A path is defined along the upper-level main girders and the displacement of the points extracted in an Excel file. The two mode-shapes are calculated by dividing the displacements by their maximum values in absolute value. Therefore, they are expressed by positive and negative values $0 \leq x \leq 1$.

The experimental ones are evaluated through the simultaneous analysis of all the accelerometers along the bridge. For each accelerometer, the spectrum of the free signal after the jump test (set up 1) is considered and the frequencies of vibrations and amplitude of the peak stored in two matrixes. As only the two bending vertical mode shapes are looked for, it is preferred to calculate the average between the two accelerometers at the same longitudinal coordinate. This technique permits the elimination of torsional effects and maximization of bending. Equation 3.9 is applied.

$$a_{av} = \frac{a_1 + a_2}{2} \tag{3.9}$$

Where a_1 is the signal of the first accelerometer, a_2 is the signal of the second accelerometer and a_{av} is the signal for which torsional effects minimized and bending effects were maximized.

Matrix $\mathbf{RMS}$ stores the peak values of the spectra. Each column corresponds to a mode, and each raw to a signal. Matrix $\mathbf{F}$ stores the natural frequencies of each spectrum. Each column comprehends slightly different values because of the different signal that has been analysed.

Therefore, each column of the matrix $\mathbf{RMS}$ is normalized. Each column corresponds to a mode-shape described in absolute value. By the calculation of the phase angles of each filtered signal, it is possible to calculate a plus/minus direction for each degree of freedom.

$$\mathbf{SIGN} = \frac{cos(\phi)}{|cos(\phi)|} \tag{3.10}$$

The multiplication of the mode and the sign matrix, permits to calculate the matrix $\mathbf{MODE}$ containing the modes of the system.

$$\mathbf{MODE} = \mathbf{SIGN} \bullet \mathbf{RMS} \tag{3.11}$$

3.8. Coordinate Modal Assurance Criterion (CoMAC)

The independence of the two modes and the correlation between the two of them by the first experiment and by the FEM model are verified through the Coordinate Modal Assurance Criterion (CoMAC). The CoMAC is an extension of the Modal Assurance Criterion (MAC), which permits the recognition of mathematical similarity and the provision of a measure of consistency between estimates of a modal vector. The COMAC is calculated over a set of mode pairs, which in this case is experimental versus analytical. The set of mode pairs represents all modes of interest in a frequency range, For the two vertical modes from both the theoretical and experimental approach, a value of COMAC is calculated for each degree of freedom.

The coordinate modal assurance criterion (CoMAC) is calculated through equation 3.12.

$$CoMAC_q = \frac{\sum_{r=1}^{L} \left|\phi_{qr}\varphi_{qr}\right|^2}{\sum_{r=1}^{L} \psi_{qr}\psi_{qr}^T \sum_{r=1}^{L} \phi_{qr}\phi_{qr}^T} \tag{3.12}$$

Where ϕ_{qr} and φ_{qr} are the two modes to compare. CoMAC assumes a value between 0 and 1, where o indicates independency and orthogonality and 1 indicates dependency.

3.9. Estimation of damping

The estimation of damping was conducted following both methods described in section 2.6. Logarithmic decrement and Half Power bandwidth are applied, and the results are compared. The four hammer tests for the two setups from experiment one are analysed and the values of damping for each mode are expressed.

The logarithmic decrement method implied the filtering of the signal for the frequency of interest. A bandpass filter was applied for the first horizontal frequency and the first and second vertical. 5 consecutive peaks were observed, and the value of damping evaluated.

Half-power bandwidth method is implemented on the spectra of the four hammer tests and average values from the tests are taken. The first three peaks are considered, and the three values of damping are calculated.

By Eurocode, usual values for damping for bridges can be written in table 2.

Table 2: Eurocode recommended damping values. Source [33]

Bridge Type	ξ Lower limit of percentage of critical damping [%]	
	Span L < 20 m	Span L ≥ 20 m
Steel and Composite	$0.5 + 0.125(20 - L)$	0.5
Prestressed concrete	$1.0 + 0.07(20 - L)$	1.0
Filler beam and reinforced concrete	$\xi = 1.5 + 0.07(20 - L)$	$\xi = 1.5$

As described in section 3.3, the Folke Bernadotte Bridge is a 97 meters steel bridge with concrete abutments and timber deck. The expected value of damping is below 0.5%.

3.10. Running Pedestrian

Experiment one and two involved 5 running and 5 marching tests. The analysis of this kind of tests is not correlated to crowd effects on pedestrian bridges but the dynamic evaluation of the Folke Bernadotte bridge and the modelling of pedestrians. The analysis aims to assess the dissimilarities in the modelling of the pedestrian as a Moving Force (MF) and as a Spring-Mass-Damper (SMD) system, and to register the maximum acceleration induced by a running pedestrian on the bridge. Moreover, it creates a reference in modelling the properties of the bridge and the pedestrians.

A theoretical and an experimental approach are conducted simultaneously, and the results compared. Stiffness, damping of the pedestrian are unknown and can be defined by matching the results if possible. The single pedestrian applies a force to the bridge which can be defined as the summation of harmonics according to ISO 2008.

$$F(t) = M_p \left(9.81 \left(1.6sin(2\pi f_{step} t) + 0.8sin(4\pi f_{step} t) + 0.2sin(6\pi f_{step} t)\right)\right) \tag{3.13}$$

In the code, it is later considered that a pedestrian does not apply an upward force on the bridge. The MF model implies the definition of the mass, stiffness, and damping matrix as independent from the pedestrian. The pedestrian is considered as the cause of the loading but no HSI effect is considered on the system. On the other hand, the SMD model implies the inclusion of the pedestrian mass, stiffness, and damping in the mass, stiffness, and damping matrixes definitions.

The dynamic response of the bridge is calculated through Newmark constant method. The two vertical modes are taken into account in the analysis and the total response is calculated through modal contributions in the analysed point. The experimental signal is filtered for frequencies higher than 5 Hz in order not to include multi harmonics effects. Therefore, the envelopes of the experimental and the two theoretical dynamic responses can be compared. A modification of the DLFs, according to Baumann and Bachmann [38], in the load description may be needed to permit a better fit of the curves.

4. Results

The following section summarises the results obtained throughout the two experiments, the FEM modelling, the verifications of the HSI model, the parametric analysis, the error surface and the running test.

4.1. Comparison of the HSI model and Newmark's method

By the HSI model, the dynamic response of the bridge is calculated by the DAF and the displacement associated with the bridge. The validity of the formulation by Colmenares et al. (2021) [37], is checked by the calculation of the error on Newmark's method. The error surface presented in section 4.3, is obtained varying the non-dimensional parameters Π_1, Π_2 and Π_3. In this section Π_1, Π_2 and Π_3 are fixed, and the associated error is calculated.

This section aims to present the results of Newmark's method displacements of the bridge and of the pedestrians, the results of the maximum steady response of the bridge, the DAF curve, and the error in % between the two formulations.

In this case, the condition of resonance is checked. The frequency of the load is set to 2.9 Hz as well as the frequency of the bridge and pedestrians. The choice on these parameters was made in order to emphasize the effect of the pedestrians on the bridge. The displacement of the bridge is checked and compared to the displacements of the pedestrians in three different positions: first quarter span, middle span and third quarter span. The condition of resonance of the pedestrians indicates the deviation of the load path, the pedestrians act as dynamic vibration adsorbers (DVA).

The dynamic properties of the bridge are set to the values which are found for mode 2 in sections 4.5, 4.6, 4.7. The damping of the bridge is set to 0.019, the frequency of the bridge equal to 1.56 Hz. The experimental mode-shape equation is taken into account. The linear mass of the bridge is set equal to 1031 kg/m.

The modal mass ratio is set to 0.04, the modal mass of all the pedestrians over the modal mass of the bridge. 50 pedestrians are positioned evenly on the bridge. The mass of the single pedestrian is found to be equal to 78.5 kg. The damping of the pedestrian is set equal to 0.35, while the stiffness is calculated from the mass and is equal to 7536 N/m. The value of stiffness, which was found, is not coherent with the literature [10]. This is because the frequency of the pedestrian is set to the natural frequency of the bridge.

By Newmark's linear method, the dynamic response of the MDOF, where the first degree of freedom corresponds to the bridge and each other mode to a pedestrian, is estimated. Figures 28, 29 and 30 represent the displacement in time of the bridge and a pedestrian positioned in the first quarter span, in the midspan, in the third midspan.

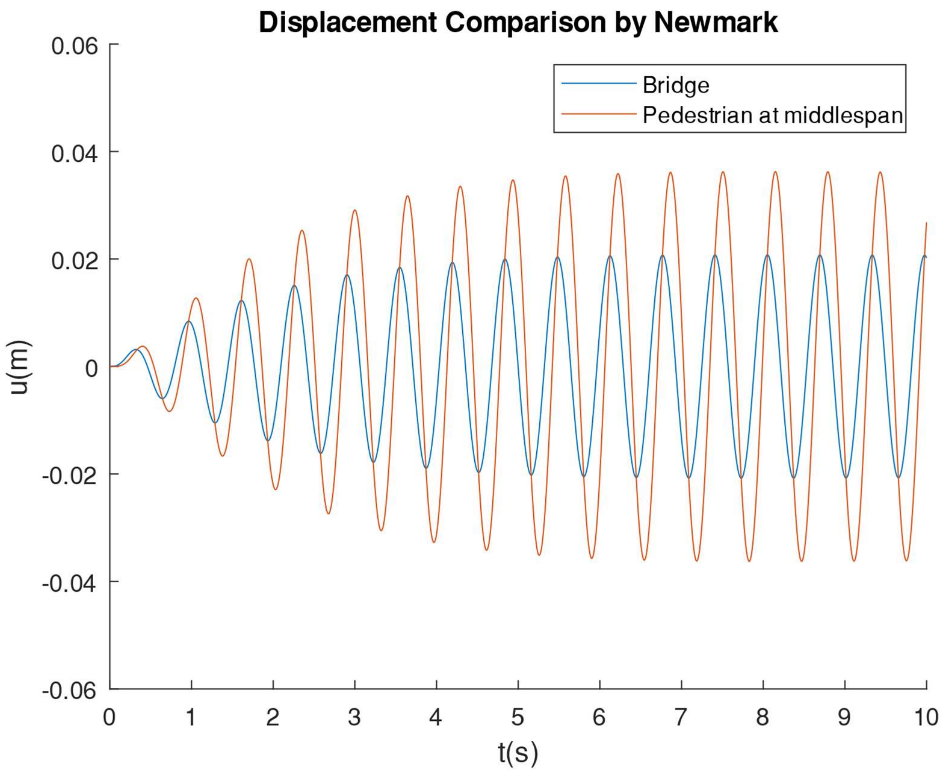

Figure 28: Displacement Comparison by Newmark. Pedestrian at middle span

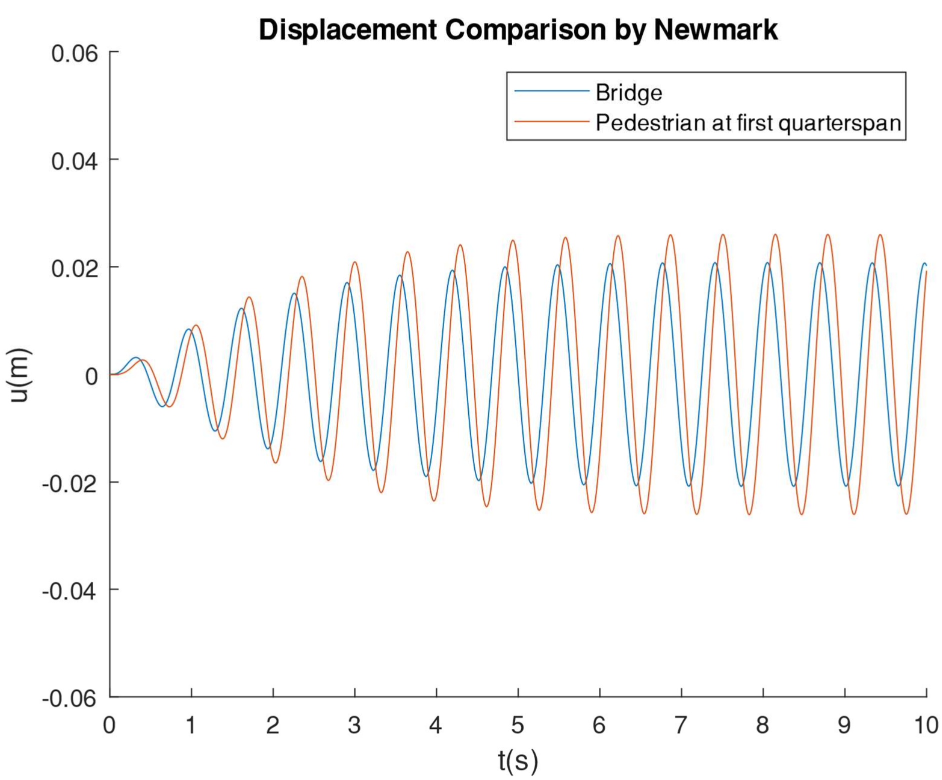

Figure 29: Displacement Comparison by Newmark. Pedestrian at first quarter span

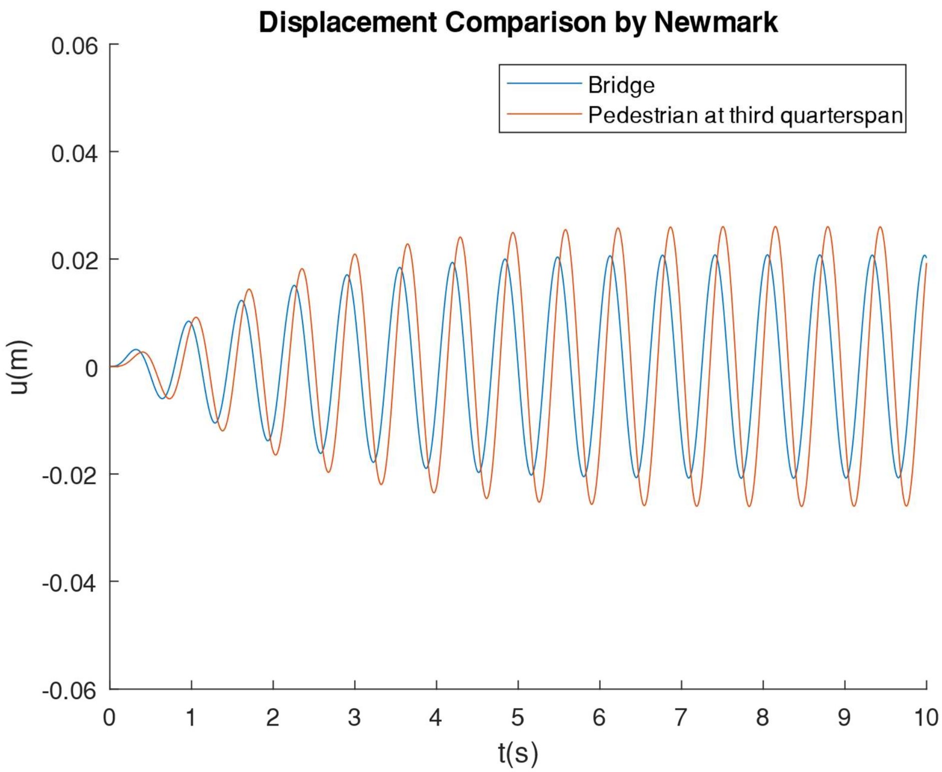

Figure 30: Displacement Comparison by Newmark. Pedestrian at third quarter span

The blue lines represent the dynamic response of the bridge while the red lines represent the dynamic response of the pedestrian in each position. As the first mode is considered, the maximum dynamic response of a pedestrian is registered at midspan. The displacements of the two pedestrians at the quarter-span are coherent as the mode-shape is symmetric. The condition of resonance of the pedestrians induces large displacements on pedestrians who dissipate energy and reduce the dynamic response of the bridge itself.

To verify the HSI model, the maximum dynamic response in the steady-state from Newmark‘s method is registered. The value of 0.0205 m is found as the peak of the oscillation in the steady-state. The DAF curve is found from the Mass matrix, Stiffness matrix and Damping matrix of the MDOF system and the value of DAF for the loading frequency is equal to 9.661.

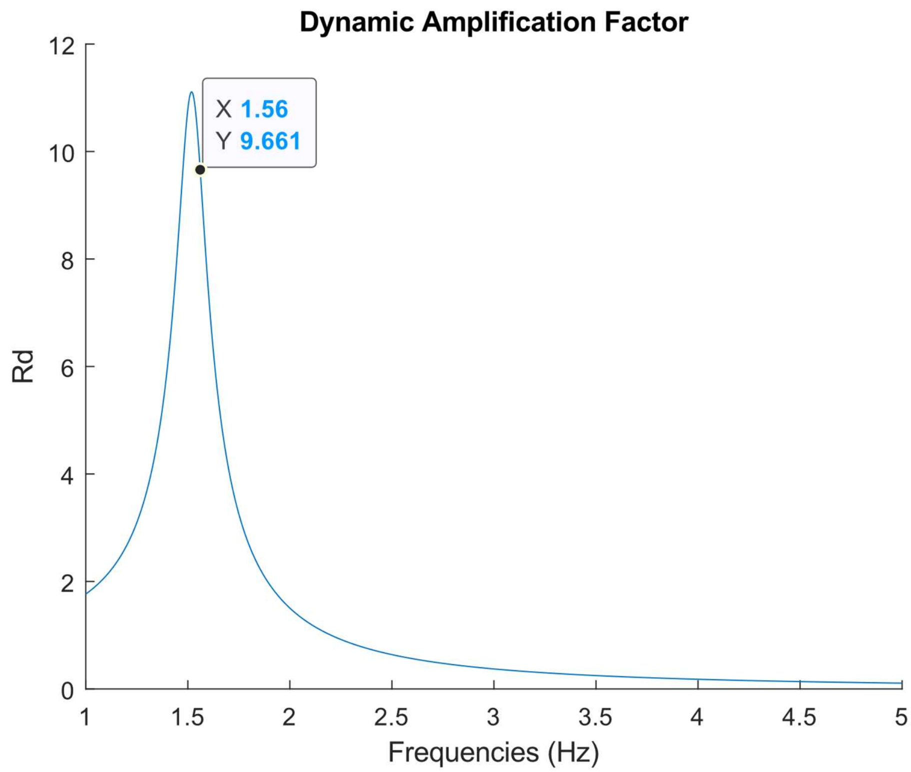

Figure 31: The Dynamic Amplification Factor (DAF) curve

The static response of the bridge is equal to 0.0021 m and it is found by the static force applied to the system and the inverse of the stiffness matrix.

By the multiplication of the static displacement and the DAF evaluated at the loading frequency, the maximum dynamic response in the steady-state is found. The error between this value and Newmark is equal to 0.0073 % indicating the equality of the two methods.

4.2. DAF curves

The Dynamic Amplification Factor (DAF) curves can be obtained for each configuration of the system. The dynamic properties of the bridge (natural frequencies, damping and mode-shapes) are calculated from the first experiment and can be inserted into the HSI model. Pedestrians' stiffness and damping are taken from the literature [10] and the result of the second experiment is predicted by simulations. The exact number of people, their distribution on the bridge and their weights are not yet known. Simulations are made in order to form an opinion on the pedestrian distribution and posture which pedestrians should assume. In this phase, pedestrians are evenly distributed on the total span of the bridge. The mass of each pedestrian is set to 70 kg, the stiffness is set to 23500 N/m as middle value in Caprani's range, and damping is assumed to be equal to 0.30. Figure 32 and

Figure 33 represent the DAF for the first and second vertical modes which are expected from the experiment. The three curves represent the DAF curve in the case of 0 pedestrians, 25 pedestrians, 50 pedestrians evenly distributed on the bridge.

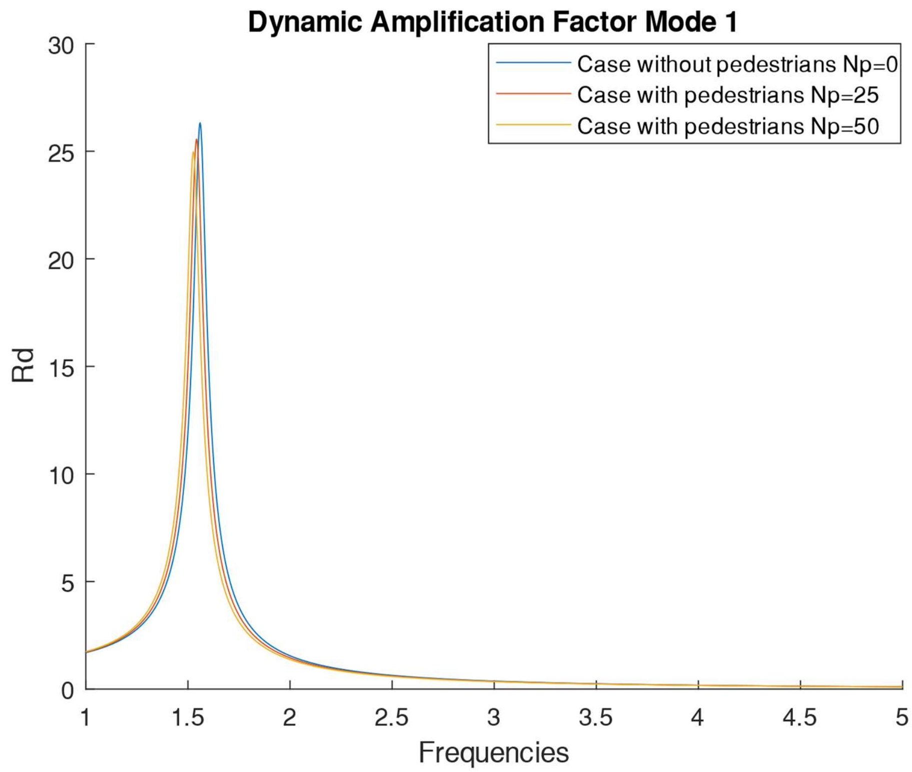

Figure 32. Comparison of the first mode DAF curve depending on the number of pedestrians

From the simulation represented in Figure 32 for the first mode of vibration, the DAF curve registers a shift towards the left and a decrease of the peak point. HSI affects the dynamic response of the model, resulting in a decrease of the natural frequency of the bridge and a lowering of the maximum DAF.

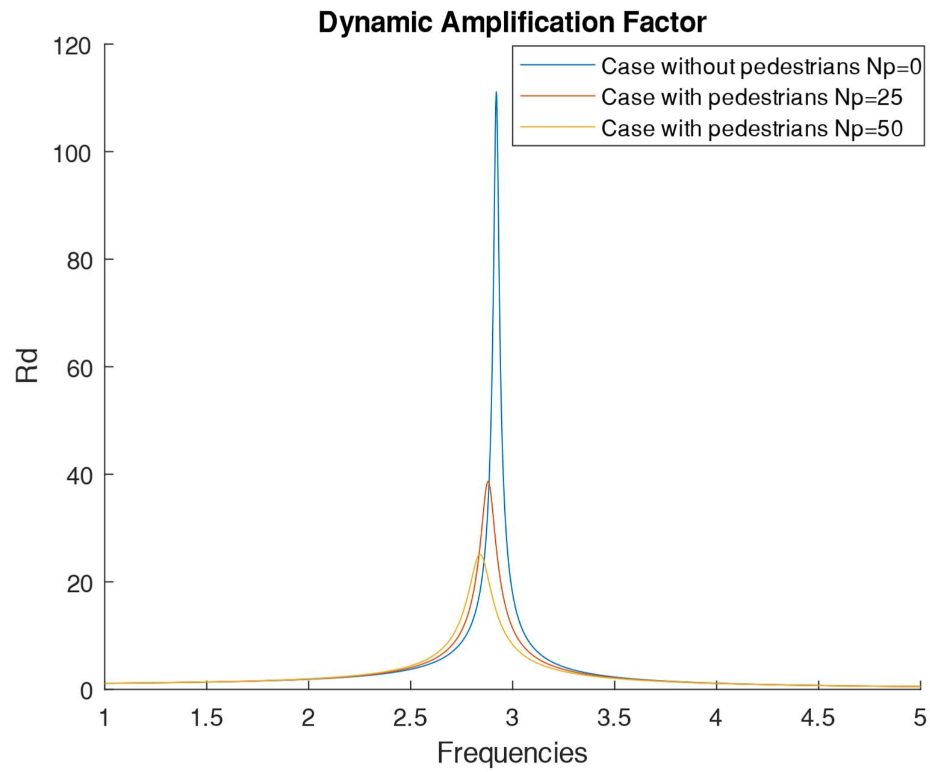

Figure 33: Comparison of the second vertical mode DAF curve depending on the number of pedestrians

The simulation on the dynamic response variation due to HSI for the second vertical mode results in a relevant change on the DAF curve. The peak value reduces by three times from the case without pedestrians and with 50 pedestrians. The shift in the natural frequency is equal to 0.08 Hz which can be measured during the experiment.

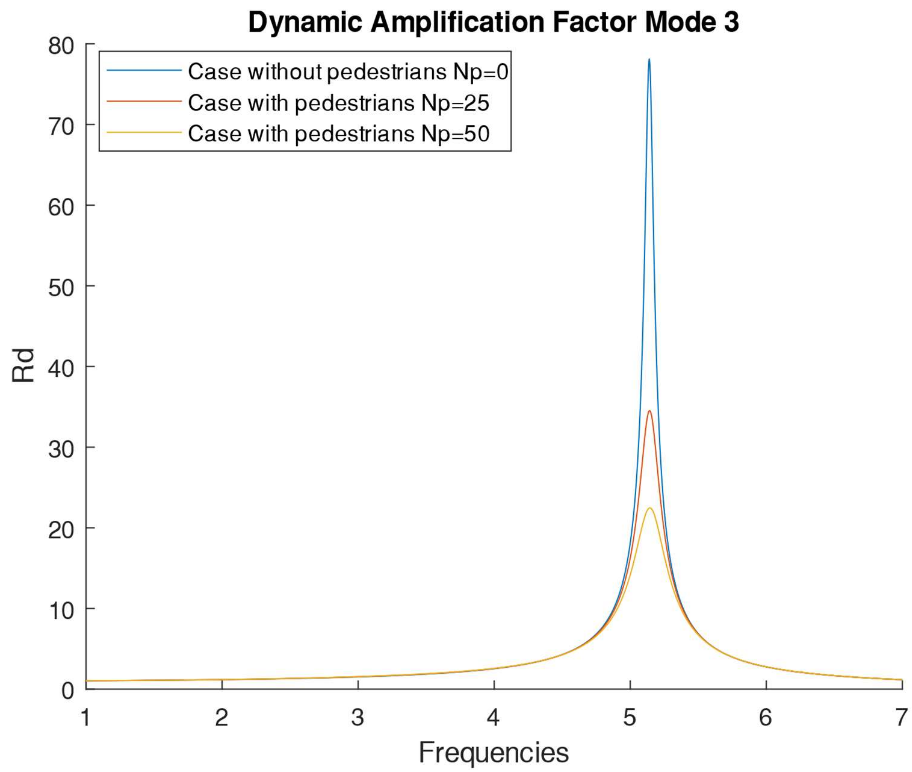

Figure 34:Comparison of the third vertical mode DAF curve depending on the number of pedestrians

The simulation on the dynamic response variation due to HSI for the third vertical mode results in a relevant change on the DAF curve. The peak value reduces relevantly from the case without pedestrians to the one with 50 pedestrians. The shift in the natural frequency is equal to 0.01 Hz which may be difficult to measure during the experiment.

Simulations permit to proceed to more effective experiments. The distribution of the pedestrians is made to increase the modal mass of the second mode as HSI effects are more sizeable and measurable.

4.3. HSI parametric analysis

The parametric analysis of the HSI model for a simply supported bridge is conducted. The results which are here reproduced, are first shown in Colmenares et al. (2021) [37].

f_p, f_{step} and $\Pi_2 = \frac{m_{pedestrians}}{m_{bridge}}$ vary. f_p is made to vary between 1 and 2.9 Hz with 0.1 step, f_{step} is made to vary between 1 and 2.4 Hz with 0.1 step, and Π_2 is made to vary between 0.02 and 0.10 with 0.2 step. As defined in section 3.2, the non-dimensional quantities are reported.

$$\Pi_1 = \frac{\omega_{loading}}{\omega_{bridge}} \qquad \Pi_2 = \frac{m_{pedestrians}}{m_{bridge}} \qquad \Pi_3 = \frac{\omega_{pedestrians}}{\omega_{bridge}}$$

The varying quantities are included in the definition of the non-dimensional parameters Π_1, Π_2 and Π_3. Figures 34, 35, 36, 37 and 38 in the first column represent the results of the parametric analysis explicating Π_1 on the x axis and Π_3 on the y axis. Π_2 variation generates 5 different surfaces. Figures 34, 35, 36, 37 and 38 in the second column show the variation of the peak point of the surface on Π_3. On the other hand, Π_4 and Π_5 are set to fixed values.

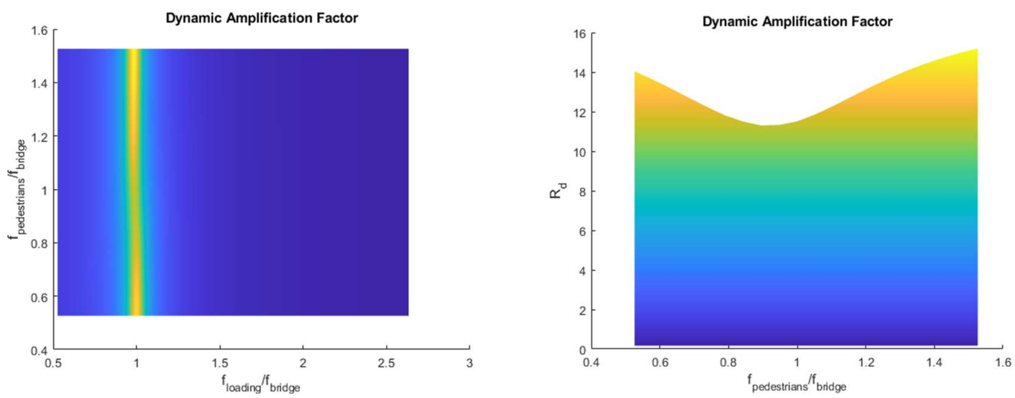

Figure 35: Parametric Analysis Surface $\boldsymbol{\Pi_2 = 0.02}$

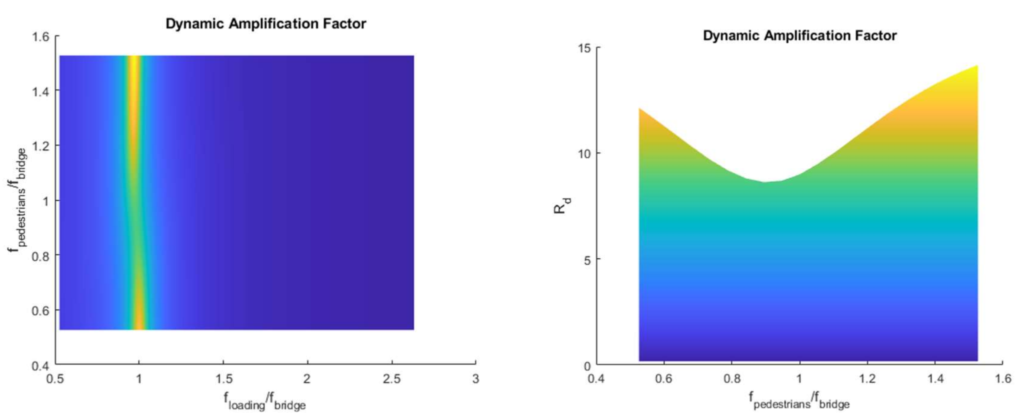

Figure 36: Parametric Analysis Surface $\boldsymbol{\Pi_2 = 0.04}$

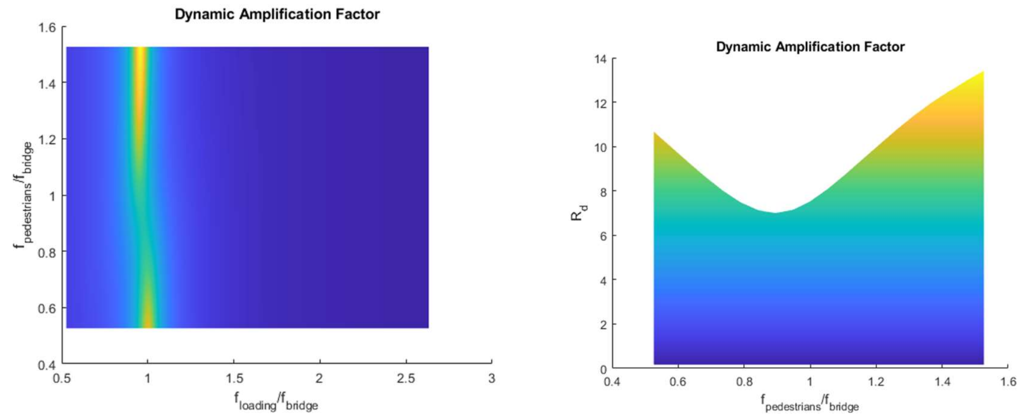

Figure 37: Parametric analysis Surface $\boldsymbol{\Pi_2 = 0.06}$

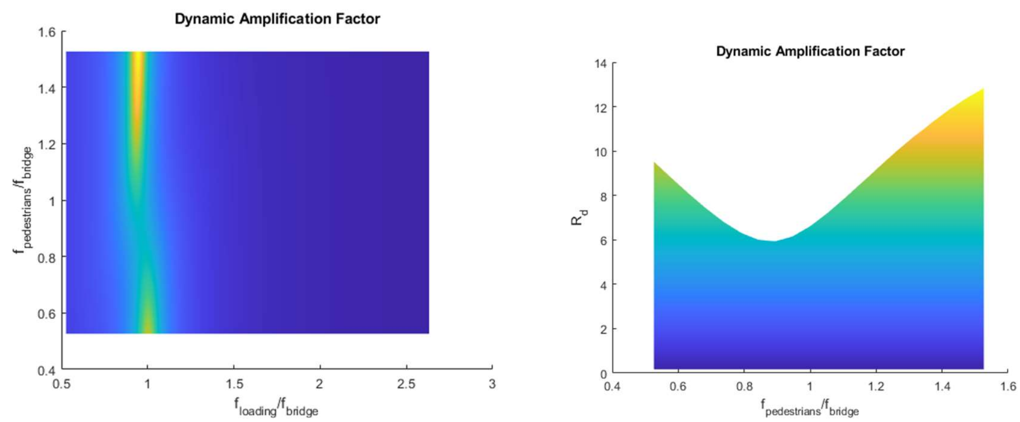

Figure 38: Parametric Analysis Surface $\boldsymbol{\Pi_2 = 0.08}$

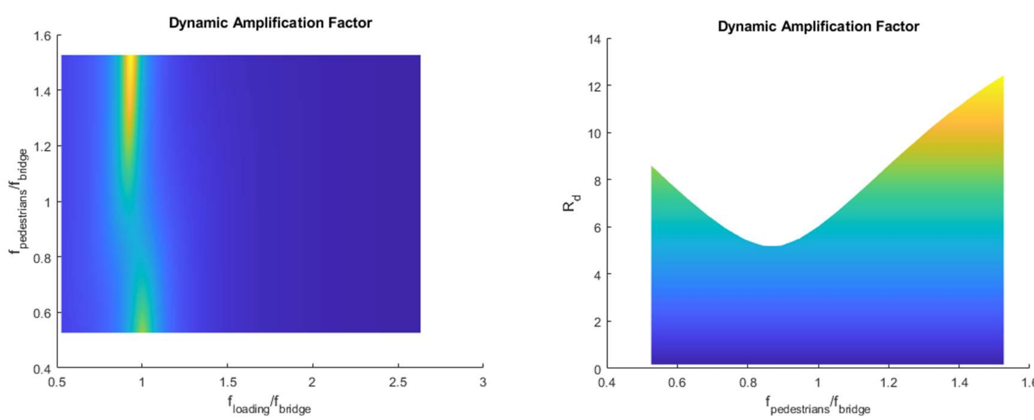

Figure 39: Parametric Analysis Surface $\boldsymbol{\Pi_2 = 0.10}$

The DAF can be read as x-z sections of the DAF surface. The ratio $f_{loading}/f_{bridge}$ indicates the condition of resonance which is verified for $f_{loading}/f_{bridge} = 1$. The ratio $f_{pedestrian}/f_{bridge}$ indicates the tuning of the system. When $f_{pedestrain}/f_{bridge} = 1$ the energy path of the system deviates, energy is dissipated by pedestrians who vibrate at the same natural frequency of the bridge. In the figures it is possible to note how the peak of the DAF curve lowers when this condition is verified. Higher mass ratios indicate a larger difference in the DAF when pedestrians are tuned to the bridge.

4.4. Error Surface

The error surfaces are a representation of the error in percentage of the difference between the Newmark linear method and the formulation of the HSI model. In parallel to the parametric analysis, the surface is calculated for the same varying quantities, the pedestrians' frequency f_p, the loading frequency f_{step} and the modal mass ratio Π_2. Figure 39 accounts five surfaces, corresponding to the five mass ratios. These results are firstly shown in [37] and here reproduced.

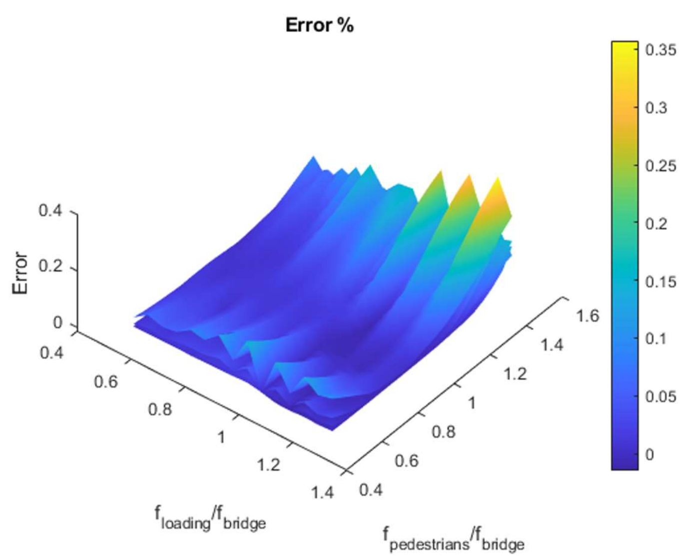

Figure 40: Error Surfaces

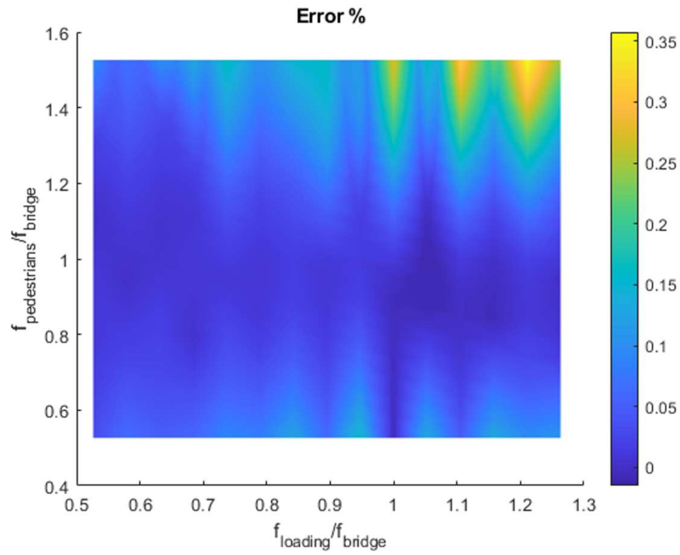

Figure 41: Error Surfaces plan view

The maximum error between the two models is below 0.35 % for the conducted parametric analysis, and it is registered for $f_p = 2.9\ Hz$, $f_{step} = 2.8\ Hz$ and the modal mass ratio $\Pi_2 = 0.10$.

4.5. Natural frequencies

The natural frequencies of the Folke Bernadotte bridge, obtained by experiment one, are shown in table 3.

Table 3: Natural Frequencies

Mode Number	Frequency (Hz)	Mode Type
1	1.25	Horizontal (1st)
2	1.56	Vertical (1st)
3	2.92	Vertical (2nd)
4	3.14	Torsional (1st)
5	3.43	Torsional (2nd)
6	5.14	Vertical (3rd)

It is possible to notice how these frequencies belong to the human loading range. The bridge goes in resonance when loading with the same frequencies is applied. A person walking has a natural frequency of 1.6 Hz which is closer to the first vertical natural frequency while a person running has a natural frequency of 2.4-3.0 Hz which is near to the second vertical natural frequency. As the first vertical horizontal mode is below the limit of 2.5 Hz, and both the first and the second vertical modes are below the limit of 5 Hz, a dynamic analysis of the bridge should be performed according to Eurocode.

By the FEM model, it is possible to extract the natural frequencies of the bridge in the two bearing configurations. A mentioned in paragraph 3.6, the first bearing configuration implies zero-translations in each direction for the two points at the base and zero-vertical translation for the four top bearings. On the other hand, the second configuration permits longitudinal translation for one of the two bearings at the base. The natural frequencies for both the configurations and for the experiment are displayed in table 4.

Table 4: Natural frequencies comparison with the FEM Model

Mode Number	Experimental Frequencies	FEM 1st Bearing Configuration	FEM 2nd Bearing Configuration	Mode Type
1	1.25	1.06	1.06	Horizontal (1st)
2	1.56	2.02	1.21	Vertical (1st)
3	2.92	2.93	2.93	Vertical (2nd)
4	3.14	3.07	3.08	Torsional (1st)
5	3.43	3.87	3.87	Torsional (2nd)
6	5.14	5.11	5.06	Vertical (3rd)

The FEM model provides coherent frequencies to the experimental ones. The experimental frequency for mode 2, corresponding to the first vertical mode-shape, lies in between the two frequencies from the first and second bearing configurations. The two frequencies create an upper and a lower bound for the measured frequency. The reason lies in the non-perfectly fixed configuration of the bearings of the Folke Bernadotte Bridge. Some translation is allowed, and the stiffness of the bearing is not at the maximum. The bearing condition could be studied by modelling the supports as springs having a certain rotational stiffness. However, for the purpose of the thesis, this study is not made. By the result by table 4, it is suggested to implement modal updating techniques in order to further improve the quality of the model in terms of frequency matching.

4.6. Damping

Damping is evaluated through the logarithmic decrement method and the half-power bandwidth method. The results are shown in table 5.

Table 5: Damping ratios

Mode Number	Frequency (Hz)	Damping ratio (%) Logarithmic decrement	Damping ratio (%) Half Power Bandwidth
2	1.56	2.05	1.9
3	2.92	0.41	0.45
6	5.14	0.59	0.64

The damping ratio is looked at for the two frequencies of interest. The first and the second vertical (mode 2 and 3), are necessary as inputs of the HSI model. It is possible to notice how damping assumes values $\xi \leq\ 0.01$ for mode 1 and 3 but assumes a higher value for the second mode $\xi =\ 0.019$-0.020. As most civil structures, the Folke Bernadotte bridge is a lightly damped structure. By Eurocode, a lower limit for the estimation of damping is 0.5. While the first mode and third mode assume values in line with the expectations, the second mode experiences higher damping.

Firstly, the logarithmic decrement is calculated by considering five consecutive peaks of the filtered signal for each mode.

Signals are filtered through the command "filtfilt" in Matlab defining a bandpass filter for frequencies 0.01 Hz higher and lower the natural frequency of interest. Peaks in position 30 to 35 are taken into consideration for the estimation of the logarithmic decrement for mode 2. Peaks in position 60-65 are taken in consideration for mode 3. Peaks in position 90-95 are taken for mode 6. For the three modes the damping ratios are calculated.

Secondly, the Half power bandwidth method is applied on the frequencies of interest to provide a term of comparison. The spectrum of the non-filtered signal is taken into account. The peak values are stored, and the procedure described in section 2.6.2 is applied. Interpolation between the points is implemented to calculate the frequencies of the peak value divided by $\sqrt{2}$. The damping ratios are calculated by the steepness of the spectrum for the first three frequencies. Figure 42 represents the spectrum of the signal.

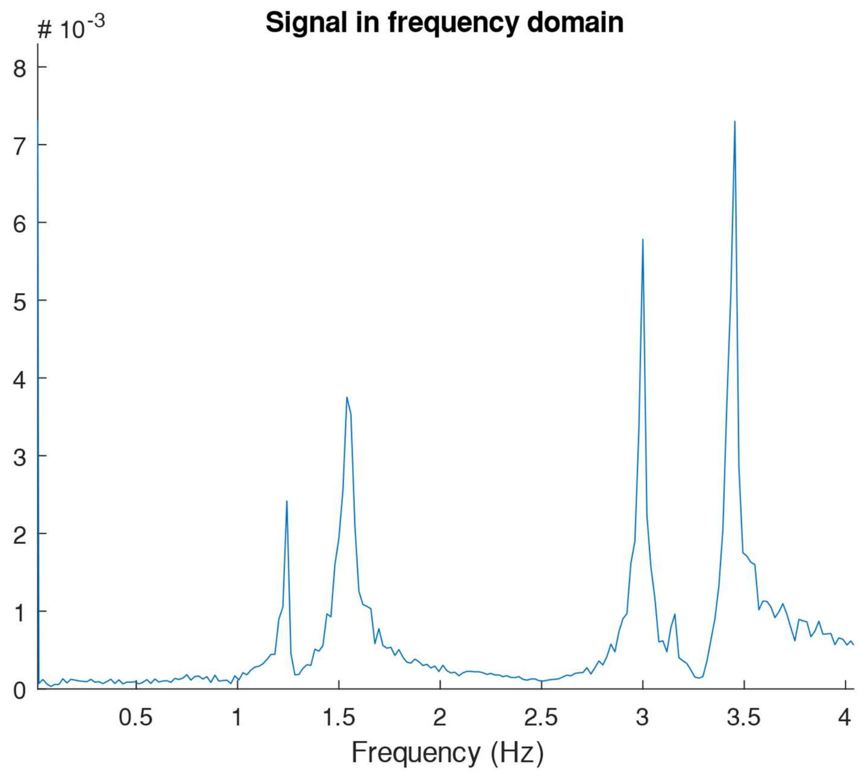

Figure 42: Signal Spectrum

4.7. Mode-shapes

In order to analyse the HSI model, the first two vertical mode-shapes are needed. The extraction of the mode-shapes from the measurements are obtained through the procedure described in section 3.7. The mode-shapes from the FEM model are extracted in parallel. The comparison is made and the curve fitting the best the experimental data is chosen as input for the HSI model.

Mode 2, 3 and 6, corresponding to the first, second and third vertical mode, from the FEM model are shown in Figures 45, 46 and 47.

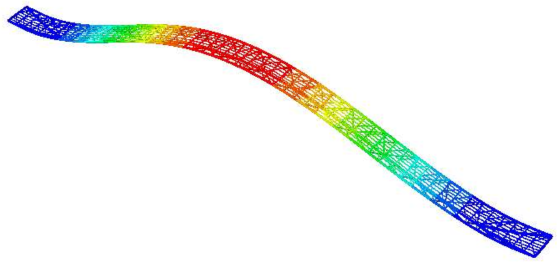

Figure 43: FEM model Mode 2, First Vertical Bending Moment

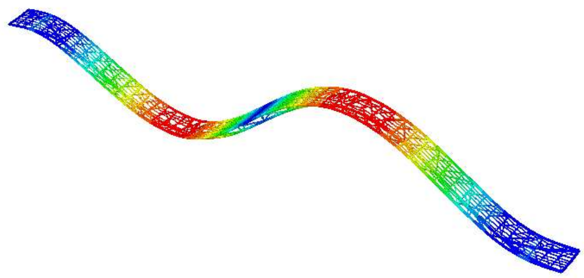

Figure 44: FEM model Mode 3, Second Vertical Bending Moment

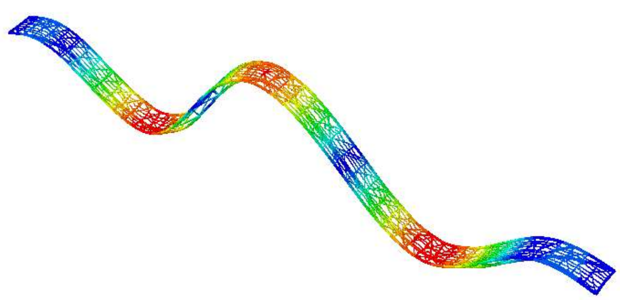

Figure 45: FEM Model Mode 6, Third Vertical Bending Moment

FEM model provides dense discrete curves for the mode-shapes. Experimental analysis provides only sampled points from setup 1 or 2.

Figure 46 shows the comparison between the curves for the first vertical mode-shape.

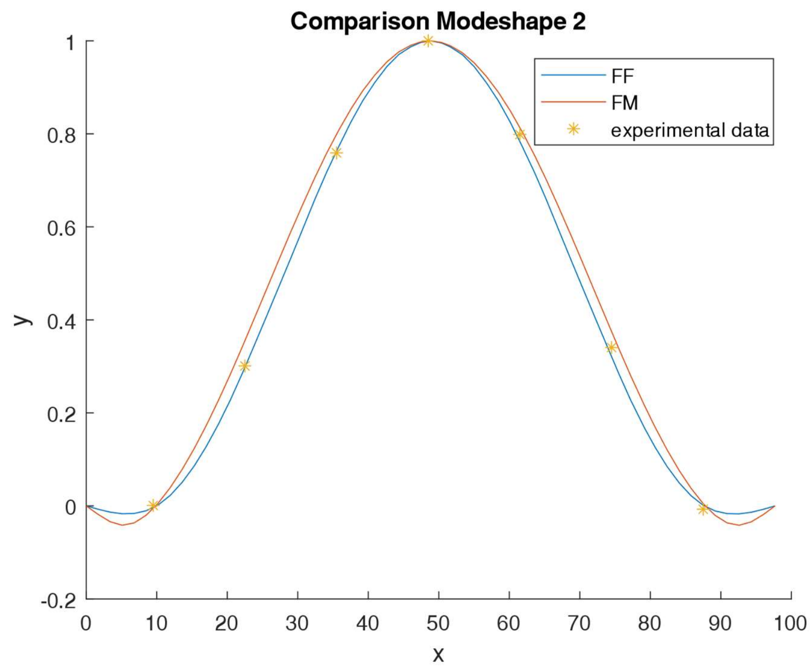

Figure 46: first vertical bending moment. Mode-shape comparison

Experimental and FEM curves are coherent. The two continuous curves represent the first (FF) and the second (FM) bearing configurations while the star points to the experimental data. Star points are in between the two configurations even though the first Fixed-Fixed may be assumed as more suitable for the description of the system.

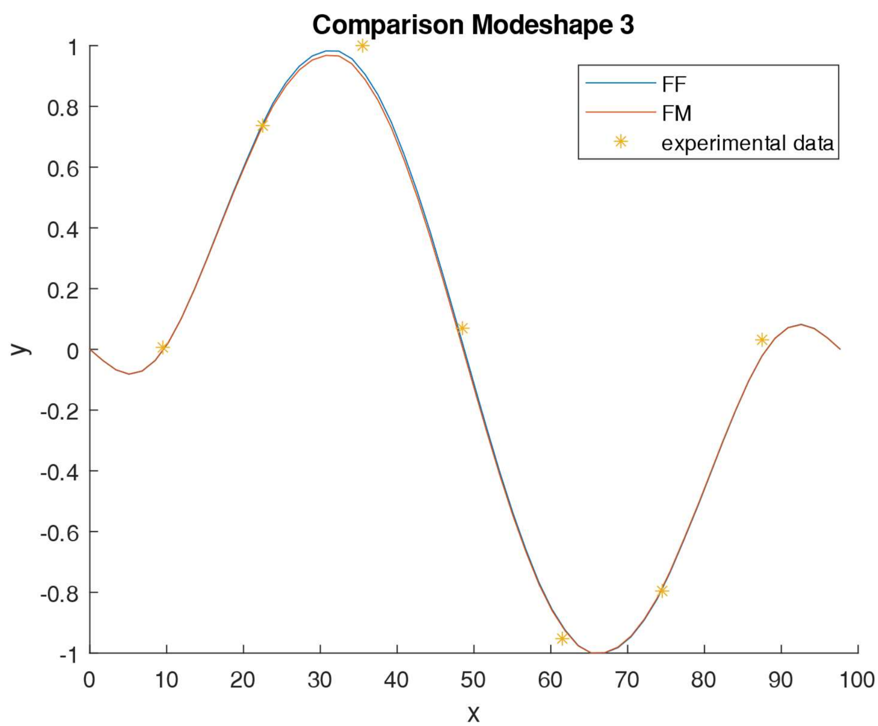

Figure 47: second vertical bending moment. Mode-shape comparison

Figure 47 shows mode-shape 3 corresponding to the second vertical. FEM Curves are coherent with the experimental data, but they assume higher values in absolute value, for points 3 and 5.

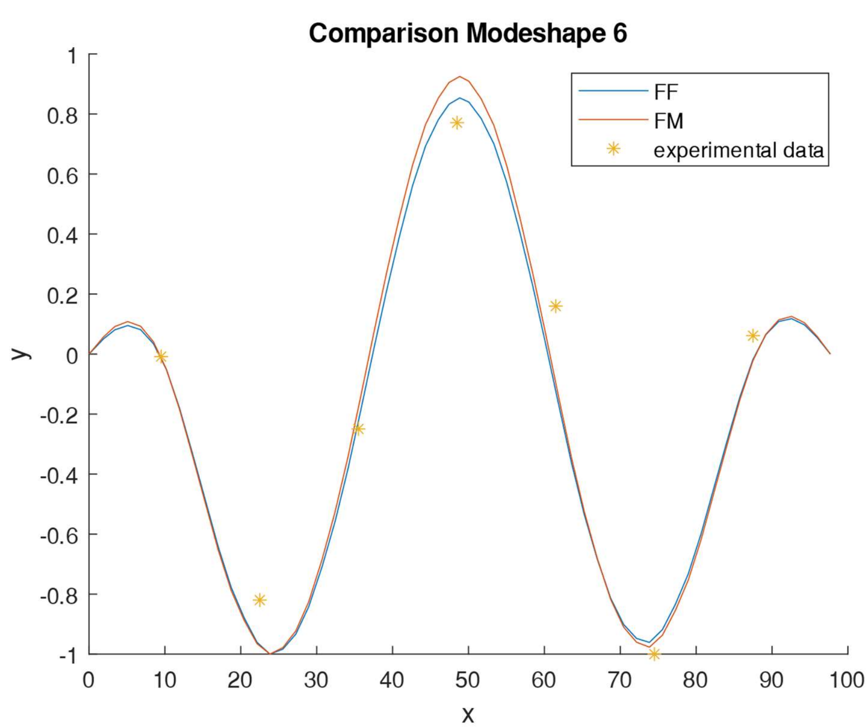

Figure 48: third vertical bending moment. Mode-shape comparison

The experimental sampled points are coherent with the FEM extracted mode shapes. Even though some experimental points are not matching the curves, the general mode shape is extracted.

The analysis of the mode-shape is conducted, and a fitting curve through the experimental data is drawn for each mode through the command fitting curve in MATLAB, sum of sine description is chosen. Sines are considered to be the most suitable choice for the description of mode-shape. Figures 49, 50 and 51 show the fitting curve for the three modes.

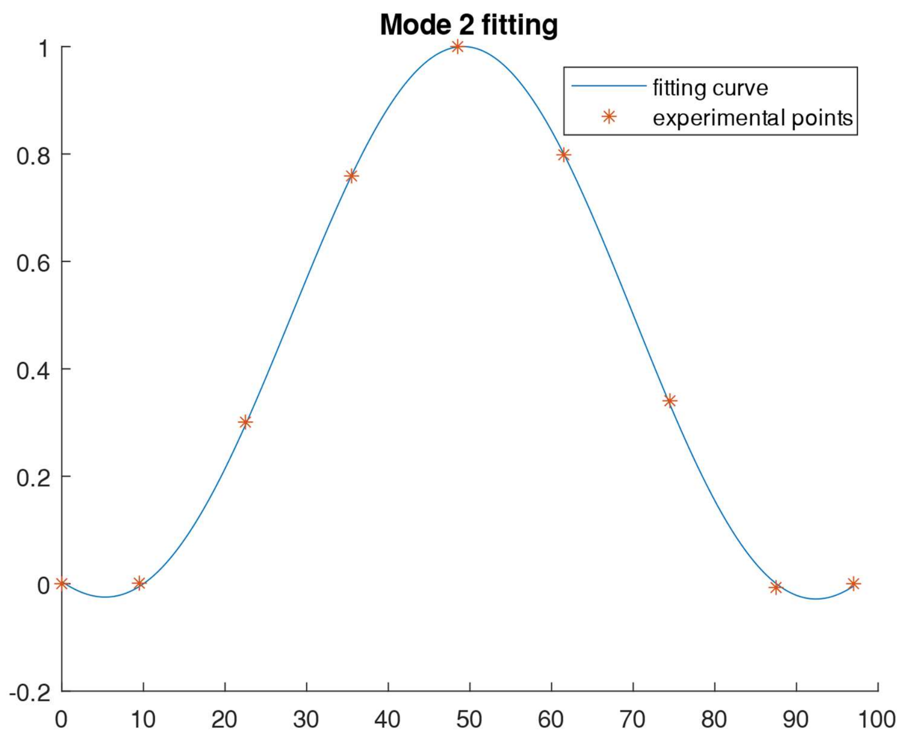

Figure 49: Mode 2 Fitting curve on experimental data

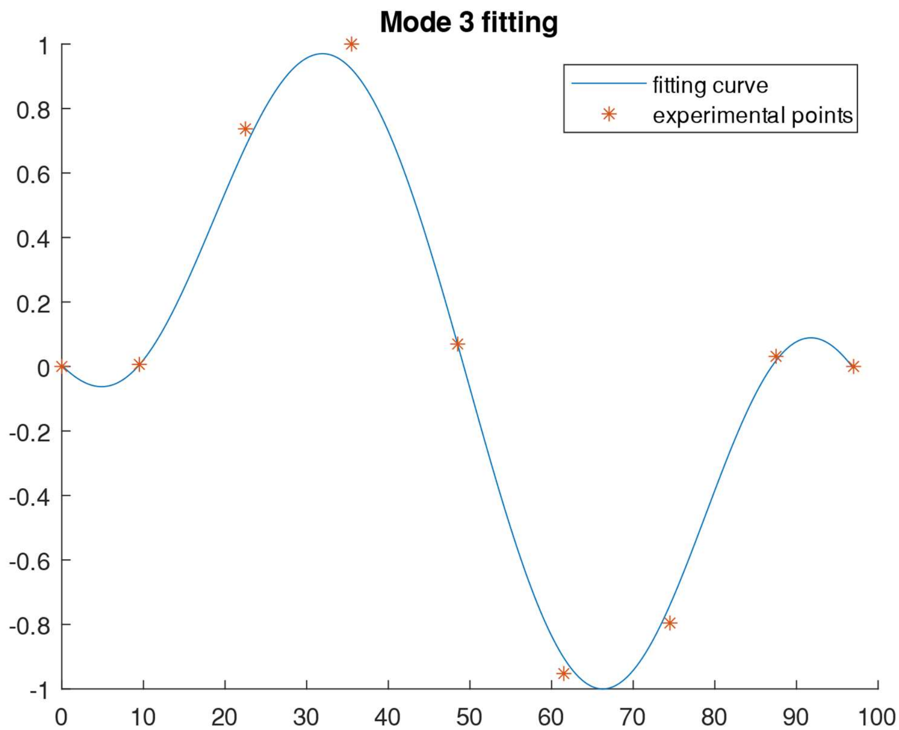

Figure 50:Mode 3 Fitting curve on experimental data

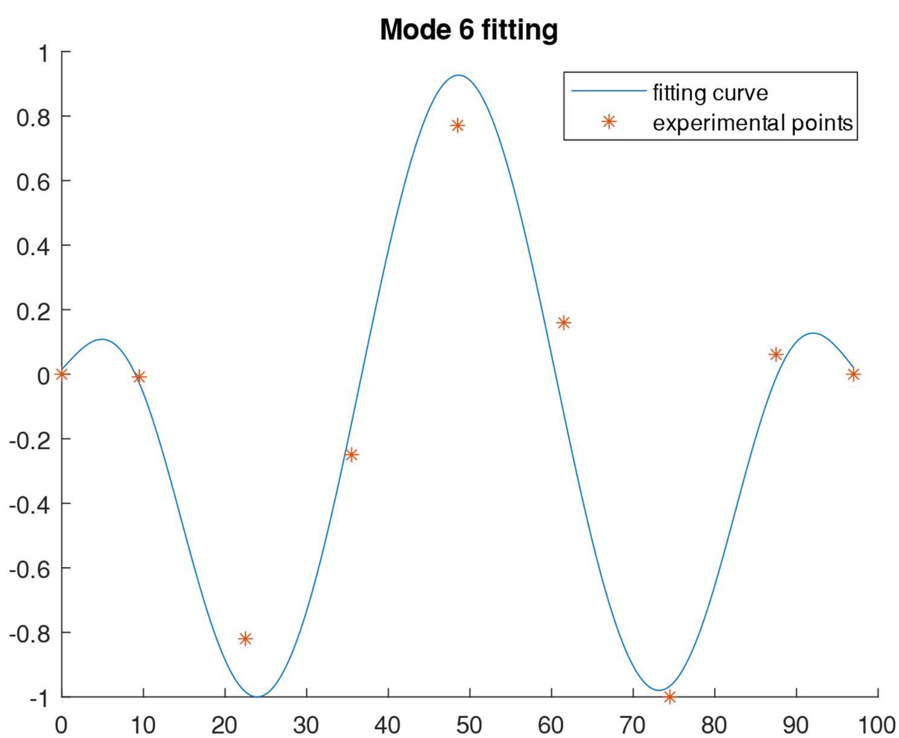

Figure 51: Mode 6 Fitting curve on experimental data

Mode 2 is described by equation:

$$f_1(x) = 0.602 sin(0.02172(x) + 0.4929) - 0.05286 sin(0.09177(x) + 3.784) \\ +0.4455 sin(0.08126(x) - 2.364)) \tag{4.1}$$

The fitting quality is assessed through the chi-square test. Mode 2 fitting is characterized by a chi-square equal to $X^2 = 0.9998$.

Mode 3 is described by equation:

$$f_2(x) = (0.7442\, sin(0.05856(x) + 0.2592) + 0.8475\, sin(0.1317(x) + 3.031) + \\ +0.4003 sin(0.1474(x) - 0.7763)) \tag{4.2}$$

The fitting quality is assessed through the chi-square test. Mode 3 fitting is characterized by a chi-square equal to $X^2 = 0.9998$.

The third mode is described by equation:

$$f_3(x) = (0.7438\, sin(0.1381(x) + 0.994) + 0.4641\, sin(0.0.1044(x) - 2.578) + \\ +0.5409 sin(0.04477(x) - 0.8249)) \tag{4.3}$$

The fitting quality is assessed through the chi-square test. Mode 3 fitting is characterized by a chi-square equal to $X^2 = 0.9662$.

The fitting curves are described by equations given by the sum of sine functions, which were preferred to polynomials due to the wave nature of mode-shapes.

4.8. CoMAC

The Coordinate Modal Assurance Criterion (CoMAC) is applied to ensure coherence between the experimental and the FEM curves and the independence between first, second and third mode. CoMAC is applied twice: the first time between the experimental fitted curve and the FEM model in the first configuration and the second time between the experimental fitted curve and the FEM model in the second configuration.

Therefore, in the first application of the CoMAC a matric comprehending the four mode-shapes vectors is composed. Equation 3.12 is applied and a symmetric matrix $4\ x\ 4$ is obtained. The main diagonal represents the identity. The formula is applied between the same mode-shape and correlation is equal to 1. The elements in position 1-2, 2-1, 3-4, 4-3, 5-6 and 6-5 indicate the dependence between the experimental and the FEM model. High values of dependence for these elements are looked for as indication of the correlation between the experiment and the FEM model for the same mode. Values in position 1-3, 1-4, 1-5, 1-6, 2-3, 2-4, 2-5, 2-6, 3-1, 3-2,3-5, 3-6, 4-1, 4-2, 4-5, 4-6, 5-1, 5-2, 5-3, 5-4, 6-1, 6-2, 6-3 and 6-4 need to be low indicating the correlation between different modes from different sources.

The result of CoMAC, applied between the first configuration (Fixed-Fixed) of the FEM model and the experimental data, can be expressed by the matrix:

$$\mathbf{CoMAC} = \begin{bmatrix} 1 & 0.9999 & 0.0069 & 0.0212 & 0.0508 & 0.0129 \\ 0.9999 & 1 & 0.0186 & 0.0097 & 0.0590 & 0.0044 \\ 0.0069 & 0.0186 & 1 & 0.9984 & 0.0574 & 0.0033 \\ 0.0212 & 0.0097 & 0.9984 & 1 & 0.0694 & 0.0177 \\ 0.0508 & 0.0590 & 0.0574 & 0.0694 & 1 & 0.9774 \\ 0.0129 & 0.0044 & 0.0033 & 0.0177 & 0.9774 & 1 \end{bmatrix} \tag{4.4}$$

Figure 52 represents the CoMAC in the described case:

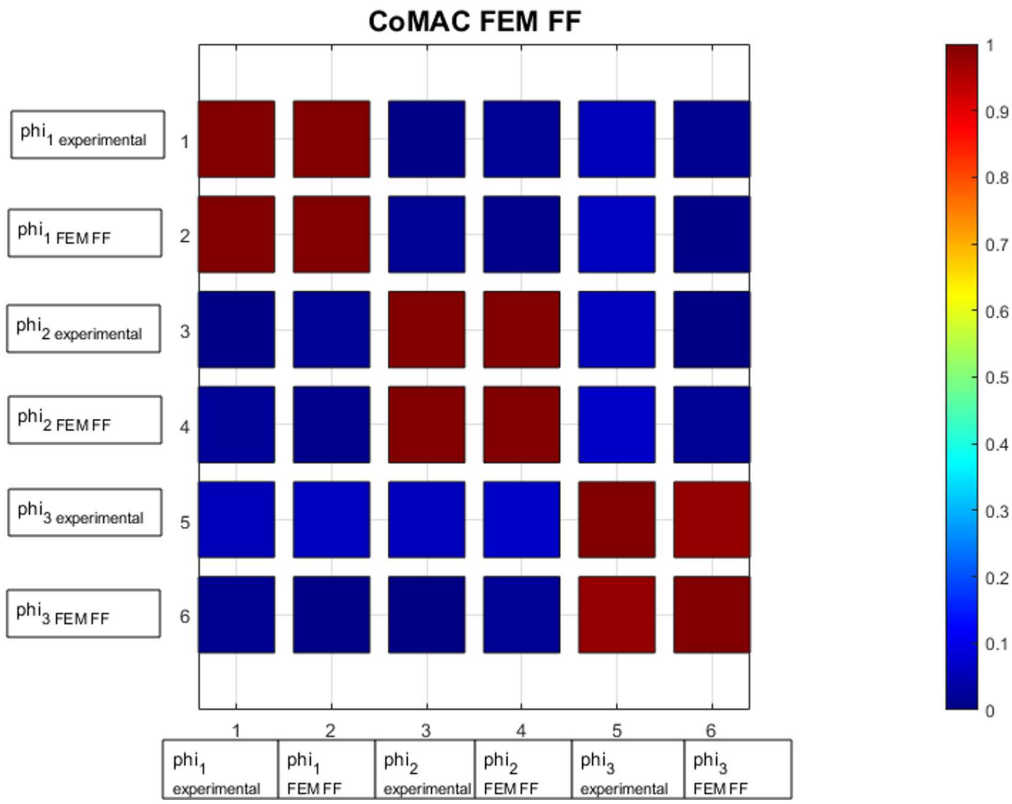

Figure 52: CoMAC FEM Fixed-Fixed configuration

CoMAC is applied in the second case for the experimental mode-shape and the second configuration (Fixed-Moveable) of the FEM model. The result is expressed in matrixial form by equation 4.5.

$$\mathbf{CoMAC} = \begin{bmatrix} 1 & 0.9992 & 0.0069 & 0.0334 & 0.0508 & 0.0342 \\ 0.9992 & 1 & 0.0204 & 0.0195 & 0.0143 & 0.0026 \\ 0.0069 & 0.0204 & 1 & 0.9980 & 0.0574 & 0.0088 \\ 0.0334 & 0.0195 & 0.9980 & 1 & 0.0716 & 0.0089 \\ 0.0508 & 0.0143 & 0.0574 & 0.0716 & 1 & 0.9785 \\ 0.0342 & 0.0026 & 0.0088 & 0.0089 & 0.9785 & 1 \end{bmatrix} \tag{4.5}$$

Figure 53 is the representation of the CoMAC in the second case.

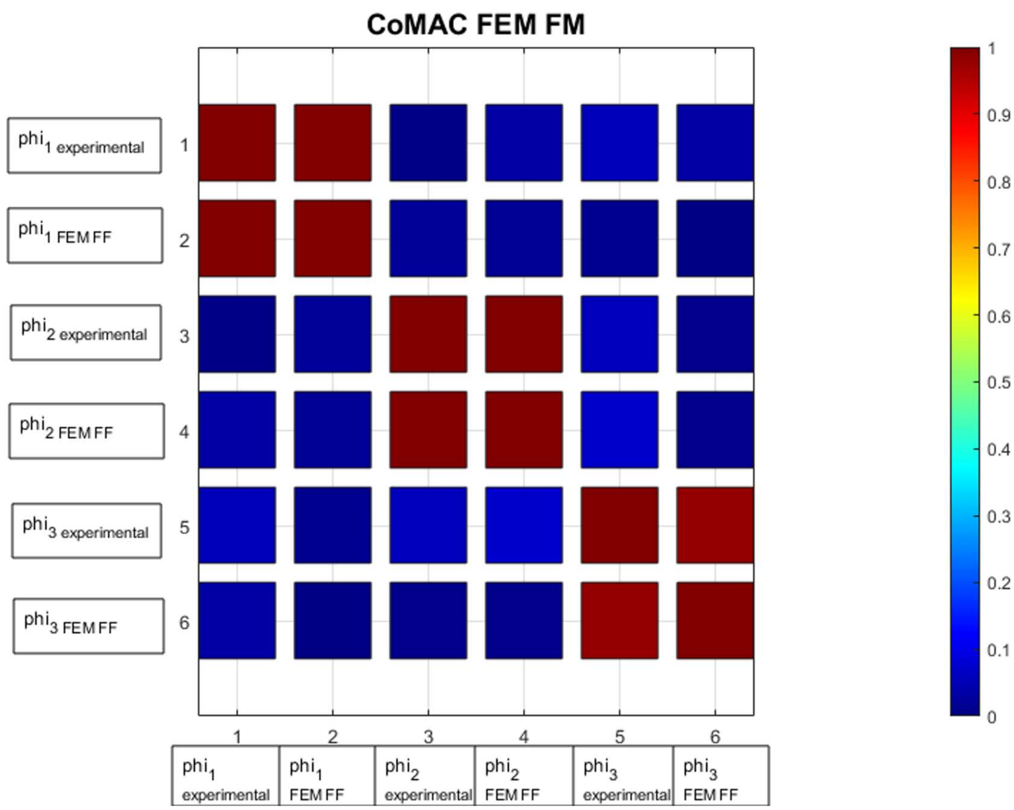

Figure 53:CoMAC FEM Fixed-Moveable configuration

High correlation is calculated for experimental and FEM model mode-shapes for both the configurations. Even though, the difference is very small the first configuration is considered more suitable for the description as the CoMAC assumes slightly lower values for the independence of mode-shapes one and two.

4.9. HSI model verification

The verification of the HSI model is proven through the matching of the theoretical and the experimental DAF curve. By experiment 2, two DAF curves are obtained. These curves describe the dynamic response of the bridge when zero or 35 pedestrians are on the bridge. The experimental curves are obtained through the determination of the Frequency Response Function (FRF) through the whole spectrum. Figure 56 is the representation of the two system conditions in experiment two.

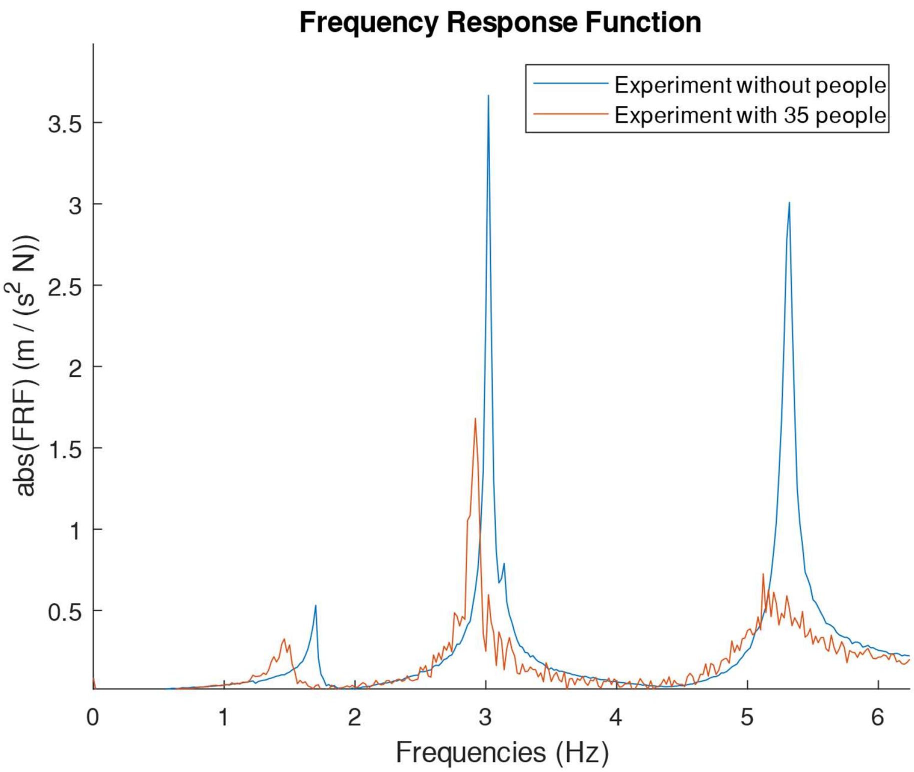

Figure 54: HSI effect in the experimental spectra

Pedestrians affect the whole spectrum of the FRF curve. The effect of HSI was expected to affect mainly the FRF or the DAF value in correspondence with the natural frequency of the pedestrians. From the experiment, the whole spectrum is affected, registering a decrease in the peak and a shift of the natural frequency.

In order to verify the HSI model, single modes need to be isolated. This procedure can be implemented by filtering the signal which is the input of the FRF function or considering just a band on the total DAF curve. The analysis is performed for three modes, the first vertical mode at 1.56 Hz, the second vertical mode at 2.92 Hz, and the natural frequency of the pedestrian at 5.32 Hz.

For each mode, a stiffness value that allows the natural frequency of the pedestrians to be in the range of the considered mode is found and adopted. Therefore, a value of damping in the range 0.25-0.35 is used to approximate the experimental curves better.

The first vertical mode is analysed. The mode-shapes and the natural frequency, found in section 4.7, are considered. The value of damping of the bridge is adjusted in order to permit matching of the peaks of the DAF curves for no pedestrians. Regarding the pedestrians, two main parameters are unknown: the stiffness and the damping. The stiffness of the pedestrian is found in order to better suit the experimental data. Even though in this first case, the matching was not pursued, the model registers a shift and lowering of the peak. The stiffness is set to 22.000 N/m which is in the range defined by Caprani [10]. Figures 57, 58 and 59 show the variation of the HSI model DAF curve when 35 people are considered on the pedestrian bridge for three values of damping. Figure 57 shows the case in which the damping of the pedestrian is taken equal to 0.25, Figure 58 shows the case in which the damping is equal to 0.30 and Figure 59 shows the case in which the damping is set equal to 0.35.

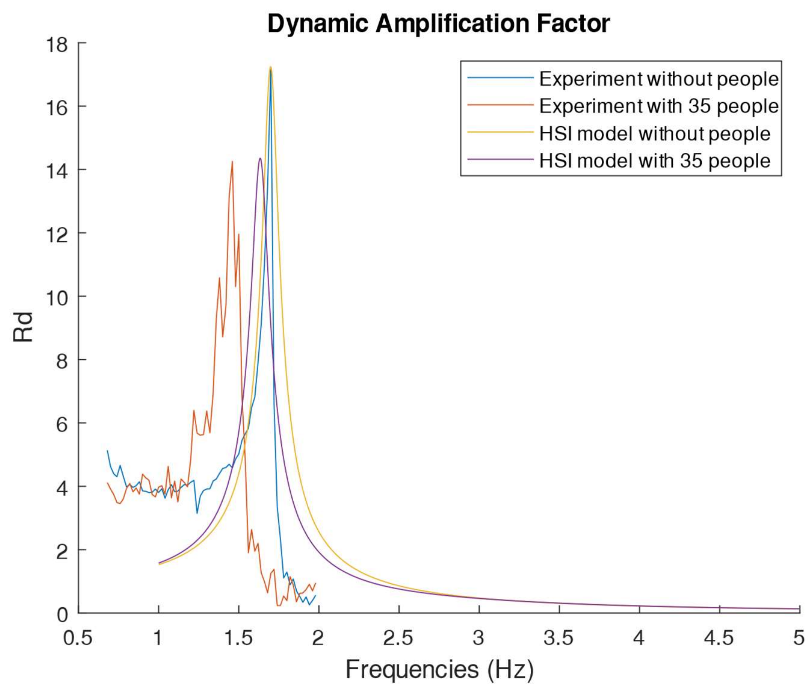

Figure 55: Mode 2 DAF curves comparison for pedestrian damping equal to 0.25.

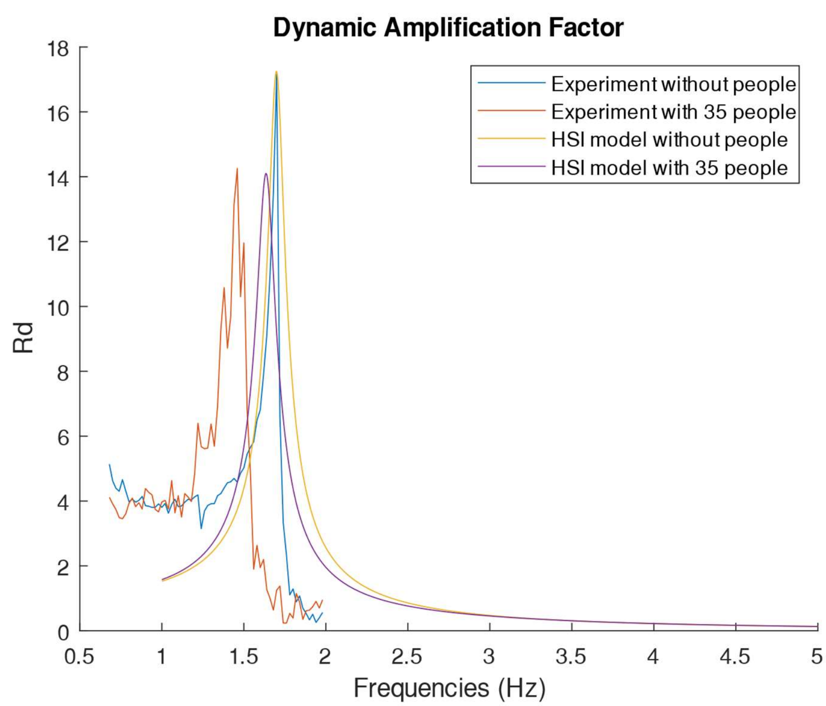

Figure 56: Mode 2 DAF curves comparison for pedestrian damping equal to 0.30

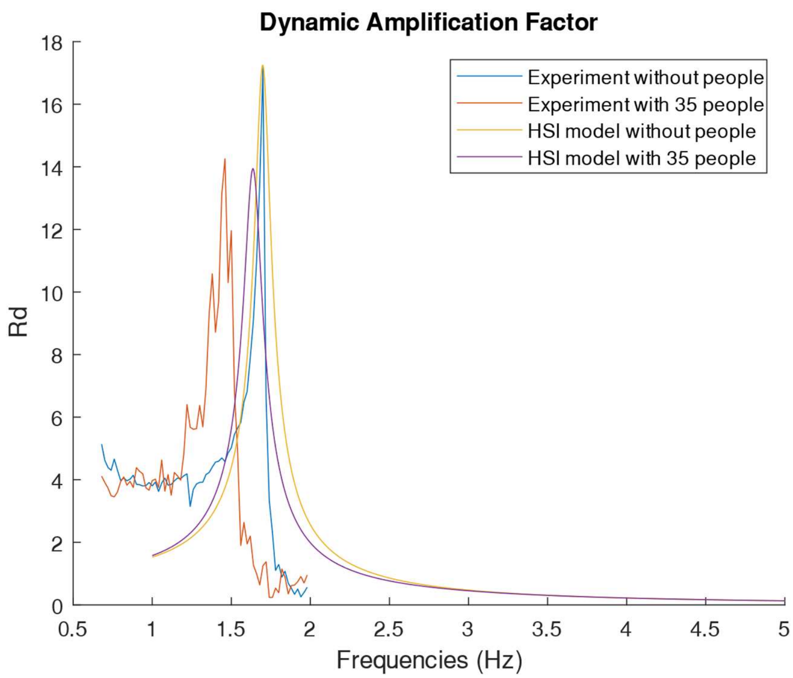

Figure 57: Mode 2 DAF curves comparison for pedestrian damping equal to 0.35

The second mode, which is analysed, corresponds to the second vertical bending moment. Mode-shape, main natural frequency and damping are found in sections 4.5 and 4.6. As for mode one, the damping is adjusted to make the peak value of the DAF curve by the HSI model matching the experimental peak value. The values of the stiffness and damping of the pedestrians are studied. Matching of the experimental and of the HSI model, in the case of 35 pedestrians, is obtained for a value of stiffness of 80.000 N/m. This stiffness value implies that pedestrians assume frequency values in the range 4.7-6 Hz. The assumed stiffness value of 80.000 N/m is not in the Caprani range [10], and the explanation of this assumption is found in Van Nimmen [32], and it is discussed in section 5.3. Figures 60, 61 and 62 represent the two experimental and the two theoretical curves for the cases in which the pedestrian damping is set equal to 0.25, 0.30 and 0.35.

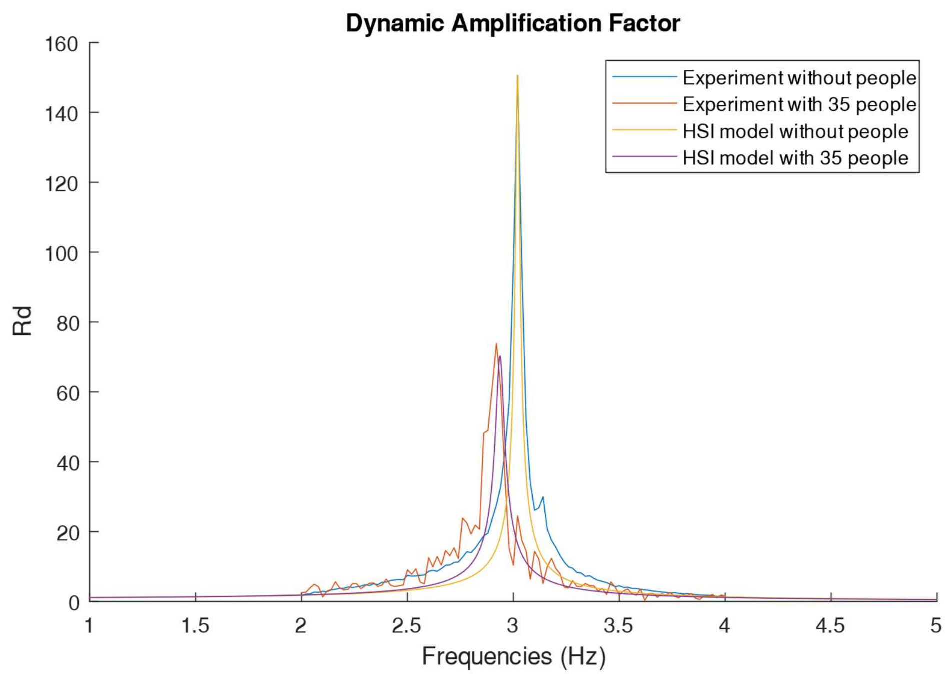

Figure 58: Mode 3 DAF curves comparison for pedestrian damping equal to 0.25.

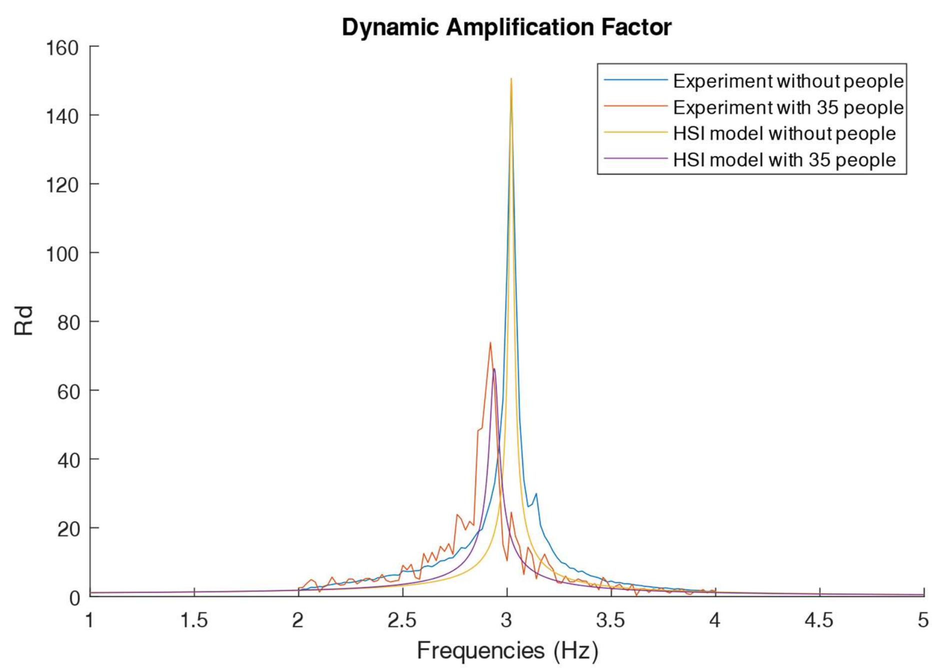

Figure 59: Mode 3 DAF curves comparison for pedestrian damping equal to 0.30.

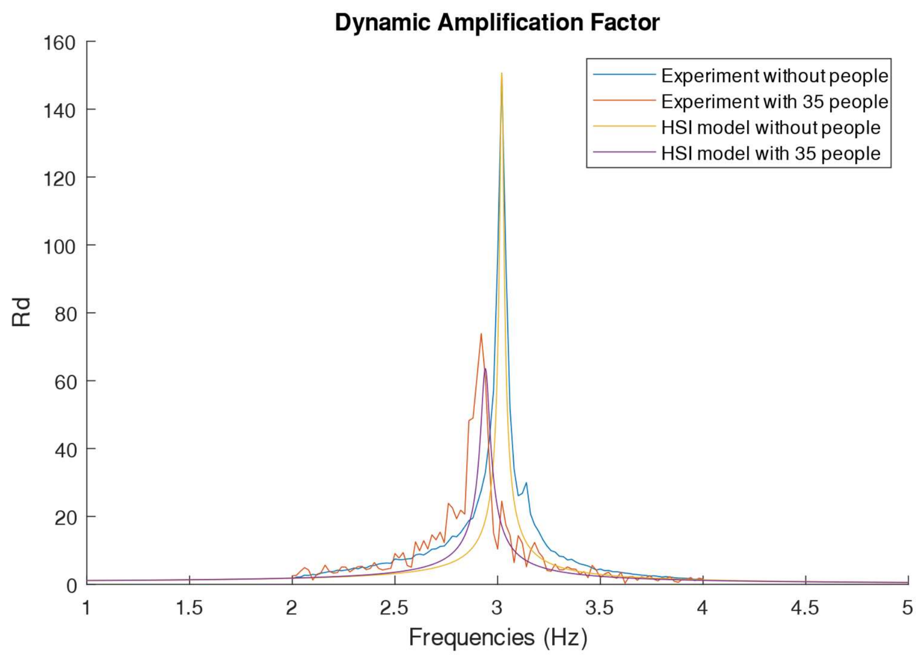

Figure 60: Mode 3 DAF curves comparison for pedestrian damping equal to 0.35.

Mode three corresponds to the third vertical mode and it is examined due to to its main frequency, which is equal to 5.14 Hz and is closer to the main frequency pedestrians assume for mode two. As a matter of fact, the experimental curves show a peak value ratio equal to 4. The structure for this particular frequency is highly affected by HSI, as pedestrians are tuned to the loading frequency. Figures 63, 64 and 65 show the DAF curves obtained for stiffness of the pedestrians equal to 80.000 N/m and a damping value of 0.25, 0.30 and 0.35.

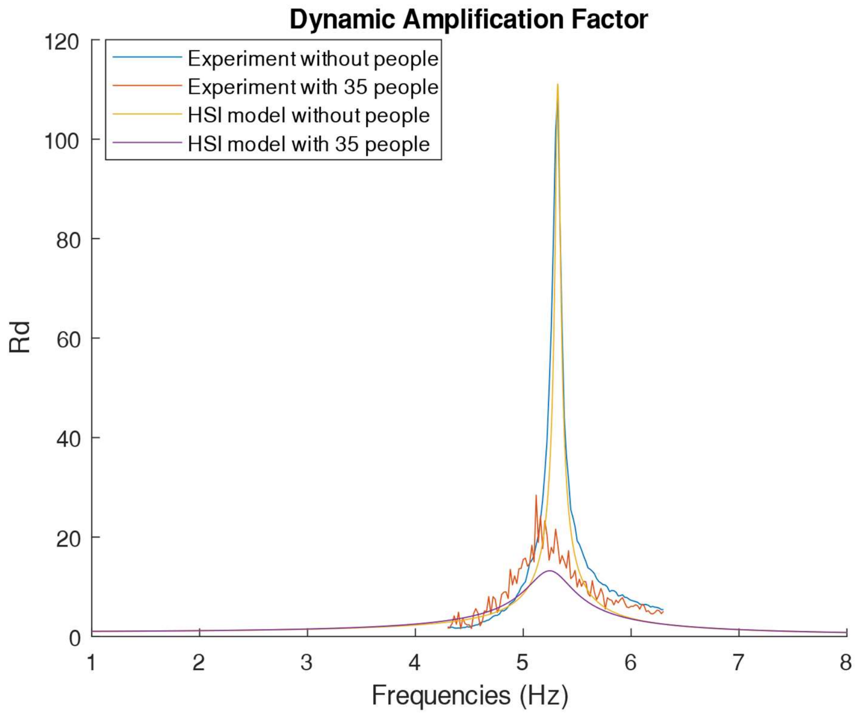

Figure 61: Mode 6 DAF curves comparison for pedestrian damping equal to 0.25.

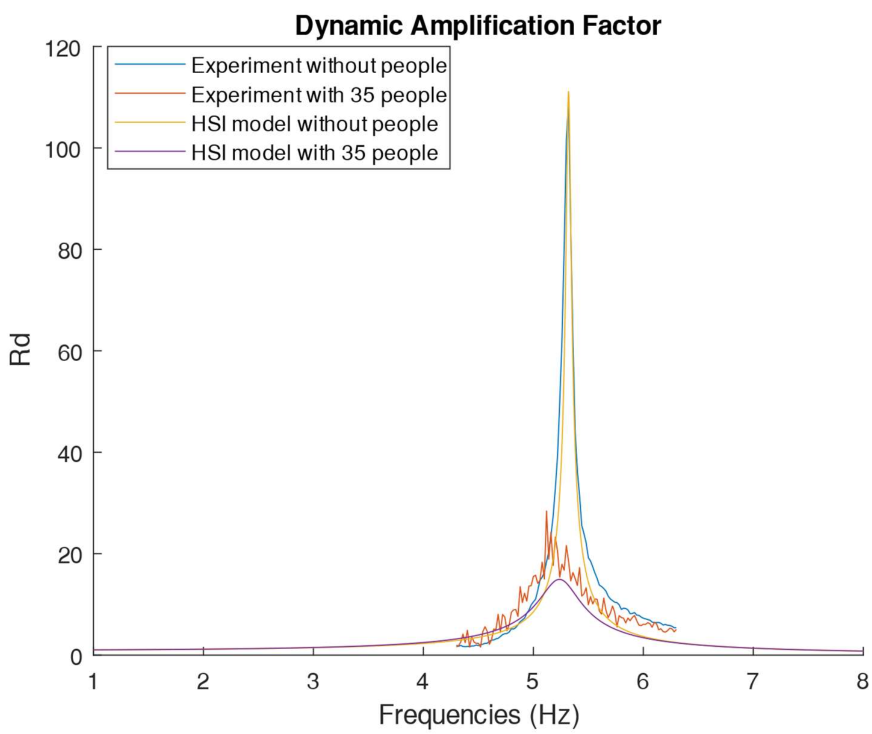

Figure 62:Mode 6 DAF curves comparison for pedestrian damping equal to 0.30

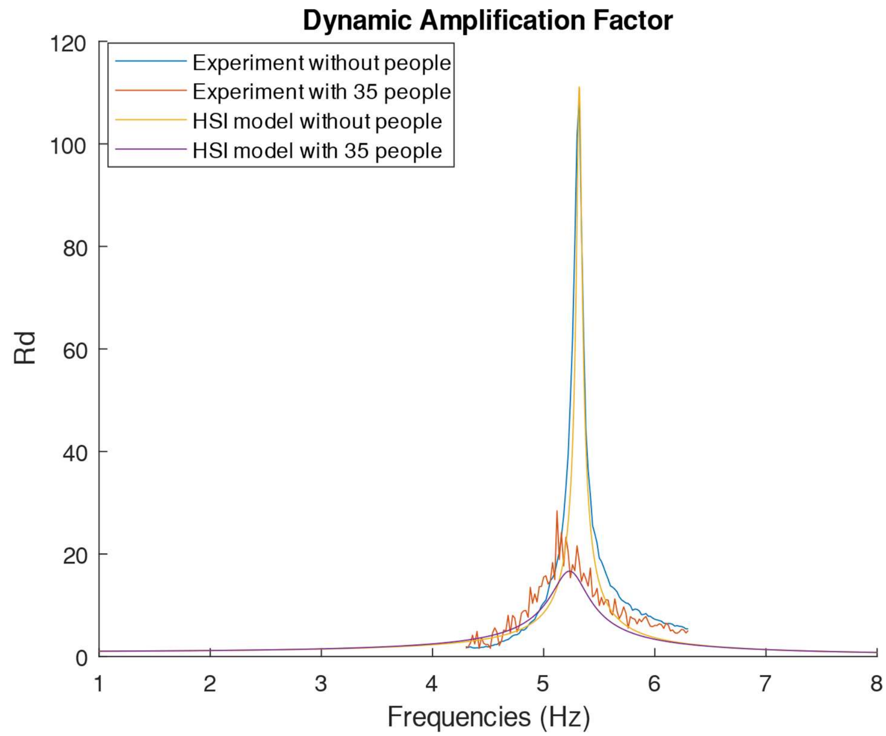

Figure 63:Mode 6 DAF curves comparison for pedestrian damping equal to 0.35.

The damping value of 0.35 better suits the experimental data.

4.10. Time history analysis of a running test

Several running and marching tests are performed on the Folke Bernadotte Bridge during the experimental campaign. In the first experiment, 5 running tests and 5 marching tests were performed at different frequencies. Loading frequencies of 1.6 Hz, 1.8 Hz, 2 Hz, 2.2 Hz and 2.4 Hz were chosen. From the analysis of the data, it was clear that in the marching tests synchronization was not obtained. As described in section 3.4.2 marching tests were executed by 4 people walking in a 2 by 2 distribution on the southern half of the bridge. The spectrum of the input signal presented more loading frequencies. Running tests presented better results. However, at least two loading frequencies were registered during the same test. In the second experiment, an experienced runner was asked to perform the test. Figure 64 shows the accelerations of the bridge measured by the accelerometer 3 by the set up from the second experiment, positioned in at 35.5 meters from the edge on the southern middle span. Higher peaks are not to be considered because of the wooden deck configuration. The timber langers of the deck are not totally fixed to the steel construction causing high peaks when the runner is approaching the accelerometer,

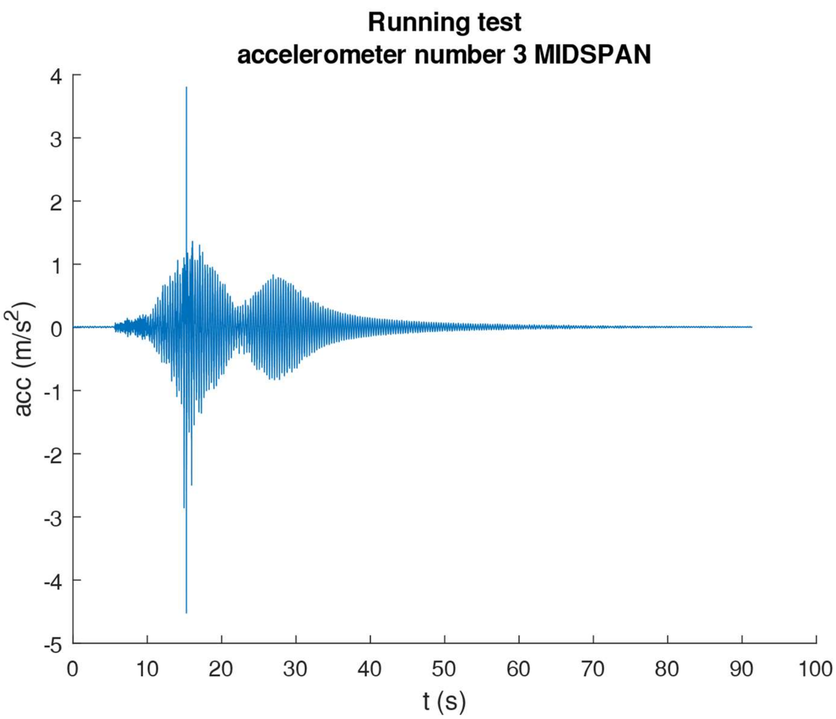

Figure 64: Running Test signal in time-domain

Figure 65 represents the spectrum of the signal. Two peaks are dominant on the frequencies 2.97 and 3.03 Hz.

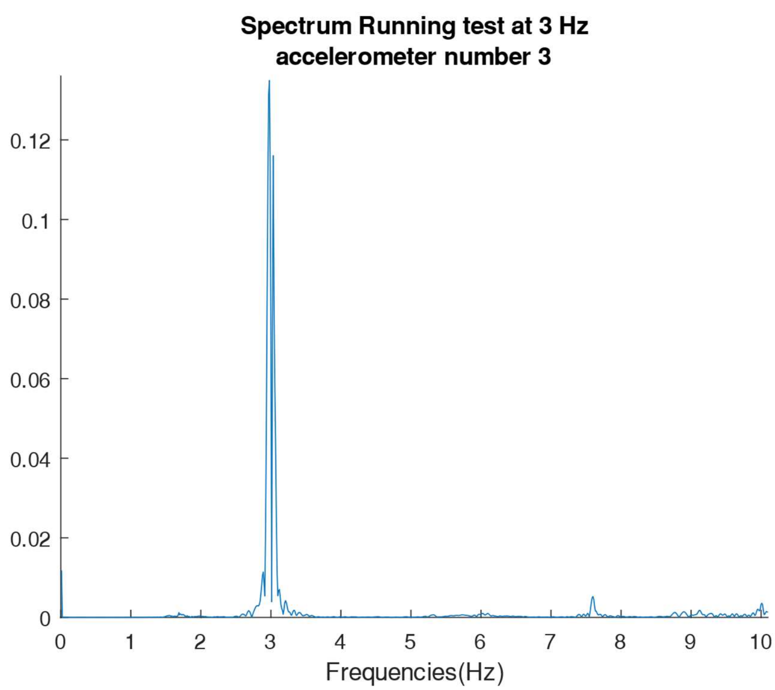

Figure 65: Running Test signal in frequency-domain

The signal is filtered with a bandpass from 1 Hz to 5 Hz to permit a loading description through a moving harmonic. The command filtfilt is used on Matlab. The filtered experimental signal is shown in Figure 66.

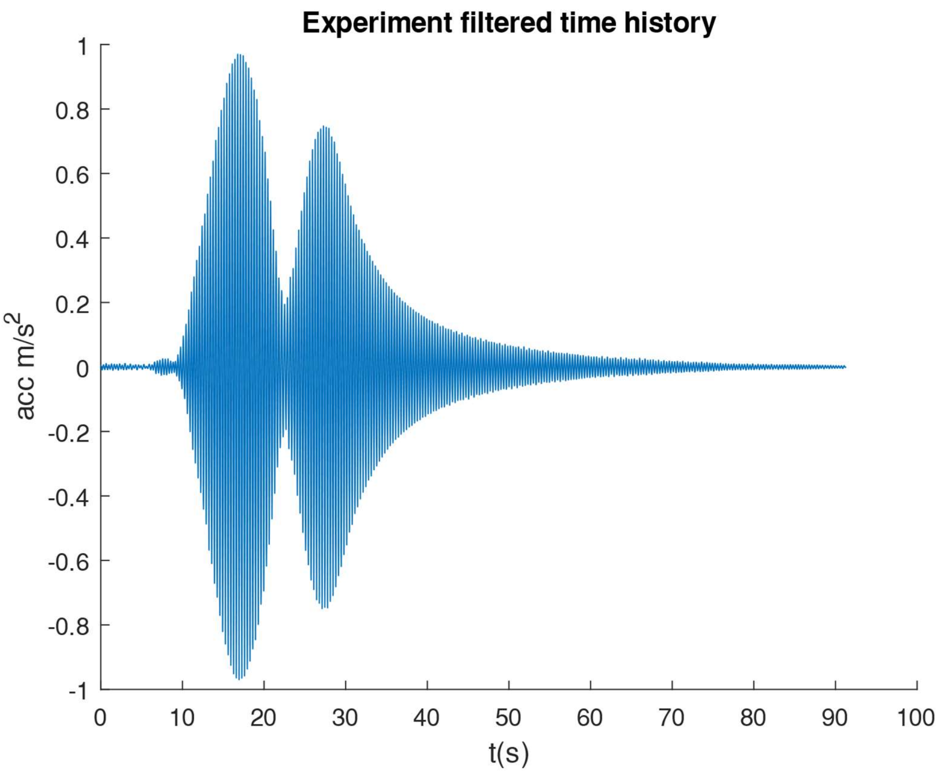

Figure 66: Experimental filtered signal

The signal shows two peaks reaching the acceleration of 1 m/s^2. The time history is modelled through a Moving Force (MF) or a Spring Mass Damper (SMD) as shown in Figures 67 and 69.

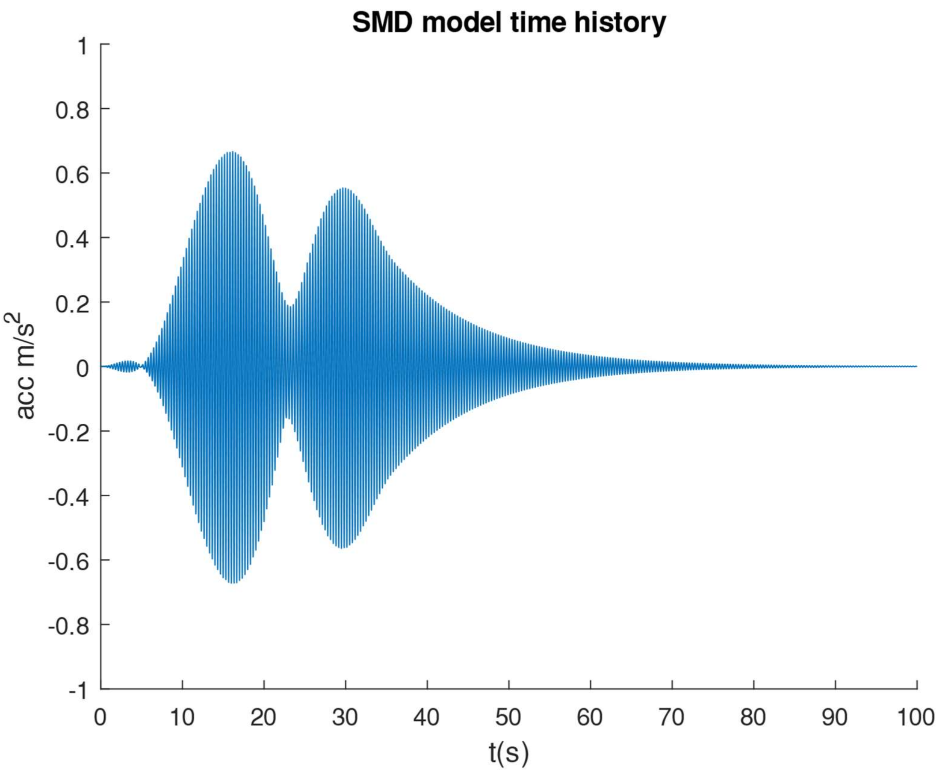

Figure 67: SMD model time history

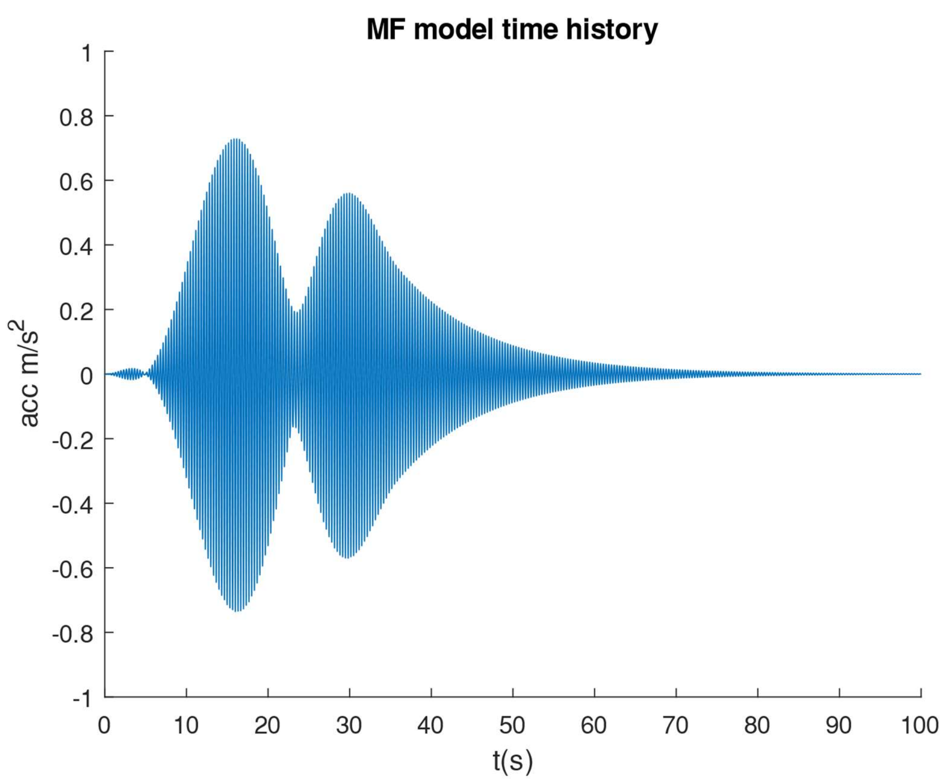

Figure 68: MF model time history

The history analysis of the pedestrian is reconstructed by modelling the load transmitted from the pedestrian to the bridge as a moving harmonic. The envelopes of the signals are shown in Figure 70.

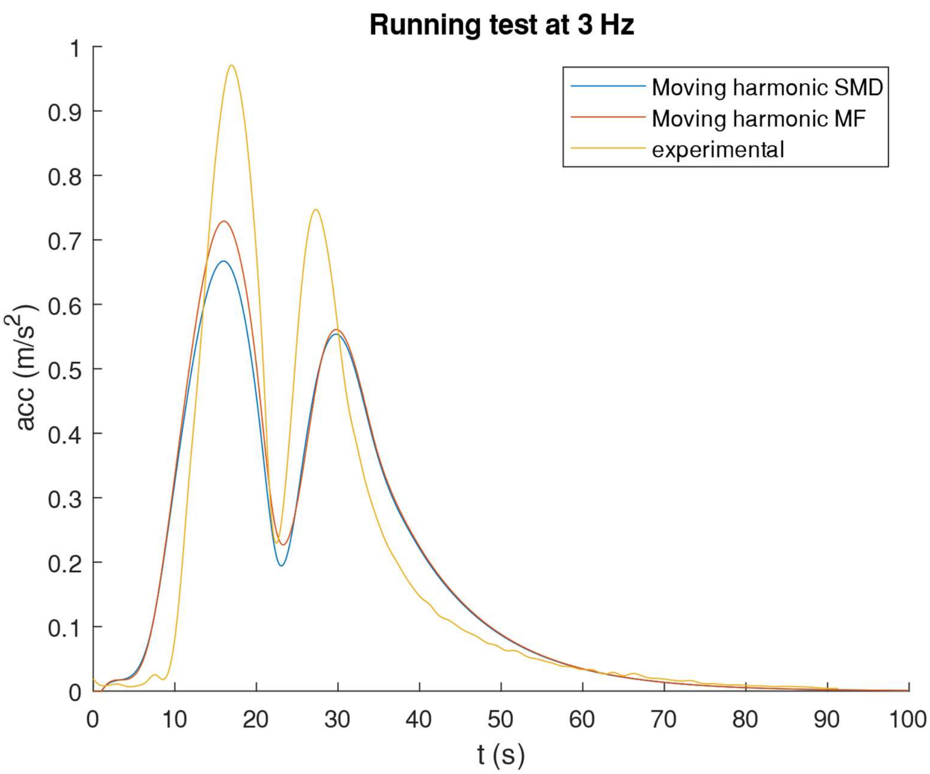

Figure 69: Comparison of the time histories envelopes

In Figure 70, the experimental time history is compared with the two theoretical models. Only the positive part of the envelopes of the signals are represented due to symmetry. The experimental envelope presents peaks over the two peaks of the SMD and MF models.

Both the theoretical and the practical envelopes present the same shape, and they are consistent. However, the difference in the peak accelerations show the large underestimation of the theoretical method rather to the experimental measures. The load definition, that was implemented in the code, is reported in equation 3.13 and is extracted from ISO 2008.

The load definition is amended in order to permit matching of the envelopes. Equation 3.13 is modified as detailed below.

$$F(t) = M_p \left(9.81 \left(2\, sin\left(2\pi f_{step} t\right) + 1.4 sin\left(4\pi f_{step} t\right) + 1.2 sin\left(6\pi f_{step} t\right)\right)\right) \tag{4.6}$$

The new Dynamic Load Factors (DLF) are equal to 2, 1.4 and 1.2 and they are defined in order to match the experimental curve according to Baumann and Bachmann [38].

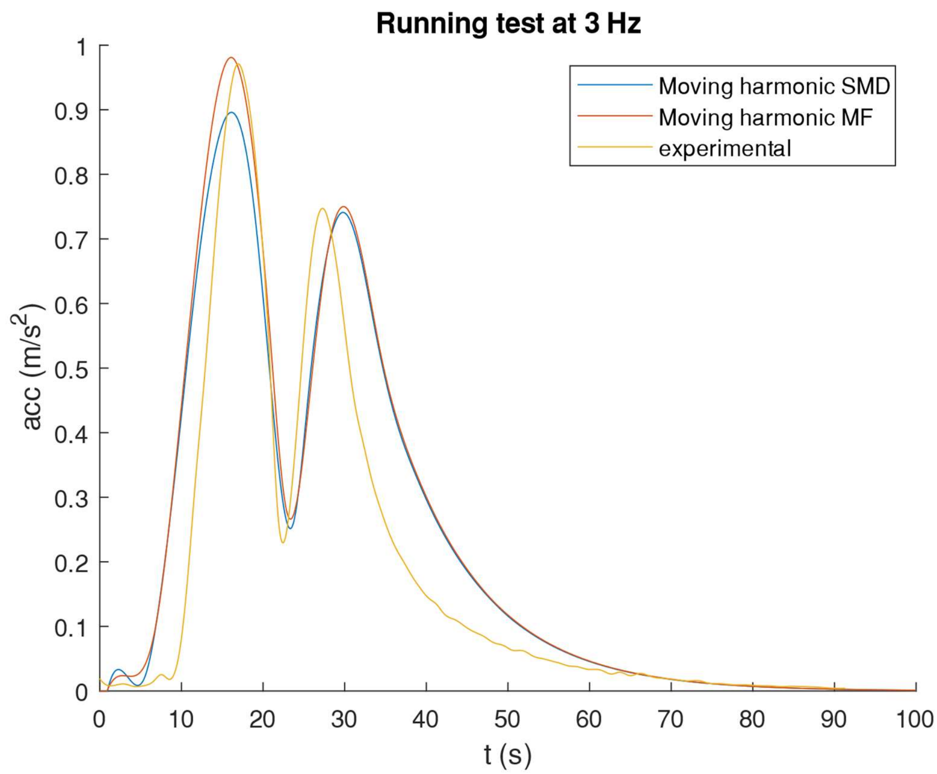

Figure 70: Comparison of the time history envelopes after the modification of the DLFs

5. Discussion

The following section aims to discuss the results, which are shown in section 4. The dynamic properties, the parametric analysis, the verification of the HSI model, are emphasized.

5.1. Dynamic properties comparison

The dynamic properties of the Folke Bernadotte bridge are estimated through the two experiments and later compared to the FEM model. The first experiment permits the estimation of the natural frequencies, the damping, and the mode-shapes of the bridge. However, to understand the dynamic response of the pedestrian bridge, a FEM model is created. The bearing condition of the pedestrian bridge has been compared with the two FEM models. The natural frequency of mode 2 (first vertical) lies in between the correspondent second modes from the two bearing configurations. Even though the executive drawings from Ramboll prescribe the fixation of the three translations in the two bearings at the base, the measures indicate imperfection. On the other hand, the first and the second mode-shapes obtained from the experiments are consistent with both the bearing configurations. The FEM mode-shapes do not differ relevantly, and the experimental measures lie in between. CoMAC shows consistency between experimental, and both the FEM extracted mode-shapes. The linear correlation between the first and the second mode from both the experiment and the FEM model is assured by values less than 0.2. High values in CoMAC above 0.9 show the high correlation between each mode from the experiment and both the FEM configurations model.

Resulting from the comparison of the values of the natural frequencies, damping and mode-shapes from the first and second experiment, the difference is negligeable.

5.2. Parametric Analysis and Error Surface

A parametric analysis of the HSI model is conducted and the results are shown in section 5.8. The parametric analysis is first implemented in [37], and later reported in this work of thesis. The choice on the variation of non-dimensional values permits to emphasize the condition of resonance of the bridge, resonance of the pedestrians, tuning of the pedestrians and bridge. The surfaces obtained for the five mass ratios, highlight the shift and the peak decrease of the DAF curve depending on the variation of Π_1, Π_2 and Π_3. When the condition of resonance occurs, the DAF curve reaches its peak. The position of this peak varies depending on the mass ratio and on the tuning of the pedestrians. As it is shown in the parametric analysis, the presence of pedestrians has a double effect. The mass of the total system increases resulting in a decrease in the natural frequency. Moreover, pedestrians act as DVA, adding damping to the system and dissipating energy. The value of the stiffness of the pedestrians is dependent on the value of the natural frequency, made to vary in the analysis. Pedestrians act as SMD systems applied on fixed points on the bridge. High values of stiffness lead to the consideration of pedestrians as attached mass of the bridge limiting their energy dissipation. Pedestrians are modelled as SDOFs with one natural frequency and one value of damping equal to 0.30, in the range 0.25-0.35 [10]. High values of damping increase HSI effects while low values decrease the effects. The natural frequency of the pedestrians is made to vary on the frequency of the bridge. When pedestrians and the bridge are tuned, the DAF curve peak has its minimum value. The reason lies in the change of the load path from the bridge to the pedestrians who go in resonance and dissipate energy. Hence, the DAF curve decreases as there is less available energy in the system.

5.3. HSI model verification

In experiment two, two hammer tests permitted to register the dynamic response of the bridge, with and without pedestrians. HSI effects can be appreciated in the two different DAF curves which have been reconstructed through the FRF functions. The shift and the decrease in the DAF curve can be appreciated through the whole spectrum of the registered signals. This effect highlights the complexity of the system. HSI effect is registered for several frequencies. Hence, the pedestrians act as DVAs the whole spectrum. The HSI model accounts for the pedestrians as SDOFs and analyses one mode at a time. Therefore, the verification is conducted considering a section of the FRF function and obtaining the DAF for a band of the spectrum.

The procedure of matching the experimental and the theoretical curves accounts for the definition of the stiffness and damping values for the pedestrians. The experimental curve without pedestrians is suited from the HSI model inserting the natural frequency, the damping and the mode-shape of the mode in analysis. On the other hand, the correspondence between the two curves with pedestrians must be ensured, by adopting reasonable values for damping and stiffness of the pedestrians. As described in section 4.9, the pedestrians are modelled differently for the first mode, second and third mode. In the first case, the stiffness is set to 22.000 N/m. The natural frequency of the pedestrian is dependent on the modal mass of the pedestrian and on the stiffness. For the mentioned value of stiffness, pedestrians assume frequency values in the range of 2.2- 3.2 which is coherent with Caprani definitions [10]. Even though the decrease of the peak value is registered by the model, the shift of the natural frequency of the system is only partially registered. On the other hand, for the second and third vertical modes, the stiffness values needed to be set to 80.000 N/m to permit the matching of the curves. For these two cases, the theoretical curve is suited to the experimental one for both the curve peak and natural frequency. Even though the assumed value of stiffness is not in the range defined by Caprani [10], it generates frequency values which are in line with the ISO 5982 and Zeng and Brownjohn. The pedestrian frequency values are found are in the range 4.7-6 according to the weight and position of the pedestrian and of the mode which is considered. Table 6 shows the usual values of natural frequency and damping which are assumed in the literature.

Table 6: Literature pedestrian natural frequency and damping. Source [32]

Author	Model type	Frequency [Hz]	Damping [%]
Vertical motion			
ISO 5982	model 2a	$f_{H1} = 5.0$	$\xi_{H1} = 36$
		$f_{H2} = 12.5$	$\xi_{H2} = 46$
Zeng and Brownjohn	model 1a	$f_{H1} = 5.24$	$\xi_{H1} = 39$
Matsumoto and Griffin	model 1a	$f_{H1} = 5.7$	$\xi_{H1} = 69$
	model 2a	$f_{H1} = 5.5$	$\xi_{H1} = 40$
		$f_{H2} = 13.9$	$\xi_{H2} = 37$
Horizontal motion			
Matsumoto and Griffin	-	$f_{H1} = 0.4 - 1.0$	-

According to ISO 5982, the natural frequency of the pedestrian should be taken as 5.0 Hz. Similarly, Zeng and Brownjohn recommend the value of 5.24. The explanation of these values can be taken by the natural frequencies of the human body. Figure 73 detects the principal natural frequencies of the human body.

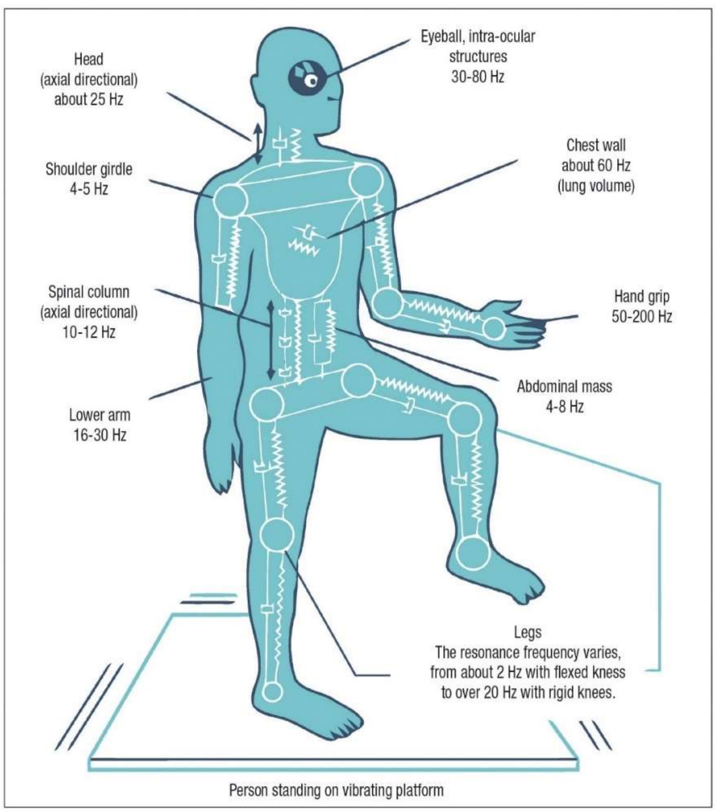

Figure 71: Human Body frequencies. Source [36]

Hence, the adoption of the value of $80.000\ \mathrm{N/m}$ for the stiffness can be justified by literature because resulting in frequency values prescribed by ISO 5982 and others.

In the analysis of the first mode, the pedestrian stiffness is set to $22.000\ \mathrm{N/m}$ and the results are shown in section 4.9. Another analysis was performed assuming the stiffness value of $80.000\ \mathrm{N/m}$ as for the other two modes. In this case, HSI has a limited effect on the bridge as the pedestrians assume frequencies in the range $4.7 - 6\ Hz$ and the natural frequency of the bridge is equal to $1.56\ Hz$. The HSI model registers the decrease of the natural frequency but not the decrease of the DAF curve. Therefore, it was hypothesized that pedestrians acted as an attached mass to the bridge. This assumption was verified through the comparison of the modal mass of the system, calculated by the summation of the modal mass of the pedestrian and the modal mass of the bridge, and an equivalent modal mass that considers pedestrians as attached mass. The percentage difference is equal to 0.77 %, and the hypothesis is verified. Assuming such a high stiffness for the first mode leads to consideration of pedestrians as attached mass rather than DVA.

5.4. Running test

The running pedestrian analysis aims to assess the dynamic behaviour of the Folke Bernadotte Bridge and the dissimilarities in the modelling of the pedestrian as an MF and as an SMD system. The time history analyses of a runner are reconstructed through Newmark's linear method and then compared with the experimental one. As described in section 4.10, an experienced runner is asked to run at a frequency of 3 Hz.

The analysis of the experimental data highlights the presence of two peaks of the envelope of the signal. The MF and the SMD models imply the definition of a harmonic loading based on the only frequency of 3 Hz. The difference in the two pedestrian modelling methods lies in the consideration of the pedestrian. The MF modelling method considers the pedestrian as only a load source, while the SMD modelling method as an SDOF system is able to dissipate energy. The MF time history envelope assumes a higher peak not taking into consideration the fact that humans dissipate energy. For a single pedestrian running, the difference in the dynamic response of the bridge is appreciable when the pedestrian is tuned to the loading frequency. The increase in the DLFs in the harmonic load description, shows a case in which ISO 2008 is not conservative. The running pedestrian problem should be further study to assess more conservative DLFs.

The maximum acceleration that is registered on the Folke Bernadotte bridge, shows a low level of comfort. The acceleration peak is equal to $1\ m/s^2$ indicate that the comfort level and the serviceability limit state of the bridge may be compromised.

6. Conclusion

Human Structure Interaction is proven to have a real effect on the variation of the dynamic properties of pedestrian bridges. The frequency shift and the decrease of the DAF curve peak are verified through the experiment when 35 people participated. Moreover, the experiment permitted the verification of the HSI model, based on Caprani and Colmenares formulations. The changes of the dynamic properties are registered and predicted from the model. Several parameters are defined and can be adjusted on the assumptions. The number of pedestrians, as well as the stiffness and damping parameters depending on the posture, are unpredictable in the design process of a pedestrian bridge. The change in the dynamic properties can be appreciated on the variation of the inserted parameters. The parametric analysis permitted to emphasize the validity of the model and the error surface highlighted the correlation of the model to Newmark's linear method.

A major effect is given when pedestrians are tuned with the loading. The experiment showed the decrease and the shift of the FRF on the whole spectrum. This result is critical in the study as the pedestrians are assumed as SDOF. Further studies in modelling the pedestrians as MDOF which several natural frequencies are considered, should be performed. The choice in modelling the pedestrians as SDOFs is made as a trade between accuracy and simplicity. More accuracy in the prediction of the dynamic properties' variation, can be obtained by increasing the degrees of freedom in modelling the pedestrians.

The running pedestrian test is not correlated to crowd effects on pedestrian bridges but modelling of pedestrians and assessing the dynamic behaviour of the bridge. The analysis aims to assess the dissimilarities in the modelling of the pedestrian as an MF and as an SMD system. In the HSI model, pedestrians are modelled as single degree of freedom (SDOF) spring-mass-damper (SMD) dynamic viscous adsorbers (DVA) systems. Moreover, the experiments emphasize the fact the Folke Bernadotte Bridge experiences large accelerations and that the comfort level and the Serviceability Limit State (SLE) may be compromised. Further studies can be done on the viscous dampers to be adopted in the Folke Bernadotte Bridge. The Dynamic Load Factors in the load description in ISO 2008 can be further studied and critically discussed.

To conclude, HSI should be considered in the design of pedestrian bridges as its large effects on the dynamic properties of the bridge has been proven. A new formulation of the design guideline including HSI would permit a more cost-efficient and environmentally efficient designing.

7. Bibliography

1) Dallard, P., A. J. Fitzpatrick, A. Flint, S. Le Bourva, A. Low, R. M. Ridsdill Smith, and others, *The London Millennium Footbridge*, *Structural Engineer*, 2001
2) Caprani, Colin C., A *Modal Precise Integration Method for the Calculation of Footbridge Vibration Response*, *Computers and Structures*, 2013
3) Živanović, Stana, Aleksandar Pavić, and Paul Reynolds, *Probability-Based Prediction of Multi-Mode Vibration Response to Walking Excitation*, *Engineering Structures*, 2007
4) Brownjohn, J. M.W., A. Pavic, and P. Omenzetter, *A Spectral Density Approach for Modelling Continuous Vertical Forces on Pedestrian Structures Due to Walking, Canadian Journal of Civil Engineering, 2004*
5) Ebrahimpour, A., R. L. Sack, and P. D. Van Kleek, *Computing Crowd Loads Using a Nonlinear Equation of Motion, Computers and Structures*, 1991
6) Rainer, J. H., G. Pernica, and D. E. Allen, *Dynamic Loading and Response of Footbridges*, *Canadian Journal of Civil Engineering*, 1988
7) Ingólfsson, E. T., C. T. Georgakis, and J. Jönsson, *Pedestrian-Induced Lateral Vibrations of Footbridges: A Literature Review*, *Engineering Structures*, 2012
8) Charles P, Bui V. , *Transversal dynamic actions of pedestrians, Proceedings of Footbridge* 2005*, second international conference*, 2005
9) Ingólfsson ET, Georgakis CT. *A stochastic load model for pedestrian-induced lateral forces on footbridges, Engineering Structures*, 2011
10) Caprani, Colin C., and Ehsan Ahmadi*, Formulation of Human–Structure Interaction System Models for Vertical Vibration*, *Journal of Sound and Vibration*, 2016
11) Ahmadi, Ehsan, Colin Caprani, Stana Živanović, Neil Evans, and Amin Heidarpour, *A Framework for Quantification of Human-Structure Interaction in Vertical Direction, Journal of Sound and Vibration*, 2018
12) Van Nimmen Katrien, Kristof Maes, Geert Lombaert, Guido De Roeck, and Peter Van Den Broeck, *The Impact of Vertical Human-Structure Interaction for Footbridges*, *COMPDYN 2015 - 5th ECCOMAS Thematic Conference on Computational Methods in Structural Dynamics and Earthquake Engineering*, 2015
13) Caprani, Colin, Junnan Qu, Stana Zivanovic, Neil Evans, and Ehsan Ahmadi, *Quantification of Human-Structure Interaction*, *EDP Sciences,* 2015
14) Ahmadi, Ehsan, and Colin Caprani, *Damping and Frequency of Human-Structure Interaction System*, *EDP Sciences*, 2015
15) Ahmadi, Ehsan, Colin C. Caprani, and Amin Heidarpour, *An Equivalent Moving Force Model for Consideration of Human-Structure Interaction*, *Applied Mathematical Modelling*, 2017
16) Younis, Adel, Onur Avci, Mohammed Hussein, Brad Davis, and Paul Reynolds, *Dynamic Forces Induced by a Single Pedestrian: A Literature Review*, *Applied Mechanics Reviews*, 2017
17) Olsson, M., *Finite Element, Modal Coordinate Analysis of Structures Subjected to Moving Loads*, *Journal of Sound and Vibration*, 1985
18) Lin Y.H. and Trethewey M.W., *Finite Element To Analysis Moving of Elastic Dynamic Beams Loads*, *Journal of Sound and Vibration*, 1990
19) Hino, J., T. Yoshimura, K. Konishi, and N. Ananthanarayana, *A Finite Element Method Prediction of the Vibration of a Bridge Subjected to a Moving Vehicle Load*, *Journal of Sound and Vibration*, 1984

20) Pu, Junping, and Peng Liu, *Numerical Calculation of Dynamic Response for Multi-Span Non-Uniform Beam Subjected to Moving Mass with Friction, Engineering*, 2010

21) Živanović, S., I. M. Díaz, and A. Pavić, 'Influence of Walking and Standing Crowds on Structural Dynamic Properties', *Conference Proceedings of the Society for Experimental Mechanics Series, 2009*

22) Živanović, Stana, Aleksandar Pavić, and Einar Thòr Ingolfsson, *Modelling Spatially Unrestricted Pedestrian Traffic on Footbridges*, *ASCE Journal of Structural Engineering,* 2010

23) Matsumoto, Y., Nishioka, T., Shiojiri, H. and Matsuzaki, K., *Dynamic Design of Footbridges, IABSE Proceedings,* 1978

24) Brownjohn, J. M. W., Pavi´c, A., Omenzetter, P. *A spectral density approach for modelling continuous vertical forces on pedestrian structures due to walking. Canadian Journal of Civil Engineering*, 2004

25) Butz, C. A *Probabilistic Engineering Load Model for Pedestrian Streams, In Proceedings of the Third International Conference Footbridge*, 2008

26) Georgakis, C. T. and Ing´olfsson, E. T. *Vertical Footbridge Vibrations: The Response Spectrum Methodology. In Proceedings of the Third International Conference Footbridge*, 2008

27) Piccardo, G., and F. Tubino, *Simplified Procedures for Vibration Serviceability Analysis of Footbridges Subjected to Realistic Walking Loads*, *Computers and Structures*, 2009

28) Yao, S., J. R. Wright, A. Pavic, and P. Reynolds, *Forces Generated When Bouncing or Jumping on a Flexible Structure, Proceedings of the 2002 International Conference on Noise and Vibration Engineering, ISMA*, 2002

29) Fanning, Paul J., Paul Archbold, and Aleksandar Pavic, *A Novel Interactive Pedestrian Load Model for Flexible Footbridges, Proceedings of the 2005 SEM Annual Conference and Exposition on Experimental and Applied Mechanics*, 2005

30) Archbold, Paul, Joseph Keogh, Colin Caprani, and Paul Fanning, *A Parametric Study of Pedestrian Vertical Force Models for Dynamic Analysis of Footbridges*, *EVACES – Experimental Vibration Analysis for Civil Engineering Structures,* 2011

31) Bruno L, Venuti F. The pedestrian speed–density relation: modelling and application. *Proceedings of Footbridge* 2008

32) Van Nimmen K. Numerical and experimental study of human-induced vibrations of footbridges. *Dissertation presented in partial fulfilment of the requirements for the degree of Doctor in Engineering Science*, 2015

33) Eurocode 5: Design of timber structures – Part 2: Bridges, EN 1995-2:2004, British Standards Institution, 2004

34) Sétra Footbridges, assessment of vibrational behaviour of footbridges under pedestrian loading, Technical guide. Service d'Etudes Techniques des Routes et Autoroutes, Paris, 2006

35) Chopra A.K., *Dynamics of Structures*, fourth edition, Pearson Education, publishing as Prentice Hall, 2012

36) Repetti G., Vulkan D., Vibroacoustics 2, - Barchemagazine.com, 2020 https://www.barchemagazi-ne.com/en/vibroacoustics-2/

37) Colmenares D., Costa G., Andersson A., Karoumi R., Surace C., Civera M., *On the quantification of Human Structure Interaction, a classical approach*, to be submitted in 2021 in Journal of Engineering Structures, 2021

38) Baumann R., Bachmann H., *Durch Menschen verursachte dynamische Lasten und deren Auswirkungen auf Balkentragwerke*, Birkhauser editor, 1988